

Real-time and Near-real-time Very Long Baseline Interferometry for
Monitoring Motion of the Observing Sites, Flux Density Variation of
Radio Sources, and Variation of Earth Orientation Parameters

Yasuhiro Koyama

Doctor of Philosophy

Department of Astronomical Science
School of Mathematical and Physical Science
The Graduate University for Advanced Studies

2003

Acknowledgements

Since the VLBI is intrinsically multi-agency activity which requires close cooperation among many research institutes, the work described in this thesis has been made possible with the vigorous supports and aid from many individuals and research institutes. First of all, I would like to express deep appreciation to Prof. Kosuke Heki at National Astronomical Observatory who kindly agreed to supervise the thesis and gave me various important suggestions to complete the thesis. I feel it is a great honor that I could ask him to be my supervisor, since I am personally respect his attitude and outstanding talent for research. I would also like to express deep appreciation to Prof. Noriyuki Kawaguchi, Mr. Yuji Sugimoto, Mr. Michito Imae, Mr. Yukio Takahashi, Mr. Noriyuki Kurihara, and Dr. Tetsuro Kondo who have kindly led me to start and continue the research in the field of VLBI as the section chief or the group leader. Prof. Kawaguchi also kindly agreed to chair the thesis evaluation committee. His enthusiasm and leadership in the various aspects of VLBI technology developments have been quite impressive and have inspired me since I started to work with VLBI in 1988. I also wish to express my gratitude to Prof. Makoto Inoue, Dr. Hideo Hanada, and Dr. Kenta Fujisawa who have kindly agreed to participate in the thesis evaluation committee.

In addition, I would like to thank the following individuals and institutes for their precious supports, productive discussions, and thorough suggestions. Many colleagues in the CRL including Dr. Junichi Nakajima, Dr. Mamoru Sekido, Dr. Ryuichi Ichikawa, Mr. Eiji Kawai, Ms. Shinobu Arimura, Dr. Toshimichi Otsubo, Mr. Hiroshi Okubo, Dr. Hiro Osaki, Mr. Moritaka Kimura, Mr. Hiromitsu Kuboki, Dr. Hiroshi Takeuchi, Dr. Hitoshi Kiuchi, Mr. Jun Amagai, Mr. Shin'ichi Hama, Ms. Yuko Hanado, Mr. Hiroshi Kuroiwa, Dr. Hiroshi Takaba, Dr. Takahiro Iwata, Dr. Taizoh Yoshino, and Dr. Fujinobu Takahashi, inspired and encouraged to complete the thesis. The developments of the real-time VLBI system realized in the KSP and the K5 VLBI system are also the cooperative work of these members in the CRL. Members of the NTT Laboratories led by Dr. Hisao Uose supported the KSP and following international e-VLBI activities by establishing the high speed research networks. Dr. Alan R. Whitney, Dr. Kevin A. Dudgeon, Dr. Michael A. Titus, Dr. David Lapsley and other colleagues at Haystack Observatory, Massachusetts Institute of Technology and Dr.

Masaki Hirabaru at CRL collaborated with us for e-VLBI efforts between Kashima and Westford VLBI stations. Internet2 for the Abilene network, NTT Laboratories for GALAXY network, and National Institute for Informatics for Super-SINET network provided the high speed network link between Kashima and Westford VLBI stations. Some of the software routines used in the work of the thesis have been developed by Meteorological Research Institute, Goddard Space Flight Center of National Aeronautics and Space Administration and by Prof. Thomas A. Herring of Massachusetts Institute of Technology. Apart from the specific items listed above, I have learned a lot from Prof. Akira Ueda, Dr. Ojars J. Sovers, Dr. John D. Anderson, Dr. Arthur E. Niell, Dr. David L. Jauncey, and many other teachers and distinguished researchers who I have met and worked with. They have influenced me not only with their wide and deep knowledge but also with their sincere attitudes and philosophies.

I would like to take this opportunity to thank CRL which has been allowing me to continue the research work at KSRC. I feel the research environment and atmosphere at KSRC have been ideal for me to continue my research. I would also like to thank National Astronomical Observatory and the Graduate University for Advanced Studies for providing the opportunity to submit the thesis for evaluation. Lastly, and most of all, I would like to thank my wife Atsuko, two sons Rio and Syuho, father and mother for their generous supports and encouragements.

I feel it is truly impossible to express my gratitude and appreciation in words alone. I hope the thesis itself remains to express and symbolize my deep appreciation towards many individuals who supported to complete the thesis.

Abstract

In this thesis, we will describe our system developments to realize real-time and near-real-time Very Long Baseline Interferometry observations and data processing. In contrast with the conventional tape based systems, the received radio signals at the observing sites are not recorded to magnetic tapes, but are transferred electrically to a correlation processing site either directly or after buffering the data on computer hard disks. We have successfully demonstrated that the all necessary procedures in the Very Long Baseline Interferometry can be fully automated and the frequency of the observations could be dramatically increased without increasing the operation costs and operational requirements. By using the developed system, we have also demonstrated their use for monitoring precise position of the observing sites, flux densities of the celestial compact radio sources, and the Earth's orientation. Especially, measurements of the Earth Orientation Parameters are the most important role of the geodetic Very Long Baseline Interferometry at present, and the system developments described in this thesis are expected to improve the prediction accuracy and the frequency of measurements of the Earth Orientation Parameters.

Contents

Acknowledgements.....	i
Abstract.....	iii
Contents	iv
List of Figures	vi
List of Tables	x
Chapter 1 Introduction.....	1
Chapter 2 Observing Systems	6
2.1 KSP VLBI Observation System	6
2.1.1 Purposes of the KSP	6
2.1.2 Antenna and Receiving Systems	9
2.1.3 Data Acquisition System	11
2.1.4 Observation Control and Monitoring Systems	13
2.1.5 Central Control Systems	14
2.1.6 Computer Network System	15
2.1.7 Redundant System Design Concepts	17
2.1.8 Optimized Observation Time	18
2.1.9 Optimized Channel Frequency Assignments	22
2.1.10 Automated VLBI Observations	22
2.1.11 Regular Observations	24
2.2 K5 VLBI Observation System	25
2.2.1 Purposes to Develop K5 VLBI System	25
2.2.2 Developments of the System	28
Chapter 3 Data Processing and Analysis Systems	31
3.1 KSP Data Processing System	31

3.1.1 Cross Correlation Processing	31
3.1.2 Initial Data Analysis	32
3.1.3 Updating Data Analysis Results	36
3.1.4 Discussions	37
3.2 K5 Data Processing System	38
3.2.1 K5 Software Correlator Programs	38
3.2.2 Test Experiment with Kashima-Koganei Baseline	42
3.2.3 Test Experiment with Multiple Baselines	44
Chapter 4 Motion of the Observing Sites	47
4.1 Daily and Sub-daily Monitoring of Site Motions in the KSP	47
4.2 Wide Area Deformation Due to Volcanic Activities	57
Chapter 5 Flux Density Variation of Radio Sources	65
5.1 Background	65
5.2 Observations	67
5.3 Flux Density Estimation Method	69
5.4 Results and Discussions	74
Chapter 6 Variation of EOP	92
6.1 Background	92
6.2 Kashima-Westford Experiments	95
6.3 Discussions	99
Chapter 7 Conclusions.....	102
References	104
List of Publications.....	111

List of Figures

2.1	Geographical locations of the four observation stations in the KSP space geodetic network. Baseline lengths range from 35 km to 135 km.	7
2.2	The 11-m antenna system at Kashima.	9
2.3	VLBI observation racks in the observation control room adjacent to the 11-m antenna at Tateyama. The rack on the left is for an antenna control unit and a video monitor system for the antenna. The second rack from the left is for controlling and monitoring the receiver. The third rack from the left is for analog unit of the backend system. The tape changing unit for the digital mass storage is located right of these three racks. The next right rack is the ATM data transfer unit for real-time VLBI data transfer.	12
2.4	Schematic diagram of the exchange of data between various equipments and the observation control workstation or the monitoring workstation.	13
2.5	Configurations of the wide area computer network system for the entire network of the KSP VLBI network. The dial-up network line between Miura and Tateyama stations becomes active when one of the other three networks happens to be unavailable. The high-speed (2.4 Gbps) ATM network lines used to transfer observed data in the real-time VLBI mode are not used for the communications between computer systems and are not shown here.	16
2.6	Data synchronization time for different observation modes and different observation data rates.	21
2.7	Three generations of the VLBI systems developed by CRL.	27
2.8	Concept of the K5 VLBI system.	27
2.9	Versatile Scientific Sampling Processor (VSSP).	28
2.10	The main board (left) and the auxiliary board (right) of the IP-VLBI board. Two boards are connected by the cable attached to the main board in the picture.	29
3.1	Tape-based KSP correlator system.	31
3.2	Schematic data flow and block diagram of the automated VLBI data analysis.	34

3.3	Offsets of the three EOP values published in the IERS Bulletin-A from the final values appeared in the IERS Bulletin-B in the period between January 1996 and August 1997.	35
3.4	A schematic diagram of the server and client mechanism developed for the distributed cross correlation processing.	40
3.5	A WWW browser screen for monitoring distributed processing status.	41
3.6	Difference of (a) group delay and (b) delay rate obtained from K4 and K5 systems. Horizontal axis is the time of the scan in hours from the beginning of the session while the vertical axis is the difference of group delay and delay rate. The error bars are one-sigma errors evaluated from $(s_{K4}^2 + s_{K5}^2)^{1/2}$ where s_{K4}^2 and s_{K5}^2 are standard deviations of the data estimated from K4 and K5 systems, respectively.	43
4.1	Length of the baseline between Kashima and Koganei stations estimated from the KSP VLBI experiments. Estimated uncertainties in the estimates are shown by the one-sigma formal error. The epoch value of the baseline length L_0 and the rate of change were estimated from the data before June 2000 by the least squares estimation and L_0 was subtracted from each data.	48
4.2	Length of the baseline between Kashima and Miura stations.	49
4.3	Length of the baseline between Kashima and Tateyama stations.	50
4.4	Length of the baseline between Koganei and Miura stations.	51
4.5	Length of the baseline between Koganei and Tateyama stations.	52
4.6	Length of the baseline between Miura and Tateyama.	53
4.7	Site position of the Koganei station in the local cartesian coordinate system. Estimated uncertainties in the estimates are shown by the one-sigma formal error. A straight line in each is showing the best-fit line to the estimated site position before June 2000.	54
4.8	Site position of the Miura station in the local cartesian coordinate system.	55
4.9	Site position of the Tateyama station in the local cartesian coordinate system.	56
4.10	Baseline length between Kashima and Tateyama stations for the period between June 1999 and August 2001. Dotted straight lines are the linear fits for two periods before June 1, 2000 and after September 1, 2000.	58

4.11	Displacement of Tateyama station in the horizontal plane. Dotted straight lines are the linear fits for two periods before June 1, 2000 and after September 1, 2000.	59
4.12	Displacement of Miura station in the horizontal plane.	60
4.13	Horizontal site velocities of four VLBI stations of the KSP VLBI Network at Kashima, Koganei, Miura, and Tateyama with respect to the North American Plate (left). Plate motion velocities around Japan with respect to the North American Plate using Nuvel-1A and Seno plate motion models (right).	62
4.14	Site displacements at Tateyama and Miura sites observed during the three months from the end of June 2000 detected by the KSP VLBI network and a model which can explain the observed crustal deformation.	63
4.15	A proposed geophysical model with a dyke and a strike slip fault which can explain the observed crustal deformation. The dyke is assumed to be 5m thick with a depth of 3km and dimensions of 20km (horizontal) and 12km (vertical). The fault is assumed to have a slip of 4m with a depth of 3km and dimensions of 5.9km (horizontal) and 10km (vertical). The model parameters were taken from a model proposed by the group of Nagoya University. The displacements were calculated by the software MICAP-G developed by the Meteorological Research Institute.	64
5.1	Geographical locations of the four observation sites in the KSP VLBI network observation sites. The names of the sites are Kashima, Koganei, Miura, and Tateyama.	71
5.2	Relationship between correlated amplitudes ρ and elevation angles θ shown for three radio sources, e.g., 3C273B (circles), 3C279 (triangles), and 1334-127 (squares). The elevation angles were evaluated by the mean of two elevation angles at two stations. The correlation amplitudes are the results obtained with the baseline between observation sites at Kashima and Miura in X band during an experiment performed for ~22.3 hours from 0200 UT on March 22, 2000. The vertical axis is $(1/\rho)-1$ and the horizontal axis is $1/\sin\theta$. The three dotted lines are the least squares fits to the observed data.	73
5.3	Flux densities of 3C273B and 2134+004 at X band and S band estimated by using (5.4) and (5.5). The correlated amplitudes obtained with the baseline between Kashima and Miura stations were used for the estimation. The error bars are $\pm 1\sigma$ uncertainties evaluated by the least squares estimation.	74
5.4	Flux densities of the 0059+581 at X band and S band.	77

5.5	Flux densities of the 3C84 at X band and S band.	78
5.6	Flux densities of the 0420-014 at X band and S band.	79
5.7	Flux densities of the 0552+398 at X band and S band.	80
5.8	Flux densities of the 0727-115 at X band and S band.	81
5.9	Flux densities of the 4C39.25 at X band and S band.	82
5.10	Flux densities of the 3C273B at X band and S band.	83
5.11	Flux densities of the 3C279 at X band and S band.	84
5.12	Flux densities of the 1308+326 at X band and S band.	85
5.13	Flux densities of the 1334-127 at X band and S band.	86
5.14	Flux densities of the 3C345 at X band and S band.	87
5.15	Flux densities of the NRAO530 at X band and S band.	88
5.16	Flux densities of the 1921-293 at X band and S band.	89
5.17	Flux densities of the 2145+067 at X band and S band.	90
5.18	Flux densities of the 3C454.3 at X band and S band.	91
6.1	Estimated values of δ_x , δ_y , and UT1-UTC estimated from routine KSP VLBI sessions. Solid curve lines are the EOP97C04 data series maintained by the IERS.	93
6.2	Deviation of the estimated UT1-UTC from the EOP97C04 values provided by IERS.	94
6.3	Configuration of the high speed network in Japan.	96
6.4	Configuration of the high speed network in the United States.	96

List of Tables

2.1	System Equivalent Flux Density (SEFD) of four VLBI antennas.	10
2.2	Optimized observation time (seconds).	20
2.3	Frequency assignments.	22
2.4	Ratio (%) of successful experiments to the total number of days in a month summarized for every month from September 1996. An experiment was considered successful for a specific station if the station coordinate was estimated or used as a reference in the data analysis.	24
2.5	Specifications of the IP-VLBI board.	29
3.1	Comparison of baseline lengths estimated from the data obtained with K4 and K5 systems.	44
3.2	Comparison of baseline lengths estimated from the data obtained with K4 and K5 systems.	45
3.3	Estimated coordinates of the Yamaguchi 32-m VLBI station.	45
4.1	Baseline lengths L_0 on the epoch of January 1, 2000 and their rates of change estimated for six baselines by the least squares estimation.	57
5.1	Compact Radio Sources Observed by the KSP VLBI Network in Regular Geodetic VLBI Experiments.	68
6.1	Statistic characteristics of the formal errors of the estimated EOP.	95
6.2	Estimated value of UT1-UTC from the Kashima-Westford e-VLBI session and reported values from IERS Bulletin B 183, May 2, 2003.	98
6.3	Time sequence from the observations to the data analysis. Time is in Japanese Standard Time and start from 22:00 on June 30.	98

Chapter 1 Introduction

The developments of Very Long Baseline Interferometry (VLBI) technique began in late 1960's [Clark *et al.*, 1985] and the technique has been extensively used in various fields of geodynamics. The research and developments of VLBI technology began in the Communications Research Laboratory in the middle 1970s. CRL (formally Radio Research Laboratory until 1988) had developed the K-3 VLBI system in the beginning of 1980s [Kunimori *et al.*, 1993]. Using the initially developed observation systems, the 26-m and 34-m antennas at Kashima Space Research Center (KSRC) of CRL have participated in global and regional VLBI sessions conducted by many organizations including CRL itself. Some of the international VLBI sessions conducted by the National Aeronautics and Space Administration (NASA) and all of the regional VLBI sessions conducted by CRL were processed by the VLBI correlator system developed at KSRC and the VLBI observations were analyzed to obtain valuable results. CRL became one of the VLBI Technical Development Centers of the International Earth Rotation Service[†] (IERS) in 1990 and has been acting as one of the leading research institutes which are responsible for the developments of VLBI observations and data analyses technologies. When the International VLBI Service for Geodesy and Astrometry (IVS) was established on 1 March 1999, CRL was designated as the Technology Development Center and also as other functions of the IVS, i.e. the Network Stations, the Associate Special Analysis Center, the Correlator Center, and the Data Center. These multiple designations can be considered as the consequences of large expectations towards CRL and its responsibilities in the research and developments for VLBI technique.

The initial results of global geodetic VLBI experiments verified the steady motions of tectonic plates that were predicted by the plate-motion hypothesis [Herring *et al.*, 1986; Heki *et al.*, 1987]. The VLBI technique thus played an important role for the progress of studies for the plate tectonics. As measurement accuracy was improved and more results were accumulated, inconsistencies between the predictions and contemporary site motions actually measured by the VLBI technique gradually became

[†] The name of the organization was changed to International Earth Rotation and Reference Systems Service in April 2003.

apparent. The first of such inconsistencies was an anomalous motion of the Kashima VLBI station north-westward with respect to the stable interior of the Eurasian plate and North American plate [*Heki et al.*, 1990]. Then the Seshan VLBI station near Shanghai was found to show eastward motion with respect to the stable interior of the Eurasian plate [*Heki and Koyama*, 1993]. Further detailed investigations also led to the conclusion that the Minami-Torishima (Marcus) and Kwajalein VLBI stations on the Pacific plate have excess westward velocities in addition to that due to the rigid plate motion [*Koyama et al.*, 1994; *Koyama*, 1996]. The discrepancies between the contemporary site motions and the predictions of the plate-motion model are contributing to our understanding of the complicated dynamics of plate tectonics [*Ryan et al.*, 1993]. Another powerful aspect of the geodetic VLBI is its ability to determine the precise earth's orientation parameters (EOP) [*Eubanks*, 1993] and the construction of the celestial reference frame [*Ma and Feissel*, 1997; *Ma et al.*, 1998]. Although data derived from the Global Positioning System (GPS) and Satellite Laser Ranging (SLR) observations can now be used to estimate the earth's pole position and the length of a day, VLBI is still the most accurate technique for determining nutation parameters and the difference between the coordinated universal time (UTC) and the time defined by the earth's rotation (UT1) [*McCarthy*, 1993]. The construction of the current celestial reference frame is relying on the data obtained by global VLBI observations.

In addition to the geodetic and astrometric applications just mentioned above, VLBI is also a very powerful and irreplaceable instrument for radio astronomy. With its unprecedented angular resolution, global scale VLBI can reveal fine structures of celestial radio sources which can not be investigated by other observational means [e.g. *Zensus*, 1997]. By using a radio telescope on orbit and other radio telescopes on the ground, the angular resolution was further improved and many radio sources have been investigated [*Hirabayashi et al.*, 2000]. It is a very interesting fact that the same hardware and software systems can be used for investigations in variety of research fields including Geodesy, Geophysics, Astrometry, and Astronomy.

Most of these remarkable achievements just summarized have been achieved by using the conventional tape-based VLBI technique, i.e. magnetic tape recorders are used to record observed data at the antenna sites and then shipped to the correlator site for cross correlation processing. The conventional tape-based VLBI, however, has a few disadvantages which can be improved. Firstly, the tape changes at the observation sites

and at the correlator site prevent fully automated operations. Recorded tapes at the observing sites also have to be packed and then shipped to the correlator site. These operations require considerable human resources and are obstacles for frequent observations. Secondly, the time to obtain results from VLBI observations is inevitably long. It is especially true when many radio telescopes in many countries are used in an observing session. At present, it can take more than two weeks to process all the data obtained from an international geodetic VLBI observing session. Shortening the time gap required to process global VLBI data is one of the current short-term technical targets wished by IVS [*Schuh et al.*, 2002]. Also, because of its nature, a problem at an observing site might not be noticed for more than two weeks since some of the problems can not be found until the data are actually processed at the correlator site. Lastly, the sensitivity and the number of baselines are limited by the capacity of the data recorders and the capability of the hardware correlator system. The minimum detectable limit of the VLBI observation is inversely proportional to the square root of the bandwidth of the observing signal and hence the data rate of the data recorders. The data rate of the data recorders with magnetic tapes have been gradually improved since the beginning of the VLBI observations but it is still limited to the current 1024 Mbps. The processing capacity of the correlator systems also have been expanded, but it is still limiting the number of radio telescopes to be included in a VLBI observing session.

All of these disadvantages of the tape-based VLBI system can be overcome by the so-called e-VLBI technique. In the e-VLBI system, the observed data are transferred to the correlator site by using high speed research network or any other high speed data transfer methods like a communication satellite link. The transferred data can then be correlated by hardware correlator systems or by software correlation programs. In the latter case, the correlation processing can be performed by multiple computer systems by using distributed computing and the processing capacity of the correlation processing can be freely expanded. In the e-VLBI system, the observed data can be correlated simultaneously with the observations, or the data can be correlated after the observations. The former case is called as real-time VLBI, whereas the latter case is called as near-real-time VLBI. In both cases, the data can be correlated much faster than in the case of tape-based VLBI, and all the procedures from the preparations of the VLBI observations to the end of data analysis can be automated.

The real-time VLBI and near-real-time VLBI are not very new form of concept.

In 1977, the first real-time VLBI observations were performed between 46-m antenna station of the Algonquin Radio Observatory (ARO) in Ontario, Canada, and 43-m antenna station of National Radio Astronomical Observatory (NRAO) at Green Bank, West Virginia, USA [Yen *et al.*, 1977]. During the observations, 20 Mbps of data obtained at the Green Bank station were transferred by using a joint communication satellite between Canada and USA called Hermes to the real-time correlation system at ARO. In early 1980's, Jet Propulsion Laboratory established the near-real-time VLBI system connecting three Deep Space Network sites at Goldstone (California, USA), Madrid (Spain), and Canberra (Australia) [Eubanks *et al.*, 1982]. By switching the observation frequency, three frequencies were observed both in S-band and X-band at the data rate of 500 kHz. The observed data were transferred by using a satellite communication link and the correlated results were processed for bandwidth synthesis to obtain precise group delay observables. At Radio Research Laboratory (now CRL), real-time VLBI observation and correlation system was developed and observations were made by using two VLBI stations at Kashima and Hiraio by using a microwave link [Kawano *et al.*, 1982]. The baseline length was 47 km and 5 frequency channels with 2 MHz of bandwidth were observed sequentially, and the correlated data were processed for bandwidth synthesis. After these remarkable pioneering works, next progress of the real-time and near-real-time VLBI technique did not happen until high speed communication networks became available by using fiber optical cables.

This thesis deals with the new efforts to develop real-time VLBI and near-real-time VLBI systems and their use for the new scientific challenges. In Chapter 2, we will describe about developments of two VLBI observation systems. One is the real-time VLBI observation system developed for the Key Stone Project (KSP). For the system, high speed dedicated fiber optical cables at the maximum data rate of 2.4 Gbps using Asynchronous Transfer Mode (ATM) were build. With the KSP VLBI system, various possibilities of the real-time VLBI were demonstrated [Koyama *et al.*, 1999]. Continuous or quite frequent VLBI observations without human operations from the observations to the data processing were made possible. Because any problem at observing stations can be detected real-time during the correlation processing, the problem can be promptly fixed and it resulted the quite high reliability of the VLBI system as a whole. The second system is the K5 VLBI observation system [Koyama *et al.*, 2003]. After the developments of the KSP VLBI system, the developments of the

K5 VLBI system began to realize near-real-time VLBI observations with international baselines by using high speed research networks based on the Internet Protocol (IP). In contrast to the costly dedicated ATM network lines, the IP networks are widely used at all over the world and the possibility to connect the VLBI observing sites in many countries is considered to be much higher than with the ATM networks. In Chapter 3, we will then describe about the developments of the KSP data processing system and the K5 data processing system. In the KSP data processing system, all the processes from the cross correlation processing to the data analysis were fully automated. Before the KSP data processing system was developed, geodetic VLBI data analysis required the analysts a lot of experiences and understanding of every aspects of VLBI technique. In addition, since the human factor of the analysts can be excluded by automating the whole procedures, it is expected that the objectivity of the estimated results will be improved. In the developments of the K5 data processing system, software correlation programs have been developed and the scheme of the distributed correlation processing has been demonstrated. In the following three Chapters from 4 to 6, we will discuss the actual applications of the real-time VLBI system and the near-real-time VLBI system. In Chapter 4, we will present results of site position monitoring by the real-time VLBI system. In Chapter 5, we will discuss the possible use of the real-time VLBI system to monitor flux densities of the celestial radio sources [Koyama *et al.*, 2001]. And finally, in Chapter 6, we will demonstrate to use real-time VLBI and near-real-time VLBI system to estimate EOP independently from any other *a-priori* information [Koyama *et al.*, 1999; Koyama *et al.*, 2003]. In the last Chapter 7, we will present conclusion of this thesis.

Chapter 2 Observing Systems

2.1 KSP VLBI Observation System

2.1.1 Purposes of the KSP

VLBI, SLR, and GPS are precise geodetic measurement methods and are often called space geodetic techniques [Anderson and Cazenave, 1986]. Since these three techniques have different characteristics in many aspects, collocation of observing facilities of the three techniques had been an idea of great interest in many years. By placing different techniques close together, one can compare the different and independently obtained results with each other. Such a comparison is very important to improve reliability of these measurement methods. Since CRL had been conducting research and technical developments in all of these three techniques, a new research project to establish a compact space geodetic network using all three of these space geodetic techniques started in 1994 [Yoshino, 1999]. Observation facilities using them were placed at four sites in the Kanto area of Japan, i.e. Koganei (Tokyo), Kashima (Ibaraki), Miura (Kanagawa) and Tateyama (Chiba). Figure 2.1 shows the geographical location of these four sites. The project was called the Key Stone Project (KSP) after an ancient mythological story originated at the city of Kashima. The relative positions of monuments at each site were precisely measured with local ground survey measurements [Xia *et al.*, 1999]. The network is relatively small considering that VLBI and other space geodetic techniques often use inter-continental baselines sometimes exceeding 10000 km. But the smallness of the network can be regarded as an advantage since many technical challenges can be easily tested or applied. The network is also very unique because three different space geodetic techniques were collocated and it can be considered as a technical test-bed for precise geodetic research.

A major motivation of the KSP network was to perform precise space geodetic measurements as frequently as possible and to investigate the dynamic behavior of a relatively small region around Tokyo associated with seismic activities and deformation of the lithosphere in the area [Kurihara *et al.*, 1996]. The area around Tokyo is seismically active and shows a complicated distribution of deformation due to plate

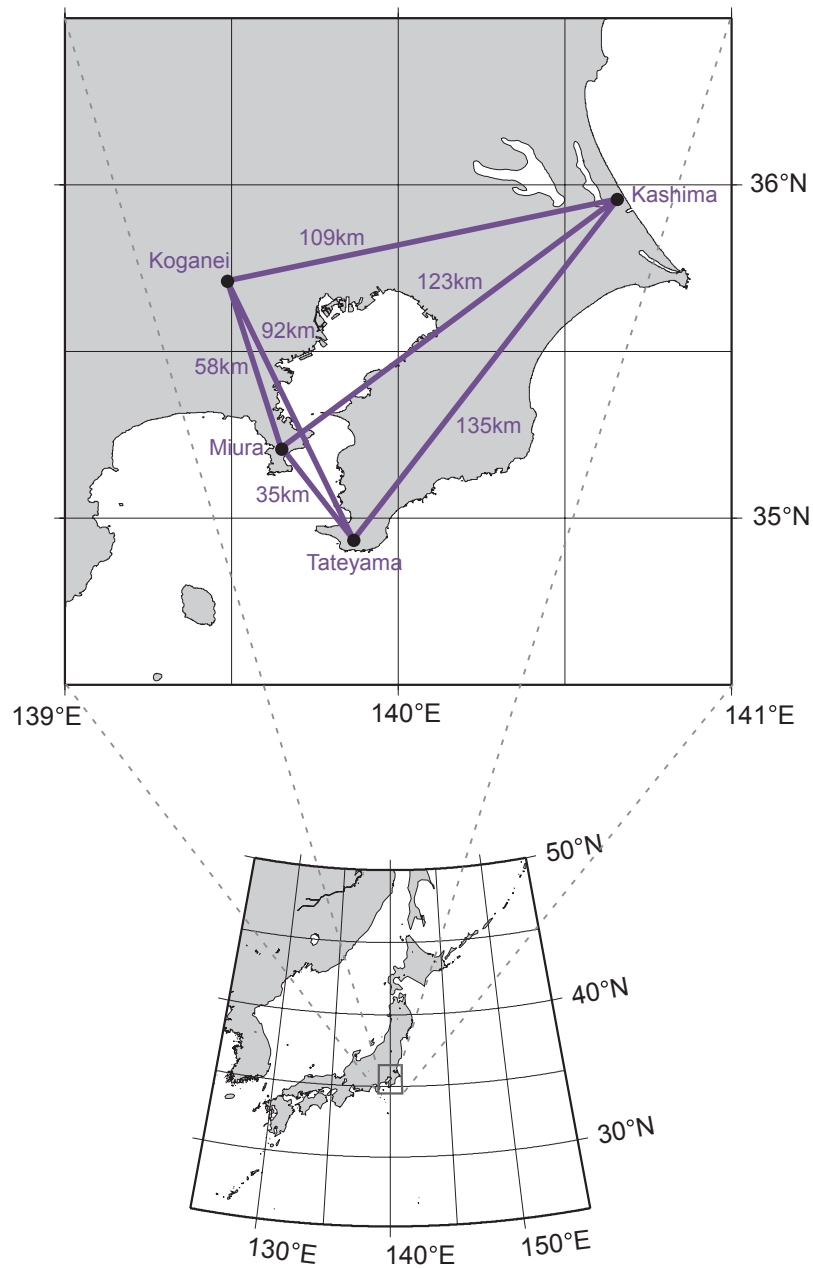


Figure 2.1 Geographical locations of the four observation stations in the KSP space geodetic network. Baseline lengths range from 35 km to 135 km.

tectonic motions of three interacting plates. Continuous monitoring of the region was therefore expected to provide valuable information about the geophysical processes occurring under the region. To achieve this objective, measurements had to be performed as frequently as possible and the results were required to be made available with minimum delay. Before the KSP, VLBI experiments used to take very long time to

coordinate and to process the observed data. In the case of Western Pacific VLBI Network experiments [*Koyama et al.*, 1994], the total time required from preparation through data correlation and analysis was usually more than a month. The KSP VLBI observation and data processing systems were designed to achieve automated operation throughout the entire process. These systems have enabled frequent and regular VLBI observations to be made and reports of analyzed results to be published quickly. This section mainly describes the observation system of the KSP VLBI network, focusing on various features providing automation and robustness.

By the year 1995, observation facilities at all of four sites of the KSP network had been constructed. At each site, an 11-m antenna for VLBI, a 75-cm telescope for SLR, and a GPS receiver had been placed close to each other. The KSP VLBI observation system was designed to improve measurement accuracy and sensitivity. The sensitivity of a VLBI observation system is proportional to the square root of the data rate. The data rate was increased from 64 Mbps (bits per second) which was possible with the previous system to 256 Mbps for the KSP VLBI system. The KSP VLBI system was the only VLBI observation network making observations at 256 Mbps on a regular basis at the time of its operation. The better sensitivity realized by the greater data rate helped to improve accuracy of the VLBI measurements since it enabled to increase the number of observations that can be made in an experiment. The frequency bandwidth is also a factor which determines the precision of the measurements. The frequency bandwidths of the KSP VLBI receivers are 900 MHz for the X-band and 400 MHz for the S-band. Assigning 10 frequency channels to the X-band observations made it possible to effectively expand the equivalent frequency bandwidth obtained from bandwidth synthesis processing. The achieved uncertainty of the baseline lengths from 24 hours observations was about 1 mm in the sense of formal error and about 2 mm in the sense of repeatability [*Kondo et al.*, 1998].

The other unique points of the KSP VLBI system were its automated features. The observation system and the data analysis system had been designed so that no human operations are needed to conduct experiments or to obtain results. Eliminating the need for human operations made more frequent experiments possible and had reduced the time needed to produce results. Experiments, 24 hours of observations each, were performed every two days. The signals observed at each station were transferred through high speed digital communication optical fibers to a correlator at the Koganei



Figure 2.2 The 11-m antenna system at Kashima.

station and were processed simultaneously during the observations. After all the observations completed, data analysis procedures were performed automatically and the results were made available within a half hour. Before the KSP VLBI system was developed, VLBI observations required highly trained personnel at all sites and the data processing and analysis required a time consuming and complicated procedures, but both of these requirements were eliminated in the KSP VLBI system.

2.1.2 Antenna and Receiving Systems

Figure 2.2 is a picture of the 11-m antenna system for VLBI observations at Kashima. The antenna systems which were constructed at all four sites were identical in design except for the heights of the antenna pedestals. The antennas were fully steerable Cassegrainian systems equipped with S-band (2000-2500 MHz) and X-band (7700-8600 MHz) receivers. Their pointing direction could be moved at a slewing rates of 3 degree per second for both azimuth and elevation angles. Table 2.1 shows the

Table 2.1 System Equivalent Flux Density (SEFD) of four VLBI antennas.

Station	SEFD (X-band)	SEFD (S-band)
Koganei	6180 Jy	3030 Jy
Kashima	4500 Jy	3320 Jy
Miura	4990 Jy	3220 Jy
Tateyama	5130 Jy	3600 Jy
34-m at Kashima	316 Jy	343 Jy

measured System Equivalent Flux Densities (SEFDs) of the receiving systems. SEFD is the flux density of a hypothetical radio source that would generate equivalent power in the receiver output to the power of the system noise; it is often used to measure overall performance of a receiver system since this value is related with a signal-to-noise ratio by an equation which will be discussed later. Although the basic designs of the receiving systems at the four stations were the same, their actual performances varied slightly. The SEFD values for the 34-m antenna at Kashima are also shown in the table for comparison. The temperature in the receiver cabinet located beneath the main reflector was maintained within 2 degrees of nominal to maintain phase stability of the signal path. A hydrogen maser system at each station was also located in a temperature controlled chamber to achieve better frequency stability.

The S-band signal was converted to the Intermediate-Frequency (IF) band between 500 MHz and 1000 MHz using a local frequency signal of 3000 MHz. The X-band signal was split and converted using local frequency signals of 7200 MHz and 7600 MHz into two IF bands between 500 MHz and 1000MHz, which correspond to 7700-8200 MHz and 8100-8600 MHz of the original signal. Three IF band signals, one from the S-band and two from the X-band, were again converted using newly developed video converter units. Since the lower side band (LSB) of the local frequency signal was used for the IF band, the LSB outputs of the video converter units were used for the S-band observations.

2.1.3 Data Acquisition System

There were two main observation modes in the KSP VLBI system: a tape-based VLBI mode and a real-time VLBI mode. In the former, the radio signals received at each antenna were digitized and recorded on D-1 standard magnetic cassette tapes using a K-4 data recorder unit whose interface unit was designed for the KSP [Kiuchi *et al.*, 1996a]. The recorded tapes were transported after each experiment to Koganei station where a VLBI correlator system was located. In this case, observation data were correlated the day after an experiment and the final analysis results became available within two days after each experiment was performed. A minimum number of simple human operations were required at three remote stations to replace tapes and transport recorded tapes to Koganei station. These simple operations were performed by a local contractor at each site. The amount of effort required was, however, much less than for conventional geodetic VLBI experiments. Once the observation tapes have been set in the digital mass storage tape changing unit, the required ones are identified by bar-code labels and are loaded or unloaded to and from the data recorder unit automatically. At Koganei correlation station, additional human operations were required to organize the observation tapes. But these are also few in number and simple. The operations at the Koganei correlation station were to ship and receive observation tapes, place them in tape changers for observations and data correlation, and then start the VLBI data correlation processing. Correlation processing and data analysis were done without human interaction throughout the all procedures. Figure 2.3 shows antenna control and data acquisition racks at one of the observing stations.

In the real-time VLBI mode, on the other hand, after the radio signals received at each antenna were digitized and formatted by the data interface unit in the same manner as in the tape-based VLBI mode, the formatted data were then transmitted to a real-time VLBI correlator located at Koganei station. Since the amount of data was huge, it was transferred by an optical fiber digital communication line using ATM. The four stations were connected by newly developed optical fibers that can transfer digital data at up to 2.4 Gbps. The design of the correlator system used for the real-time VLBI mode was identical with the correlator system used for the tape-based VLBI data processing. The ATM data transmitter and receiver interfaces were the key technical components developed for the real-time VLBI system of the KSP [Kiuchi *et al.*, 1996b]. In the case

of real-time VLBI mode, no human operations were required at either the remote stations or the Koganei data correlation station. All the processes required during observations and data analysis were fully automated. The analyzed results became available immediately after the final observation of an experiment. Recent developments in the high speed data communication technology were remarkable. Maximum speed capability is glowing very fast and soon the real-time VLBI is expected to become realistic for much longer baselines. The real-time VLBI technique has a potential to expand observation bandwidth and to improve the sensitivity which has been limited by the speed limitation of the data recording technology.

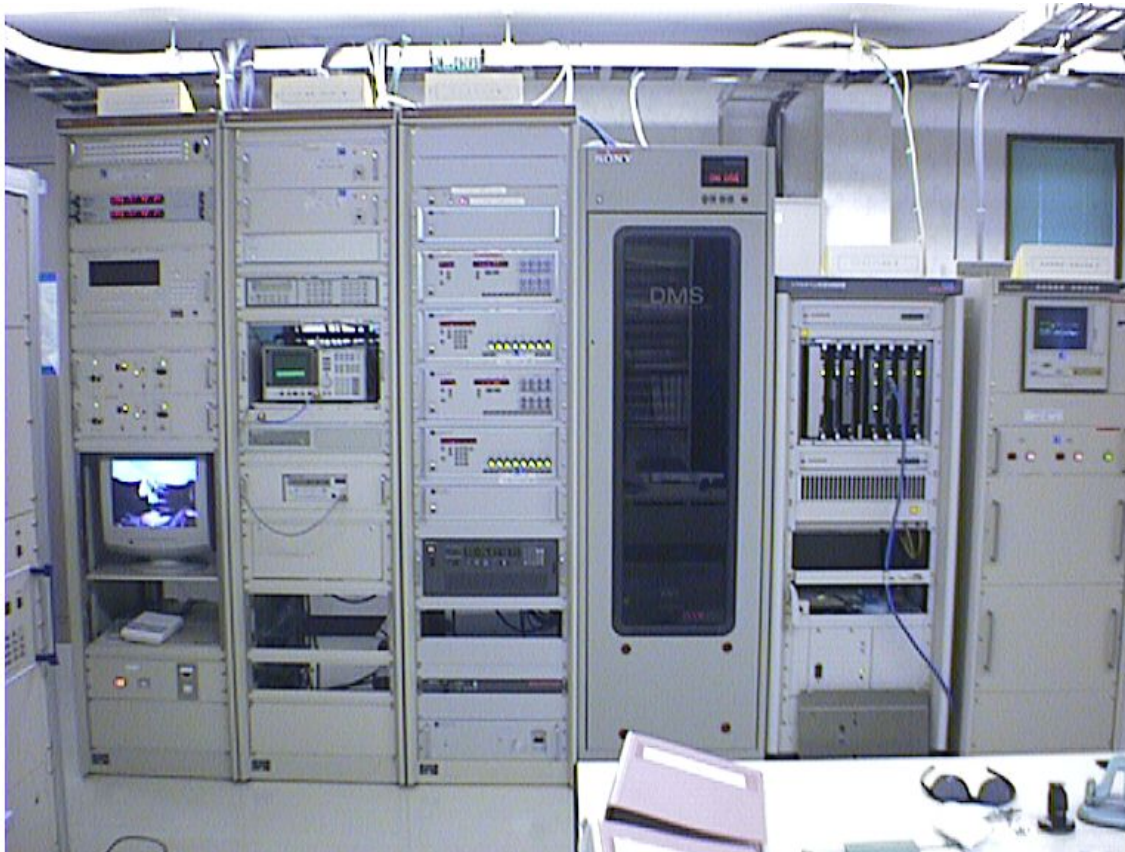


Figure 2.3 VLBI observation racks in the observation control room adjacent to the 11-m antenna at Tateyama. The rack on the left is for an antenna control unit and a video monitor system for the antenna. The second rack from the left is for controlling and monitoring the receiver. The third rack from the left is for analog unit of the backend system. The tape changing unit for the digital mass storage is located right of these three racks. The next right rack is the ATM data transfer unit for real-time VLBI data transfer.

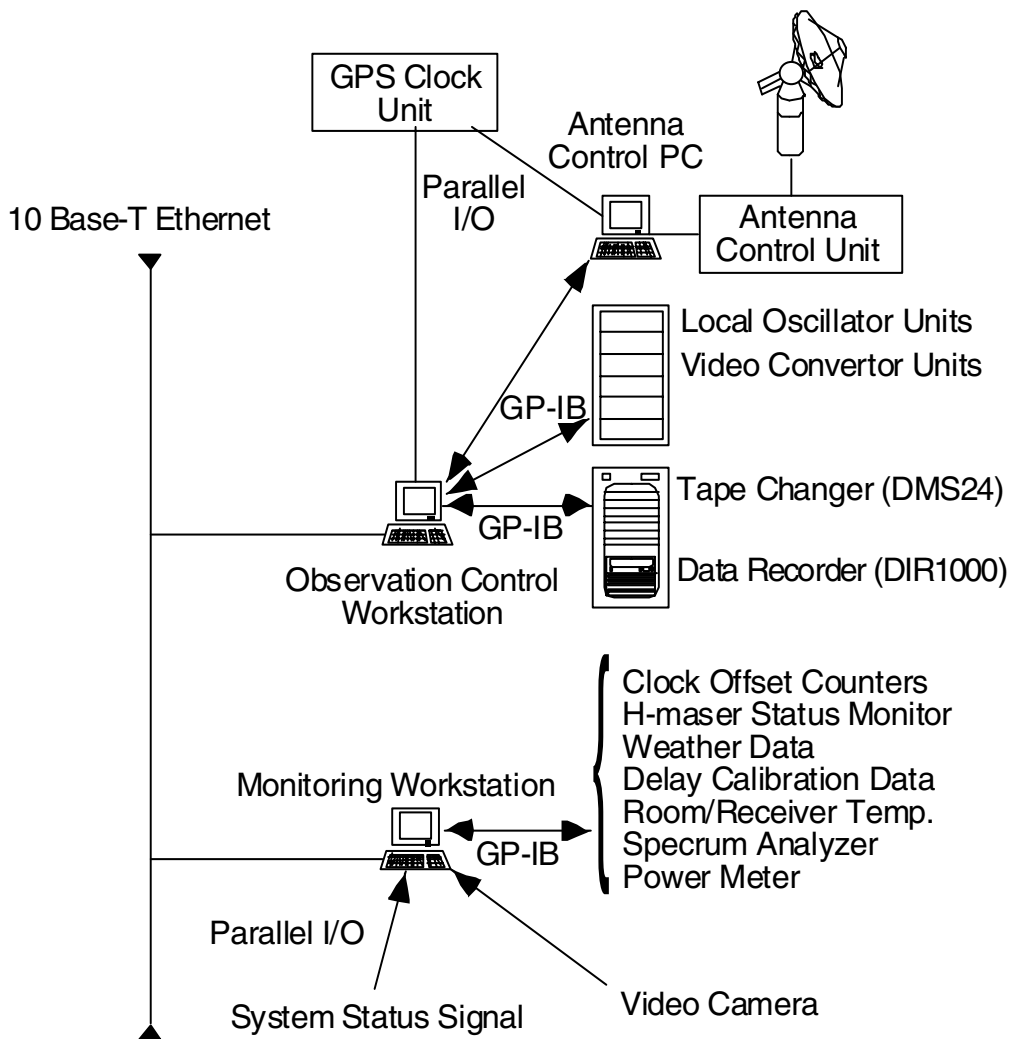


Figure 2.4 Schematic diagram of the exchange of data between various equipments and the observation control workstation or the monitoring workstation.

2.1.4 Observation Control and Monitoring Systems

At each station, two workstations and one PC system were used to perform all the automated tasks necessary for VLBI observations, as shown in Figure 2.4. The PC system, which was used to control tracking of the antenna system, is called antenna control PC. When it was given the right ascension and the declination of a celestial radio source, the antenna control PC calculates its azimuth and elevation angles and sends necessary commands to the antenna control unit, which actually controls the

motor servo systems of the 11-m antenna. The antenna control PC was connected to a Unix workstation called observation control workstation via a GPIB (General Purpose Interface Bus) communication interface. The observation control workstation provides right ascensions and declinations of target radio sources during a VLBI experiment according to an observation schedule file. Tape changing and data recording are also controlled by the observation control workstation in the tape-based VLBI mode of operations. The observation schedule file also specifies local frequencies and video-bandwidth of 16 observation channels, and necessary commands are sent from the observation control workstation to the data acquisition terminal via the GPIB communication bus to set up observation configurations at the beginning of each experimental session.

2.1.5 Central Control Systems

At Koganei and Kashima stations, there were additional Unix workstations called central control workstations. Their role was to organize observations performed by the observation control workstations at the four stations and to collect status and monitoring data from the monitoring workstations. The graphical user interface of the central control workstations was designed to be easy to use so that untrained operators can easily perform remote operations and various checks on the observation systems at remote sites. Observations at remote sites can be started, interrupted, and resumed after an interruption from the central control workstations. Receiving systems and data acquisition systems can be controlled remotely, and the results of the operations can be confirmed with video camera images over the computer network. Any problems detected by an observation control workstation or a monitoring workstation are reported to the central control workstations and such events are logged in a file and sent over the network to pre-registered e-mail addresses to notify the designated persons in charge that there is a problem. Observation programs on the observation control workstations are executed by commands from two central control workstations. These two commands are issued at different times with a certain arbitrarily-chosen interval between them. In the usual case, the first command starts the observations at all four sites, and the second command is ignored. However, if the first command fails to reach the observation control workstation at any station for some reason, then the second command becomes

effective and prevents the experiment from failing as a result of an unexpected situation.

After all the observations in an experiment completed, observation log files are transferred and merged with other data files obtained by monitoring workstation at each site. The merged log files are then used in the data correlation processing and when the database files are created. Before the experiment, the central control workstations perform check routines at all four stations to examine whether the observation tapes are ready. If any of the observation tapes are not properly set in the tape changer unit or have a problem, an e-mail message is sent to the responsible persons to inform them that the station is not ready for the observations. The tapes to be used in the experiment are specified in a master control file stored on each central control workstation. The central control workstations interpret the master control file to determine which stations will participate in the next experiment and which tapes should be used at each station. The master control file is updated every month automatically so that regular experiments can be done without human interaction. The master control file can also be modified at any time by an operator on a central control workstation in order to change the participating stations and tapes to be used. Every time the file is modified, the master control file is sent to the other central control workstation to ensure consistency between these files on the two central control workstations.

2.1.6 Computer Network System

At each station, a TCP/IP local area network over Ethernet connects the observation control workstation and the monitoring workstation; at Koganei and Kashima stations, it also connects the central control workstation. Other computers are connected to the same network to acquire data from a GPS receiver and a seismometer. In addition, at Koganei station, correlator units and additional workstations required for the correlation processing and data analysis are connected to the network. An intelligent network bridge is located between the segment for correlators and the segments for other computers to keep the huge amount of correlated data on one side.

All four VLBI stations were connected together by dedicated computer network lines. The configuration of the network system is shown in Figure 2.5. Three dedicated computer network lines connected Koganei to Miura, Koganei to Kashima, and Kashima to Tateyama. Since the data traffic on the computer network was not very

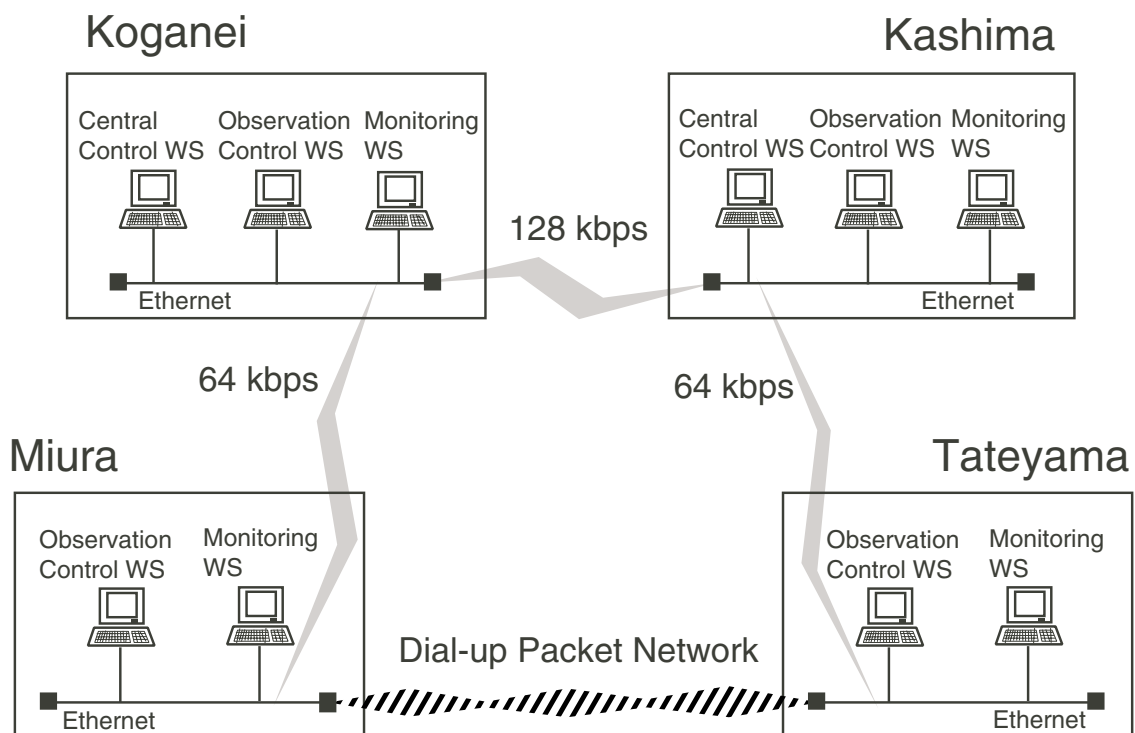


Figure 2.5 Configurations of the wide area computer network system for the entire network of the KSP VLBI network. The dial-up network line between Miura and Tateyama stations becomes active when one of the other three networks happens to be unavailable. The high-speed (2.4 Gbps) ATM network lines used to transfer observed data in the real-time VLBI mode are not used for the communications between computer systems and are not shown here.

high and there were no requirements for high-speed responses between the computer systems, 64 kbps was sufficient as the data capacity of the network system. However, the data rate between Kashima and Koganei was doubled to 128 kbps because most of the communications were done by two central control WS systems at Kashima and Koganei with other WS systems and therefore the data traffic on this segment is about twice as large as the other two segments. In addition to three dedicated computer network lines, Miura and Tateyama stations were connected by a dial-up packet line, which becomes active if one of the three dedicated lines becomes unavailable. This configuration ensures that each station is always reachable from any other station, so observations can be performed as usual unless two or more network lines fail at the same time.

The network was connected to the Internet through the data analysis workstation at Koganei. This workstation has two network interfaces: one was connected to the KSP network and the other was connected to the laboratory network, which was then connected to the public Internet. This workstation acts as a firewall system. Necessary connections between two network segments can be made through the workstation, but unauthorized access to the KSP network from the public Internet is prevented.

The antenna control PC and observation control workstation at each station had parallel data interfaces, which were connected to an Inter-Range Instrument Group (IRIG) time-code signal generator of a GPS receiver. The internal clock of these computer systems were synchronized to the coordinated universal time (UTC) provided by the GPS receiver every day during the observation preparation procedures. The precise time information maintained in the antenna control PC was necessary to point the antenna to the direction of a radio source accurately. The observation control workstation disseminates precise time information by Network Time Protocol (NTP) as a server. The monitoring workstations and central control workstations are configured as NTP clients and the internal clocks of these systems are always synchronized to the UTC.

2.1.7 Redundant System Design Concepts

Since the VLBI observation system of the KSP was intended to achieve automated operation as much as possible, it was designed with a redundant configuration to improve overall reliability. The network system described in the previous section was one example which had been designed with the redundant concept. Each observation control workstation is also accessible via a public telephone line using a modem, and observations can be controlled remotely even if the network connection to the station is unavailable.

The two central control workstation systems at Koganei and Kashima are identical and operate independently from each other. This dual operation guarantees that regular observations can be made at all stations even if one of the central control workstations malfunctions. The combination of redundant designs made the entire VLBI observation system robust against many possible irregularities. If any one station goes

down for any reason, the other three stations can still continue observations because they are accessible from at least one of the central control workstations via the dial-up packet network line. Some of the software components related to automated experiment management were also written with redundant design. For example, the observation schedule file is created two weeks before each experiment. This file contains all the information necessary to carry observations and correlation processing of an experiment. Especially, the sequence of radio sources to be observed can not be the same and the schedule file have to be made every time. But whether the file was actually created or not is checked again on the day of the experiment. If the file was not found, it is created at this time. In this way, the schedule file can be replaced anytime during the two weeks before the day of the experiment if a special experiment have to be coordinated, and on the other hand, the risk of the loss of the experiment because the schedule file was not created can be reduced considerably. This kind of redundancy is quite effective to improve the reliability of the automated observation system.

2.1.8 Optimized Observation Time

The KSP VLBI system used relatively small and fast slewing antennas. Each antenna was equipped with low-noise amplifiers for the X- and S-band frequencies that operate without a cryogenic system. Using non-cryogenic receivers reduces the amount of maintenance and the likelihood of system failure but increases the system noise temperature compared with using cryogenic ones. Both the small antenna aperture and the high system noise temperature contribute to reduce the sensitivity of the receiving system, so only strong radio sources had to be selected for the KSP VLBI experiments. To obtain sufficient signal-to-noise ratio (SNR) R within a reasonable correlation integration time T , the necessary flux density F_s (Jy) of an observation target radio source after a cross correlation can be determined from the following relationship.

$$R < (\pi/2) \text{sqrt} (2BT F_1 F_2) / F_s \quad (2.1)$$

where B is the total frequency bandwidth (Hz), and F_i ($i=1,2$) are SEFDs (Jy) of the receiver systems at two stations. The factor $\pi/2$ is a result of a loss due to the 1-bit sampling digitization error. If we limit the maximum correlation integration time to 320

seconds and minimum SNR to 10, then the minimum flux density of the radio sources with an observation data rate of 64 Mbps is 1.8 Jy in the X-band and 0.57 Jy in the S-band. From the list of radio sources whose positions are known precisely in the International Celestial Reference Frame, 16 strong radio sources that satisfy the requirements were selected. Then the optimal integration time of cross-correlation processing for each source was determined to get a sufficient SNR of 20 in both the X- and S-bands for all baselines. The maximum correlation integration time is limited to 320 seconds even if the desired SNR is not obtained and the minimum correlation integration time of 50 seconds is kept.

To determine an adequate observation time for the target radio sources, a certain amount of time required to synchronize data in correlation processing should be added to the optimized integration time. Figure 2.6 shows the distribution of the data synchronization times for two data rates and two observation modes. It reveals a clear difference in the data synchronization times between tape-based and real-time VLBI modes. In the real-time VLBI mode, the data synchronization time was about 10 seconds for data rates of both 256 and 64 Mbps, and more than 95% of the data were less than 12 seconds. On the other hand, in the tape-based VLBI mode, the data synchronization was achieved by adjusting the data reproducing timing mechanically, which takes longer than the data synchronization using data buffers, as is done in the real-time VLBI mode. The distribution of time required to perform data synchronization in this case has a peak at about 30 seconds, and it takes 40 seconds to cover 95% of all the data. The observation time for each radio source was determined by adding the correlation integration time determined from the SNR requirements and the data synchronization time, which is 12 seconds for the real-time VLBI mode and 40 seconds for the tape-based VLBI mode. The results are shown in the Table 2.2. The maximum number of observations in one experiment is achieved at a data rate of 256 Mbps in real-time VLBI mode. In a typical experiment with 24 hours of duration, about 600 observations are possible at 256 Mbps in real-time VLBI mode, compared to only about 380 at 64 Mbps in tape-based VLBI mode. The uncertainties of the estimated site coordinates are proportional to the inverse of the square-root of the number of observations if the signal-to-noise ratio is kept and each measurement can be regarded as independent from other observations. Therefore the final results were expected to be improved by about 26% by making observations at 256 Mbps in real-time VLBI mode

compared with ones at 64 Mbps in tape-based VLBI mode. However the actual improvements were not so remarkable probably because the measurement errors can not be regarded as a white noise.

Table 2.2 Optimized observation time (seconds).

Radio sources	Real-time VLBI mode		Tape-based VLBI mode	
	256 Mbps	64 Mbps	256 Mbps	64 Mbps
0059+581	332	332	360	360
3C84	62	62	90	90
0420-014	117	222	145	250
0552+398	62	67	90	95
0727-115	126	239	154	267
4C39.25	62	62	90	90
3C273B	62	62	90	90
3C279	62	62	90	90
1308+326	108	204	136	232
1334-127	62	98	90	126
3C345	62	62	90	90
NRAO530	62	62	90	90
1921-293	62	62	90	90
2134+004	62	62	90	90
2145+067	62	94	90	122
3C454.3	62	62	90	90

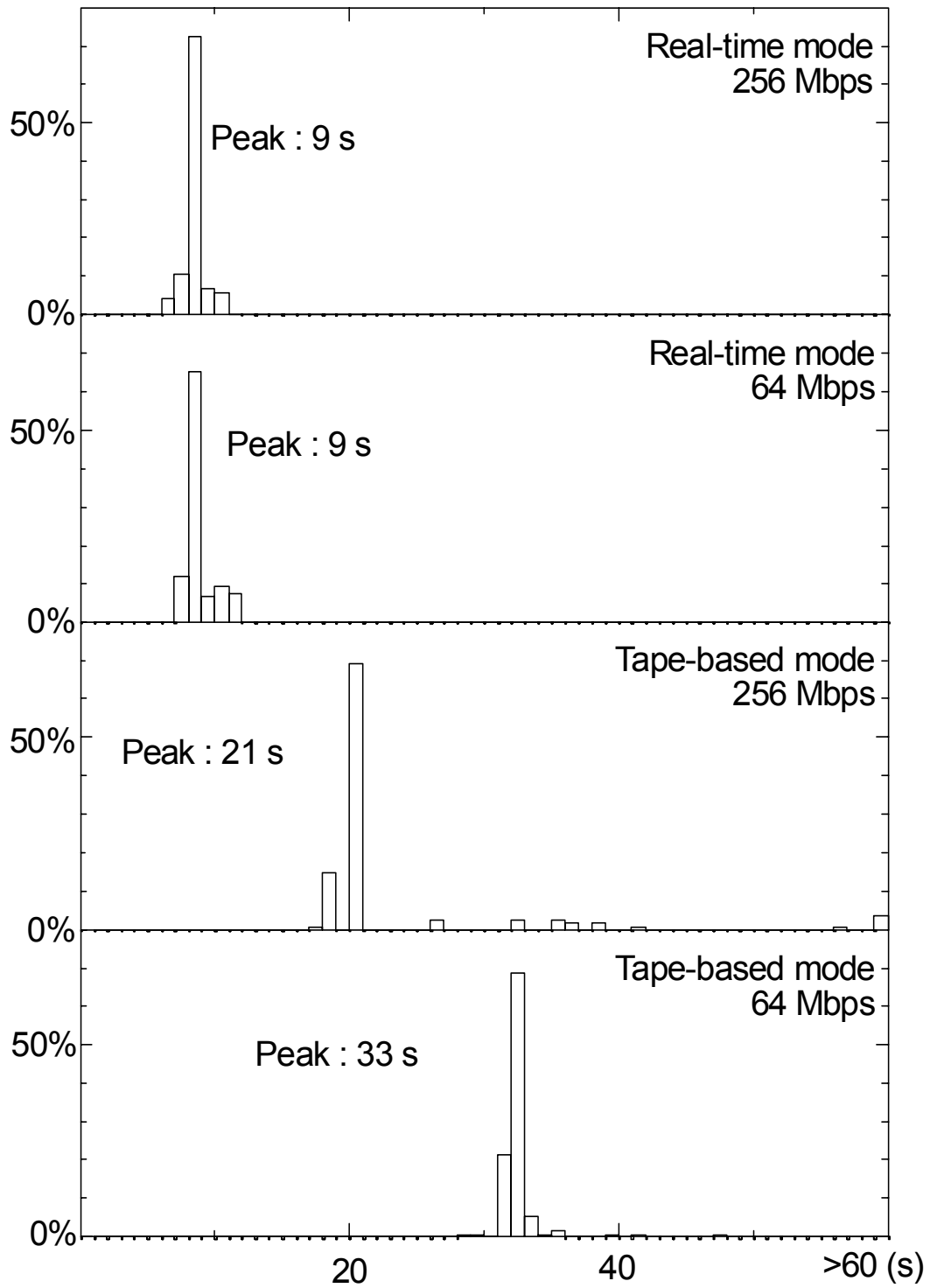


Figure 2.6 Data synchronization time for different observation modes and different observation data rates.

Table 2.3 Frequency assignments.

X-band		S-band	
Ch. No.	Local Freq. (MHz)	Ch. No.	Local Freq. (MHz)
1	7714.99	11	2154.99
2	7724.99	12	2164.99
3	7754.99	13	2234.99
4	7814.99	14	2294.99
5	8034.99	15	2384.99
6	8234.99	16	2414.99
7	8414.99		
8	8524.99		
9	8564.99		
10	8584.99		

2.1.9 Optimized Channel Frequency Assignments

The KSP VLBI observation system can perform observations with 16 video channels. Ten channels were assigned for the X-band and the other six for the S-band. The frequency assignments of observation channels were determined to achieve a wide equivalent frequency bandwidth after bandwidth synthesis processing while the side-lobe peak height of the bandwidth synthesis function was kept small. Table 2.3 shows the frequency assignments used at present. The phase calibration signal is injected into the received signal at 5 MHz frequency intervals, and the local frequency of each channel is chosen to have the phase calibration signal at 10 kHz.

2.1.10 Automated VLBI Observations

In both tape-based and real-time VLBI experiments, the observations at four stations are performed without any operators. First, the observation schedule file is created by the software SKED using its AutoSKED capability. This software has been

developed by NASA Goddard Space Flight Center and can produce an optimized observation schedule automatically [Steuftmehl, 1983]. The software is run by a clock daemon (cron) process on a workstation which is running the HP-UX operating system two weeks before the actual observations. The observation schedule file is duplicated and transferred to two central control workstations. For better reliability, the observation schedule for the day is checked by a different cron process. If the schedule file was not actually prepared two weeks ahead, the schedule file is newly produced at this time. The observation mode and starting and ending times are specified in a parameter file and the observation schedule is produced according to its contents. These parameters can be easily modified using one of the widely available browsers for the World Wide Web (WWW). If a special observation schedule is required temporarily, an operator at Koganei central station can create the schedule file using a WWW browser.

On the day of the experiment, the two central control workstations independently transfer the observation schedule file to the four observation control workstations. Stations to be included in the session are controlled by the master control files on the central control workstations. Then the observation control program on the observation control workstation is started by a command from the central control workstation. Before the first observation is begun, the internal clock of the observation control workstation is synchronized to UTC using the time code generator of a GPS receiver, and then the input interface units of the data acquisition system are synchronized to the internal clock of the observation control workstation. This step is especially important when a leap second is introduced. The frequency settings of the video converter units and the observation data rate of the data acquisition system are properly set according to the information in the observation schedule file. During an experiment, the status of each site was reported to an operator at Koganei central station by e-mail once every hour. After all observations in the experiment have finished, the log files are transferred to the central control workstations and merged with the weather calibration data file, delay calibration data file, and time difference data files for the correlation processing and the following data analysis procedures.

Table 2.4 Ratio (%) of successful experiments to the total number of days in a month summarized for every month from September 1996. An experiment was considered successful for a specific station if the station coordinate was estimated or used as a reference in the data analysis.

		Koganei	Kashima	Miura	Tateyama
1996	September	96.7	96.7	83.3	93.3
	October	96.8	93.5	96.8	93.5
	November	93.3	80.0	93.3	83.3
	December	96.8	90.3	100.0	100.0
1997	January	90.3	96.8	100.0	100.0
	February	100.0	100.0	100.0	100.0
	March	90.9	100.0	100.0	86.4

2.1.11 Regular Observations

The first VLBI experiment with the KSP network was performed for 24 hours on August 29, 1994 with the single baseline between Koganei and Kashima. Daily VLBI experiments began on January 31, 1995 with the same baseline. In the daily experiments, observations were usually performed for 5.5 hours from midnight. Full network experiments with the four stations shown in Figure 2.1 started on September 1, 1996 on a daily basis. Table 2.4 shows how the reliability of the observation system of the KSP VLBI network has improved since full network experiments began in September 1996. The ratio of the number of successful experiments to the number of days in the month is shown in the table for each station. Here, an experiment was considered to be successful for a station if the station position could be estimated from the obtained data. As shown in the table, the ratio gradually improved, and all the experiments were successful for every station in February 1997. This demonstrates the reliability of the observation system designed for the KSP VLBI system.

Until September 29, 1997, daily VLBI observations were performed from 15:00 UT to 20:30 UT. From September 30, 1997, the frequency of experiments was reduced from every day to alternate days and the duration of an experiment was

extended to 23.5 hours in the expectation that this would reduce systematic errors in the data analysis results.

2.2 K5 VLBI Observation System

2.2.1 Purposes to Develop K5 VLBI System

Currently, minimum delay time to obtain results from global geodetic VLBI observations can become more than two weeks for typical one day global experiments with several observing stations. This delay becomes shorter for so called intensive sessions where only one baseline is used and the duration is only about 1.5 hours, but it is still about one week or more. The purpose of the intensive sessions is to estimate the value of UT1-UTC by geodetic VLBI observations and the sessions are performed four or five times every week by using either Kokee Park (Hawaii, USA)-Wettzell (Germany) baseline or Tsukuba-Wettzell baseline. Since only the geodetic VLBI technique can precisely measure UT1-UTC value independently from any other measurement techniques, the results of the intensive sessions are used as essential information to generate predicted values of the UT1-UTC [McCarthy, 1993]. Since UT1-UTC randomly varies reflecting the dynamic phenomenon on the surface of the Earth and the interior of the Earth, the accuracy of the predicted UT1-UTC values deteriorates with time. Therefore, it is expected that the accuracy of the predicted UT1-UTC can be improved by shortening the delay time from the observations to the data processing of geodetic VLBI. The report of the IVS Working Group 2 for Product Specification and Observing Program [Schuh, *et al.*, 2002] pointed out it is very important to shorten this processing time delay to improve the accuracy of the EOP including UT1-UTC. The report also set the goal of the IVS observing program to make the time delay from observing to product less than one day by the year 2005.

To achieve this goal, it is necessary to transfer observation data electrically over the high speed global communication network from the observing sites to the correlator site. As described in the previous section, operational real-time VLBI was realized with the KSP VLBI system by using the ATM-based dedicated high speed research network. In the KSP VLBI system, four VLBI observing sites were connected with 2.4 Gbps ATM network optical fiber lines and the one day geodetic VLBI sessions

were performed every two days. However, maintaining dedicated high speed ATM network is quite costly, and it was only possible because of the close collaboration between CRL and NTT Laboratories. Therefore, it is not feasible to connect many VLBI sites located in many countries by using such kind of dedicated ATM network lines. On the other hand, high speed shared research networks based on IP are being constructed at many countries and regions. Under these circumstances, new system developments were initiated to realize e-VLBI over the IP-based shared high speed networks. The new system was named K5 VLBI system to distinguish it from previously developed systems at KSRC. The K5 VLBI system is characterized by the use of conventional PC systems and the shared network based on IP. The data correlation can be performed by hardware correlators and also by software correlation programs using multiple PC systems and distributed processing methods. In contrast to the K5 VLBI system, the K4 VLBI system can be characterized by the use of rotary-head, cassette type magnetic tape recorders and the dedicated network based on ATM. Similarly, the K3 system can be characterized by the use of open-reel magnetic tape recorders. Figure 2.7 shows these three generations of the VLBI observation and data processing systems developed by CRL.

As shown in Figure 2.8, the concept of the K5 VLBI system is to realize VLBI observations and data processing by combining various hardware equipments and conventional PC systems. If the data rate of the A/D sampling is less than 16 MHz per each channel, the IP-VLBI board is used for the data acquisition. The board is capable to sample the analog signals from base band converters the sampled data can be directly accessed by conventional PC systems through PCI data bus. On the other hand, if much faster sampling data rate is required, two hardware sampler units, i.e. ADS1000 and ADS2000, are available. Both of the units have data output interfaces which are compliant with the hardware specifications of the VLBI Standard Interface (VSI) [Whitney, 2001]. The PC-VSI board shown in the figure is an interface between the VSI data stream and the conventional PC systems. The board is also installed on the PCI data bus of the PC. It is planned to use the same board to output the data streams from the PC systems in the VSI compliant data streams for correlation processing by hardware correlators.

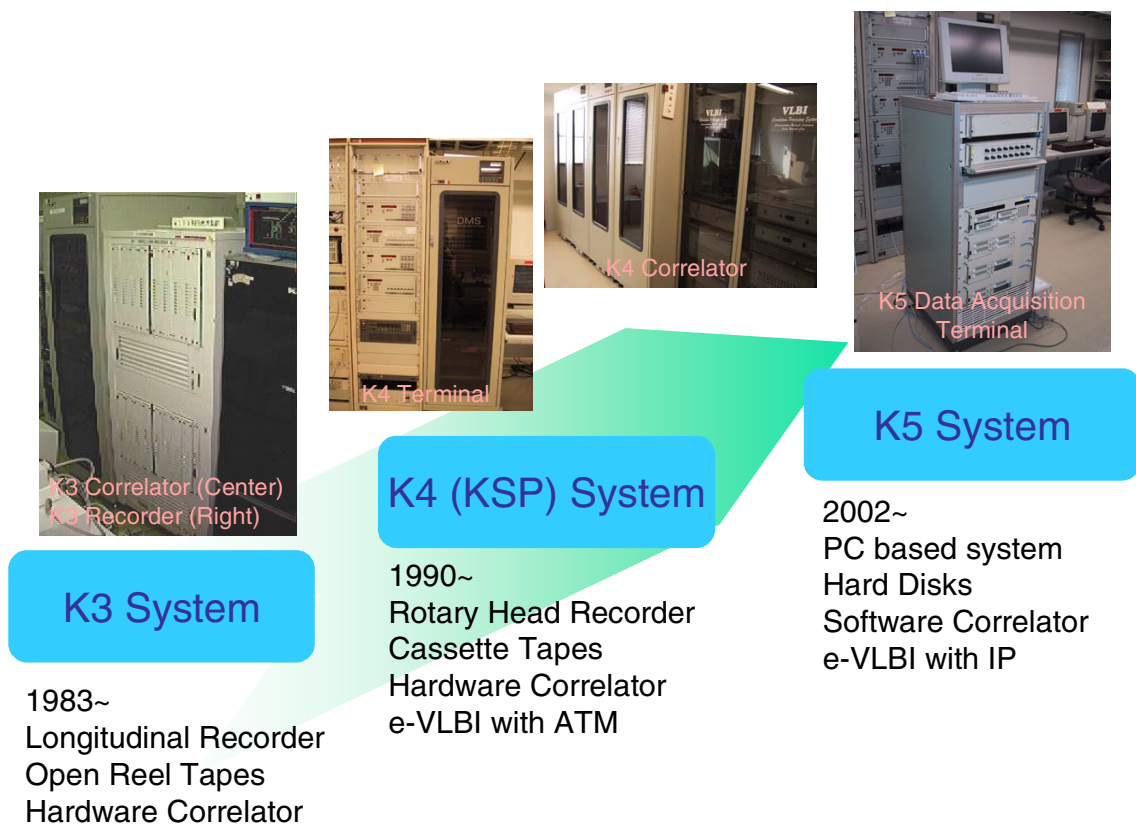


Figure 2.7 Three generations of the VLBI systems developed by CRL.

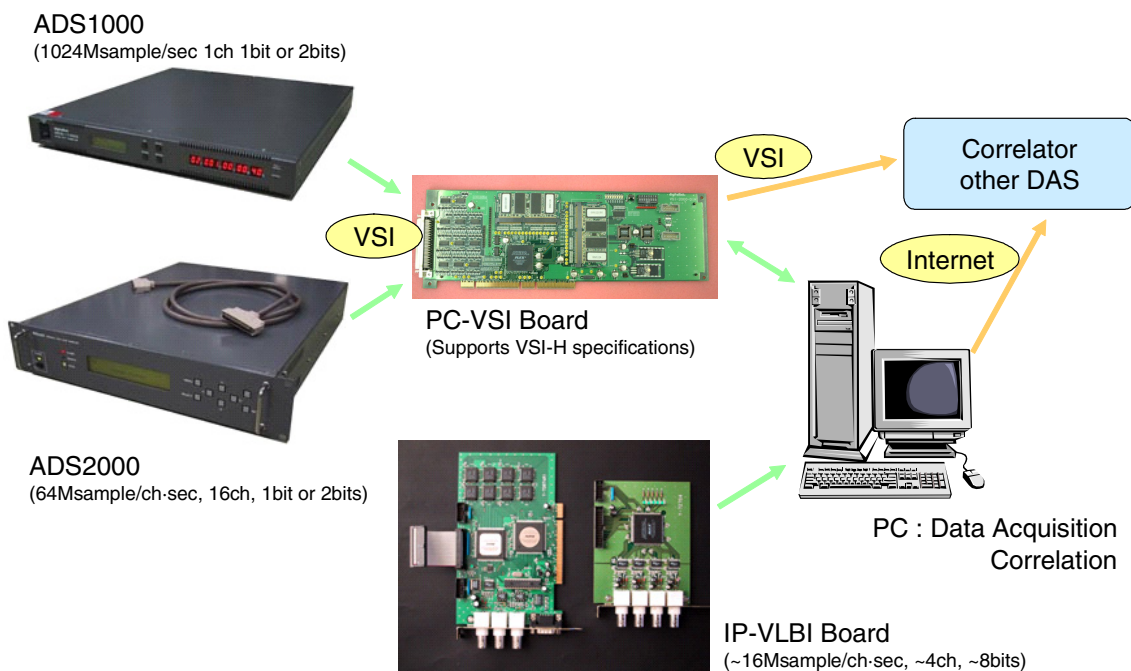


Figure 2.8 Concept of the K5 VLBI system.



Figure 2.9 Versatile Scientific Sampling Processor (VSSP).

2.2.2 Developments of the System

IVS Technology Development Centers including Haystack Observatory and CRL have been concentrating their efforts to realize the e-VLBI in the global geodetic VLBI observations. At CRL, the K5 VLBI system has been developed based on the UNIX PC systems while the Mark-5 VLBI system has been developed at Haystack Observatory [Whitney, 2003].

As one of the actual realization of the K5 VLBI system concept given in the Figure 2.8, the Versatile Scientific Sampling Processor (VSSP) system has been developed. Figure 2.9 shows the picture of the actual VSSP system developed by CRL.

Table 2.5 Specifications of the IP-VLBI board.

Reference Signals	10MHz (+10dBm) and 1PPS
# of Input	Ch. 1 or 4
A/D bits	1, 2, 4, or 8
Sampling Freq.	40kHz, 100kHz, 200kHz, 500kHz, 1MHz, 2MHz, 4MHz, 8MHz, or 16MHz
Bus Interface	PCI
OS	FreeBSD, LINUX, or Windows2000

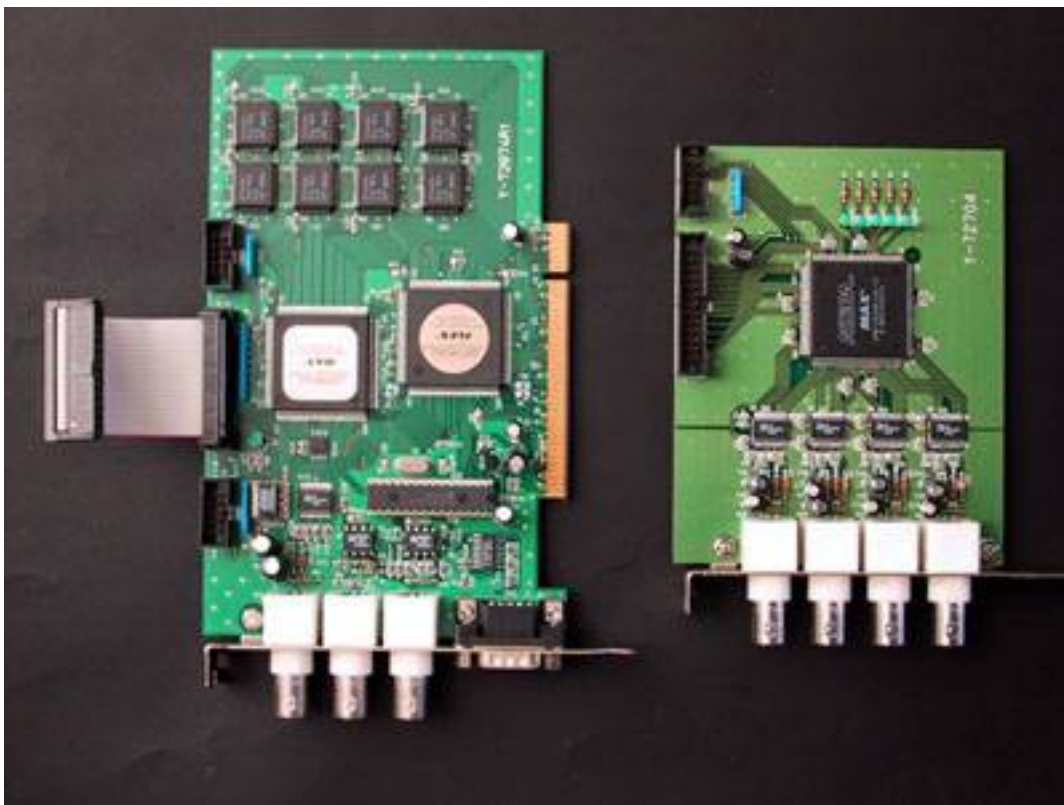


Figure 2.10 The main board (left) and the auxiliary board (right) of the IP-VLBI board. Two boards are connected by the cable attached to the main board in the picture.

The VSSP system is consist of four UNIX PC systems and each system has one IP-VLBI board on its PCI interfacing bus. The IP-VLBI board is consist of one main board and one auxiliary board connected to the main board by a special data cable as shown in Figure 2.10. Table 2.5 lists the specifications of the board. The board can

sample 4 channels of base-band signals at various sampling rates ranging from 40 kHz to 16 MHz. The timing of the sampling is controlled by the provided 10MHz and 1-PPS reference signals so that precise timing information can be reproduced from the sampled data. Quantization bits can be set from 1, 2, 4, and 8. Because the board has these many sampling modes, it has many possibilities to be used not only for VLBI observations but also for various other scientific research fields which require precise timing information in the data.

Device driver software of the board has been developed on LINUX, FreeBSD, and Windows2000 operating systems, and FreeBSD is used in the VSSP systems. As of January 2004, four VSSP systems have been manufactured. Two of these systems are now used at KSRC, while one VSSP system has been installed to the Tsukuba 32-m antenna VLBI station of the Geographical Survey Institute (GSI), and the remaining one system will be installed to the 11-m antenna VLBI station at Syowa station of the National Institute of Polar Research. In the VSSP system, four PC systems are mounted in the lower part of the 19-inch standard rack, while a signal distributor unit for 1-PPS and 10 MHz signals and 16-channel base-band signal variable amplifier unit are mounted in the upper part of the rack. The monitor and the keyboard on the top of the rack are connected to the four PC systems by using a four-way switch unit. Each PC system is equipped with four removable hard disk drives of the data capacity of 120 GBytes each. The sampled data can be transferred to the network by using IP protocol or can be recorded to internal hard disks as ordinary data files. The maximum recording speed is restricted by the speed of the CPU and the speed of the PCI internal bus. Currently, the total recording speed of 512 Mbps has been achieved. It can be expected to record data up to 1024 Mbps by using faster PCI bus and faster CPU in near future.

Chapter 3 Data Processing and Analysis Systems

3.1 KSP Data Processing System

3.1.1 Cross Correlation Processing

The cross correlation processing of the observed data by the KSP VLBI stations was done by the KSP correlator system located at Koganei station, shown in Figure 3.1. There are two sets of cross correlation processing units: one is used for the tape-based VLBI mode and the other is for the real-time VLBI mode. No human operations are required in the real-time VLBI mode. The correlation management program is always running, and the cross correlation processing is performed whenever the observations are performed [Kondo *et al.*, 1996]. In the tape-based VLBI mode, on the other hand, a human operator must set the data tapes in the tape changing unit of the correlator system and start the correlation management program. Once the cross



Figure 3.1 Tape-based KSP correlator system.

correlation processing begins, all procedures are then performed automatically until the database files are created from the observation data.

3.1.2 Initial Data Analysis

In both tape-based and real-time VLBI modes, the output data from the correlator system at Koganei station are processed by the bandwidth synthesis program to determine time delays for all combinations from participating stations. The set of obtained time-delays and their rates of change is then combined with auxiliary data including meteorological data and delay calibration measurements and is stored in two database files, one for X-band data and the other for S-band data. Only the X-band database is used for data analysis and the S-band database is mainly used to obtain correlated amplitudes of observed radio sources. The databases are created using Mark-III database handler software developed at NASA Goddard Space Flight Center and the file format of the databases is based on the Mark-III database file format, which can be handled by any software programs based on the Mark-III database handler routines.

Once the X-band database file is created on the data analysis workstation at Koganei station, a set of data analysis programs starts processing the database file until the initial analysis results are obtained. Figure 3.2 illustrates the entire process of data analysis. At first, the DBUPDATE routine updates the database with the latest *a priori* information. The *a priori* information to be updated includes coordinates (δx and δy) of the Earth's rotation pole with respect to the conventional pole, UT1-UTC, nutation offsets from the IAU80 standard model, terrestrial coordinates of reference points of VLBI stations, and coefficients for site displacements due to ocean loading effects. The same routine is used in the re-analysis procedures when a part of the *a priori* information is improved. In the next step, the CALC routine calculates theoretical delays and delay rates based on the *a priori* information. It also calculates a Jacobian matrix with various parameters for the least squares estimates. After the CALC routine, the database is ready for the least squares analysis. DATSET then extracts necessary information from the database and stores it in a work file. After these procedures, the VLBEST routine runs three or more times and least squares analyses are performed using different combinations of estimation parameters depending on the stage of the

analysis. In the first step, only the clock offsets and their rates of change with respect to a reference station are estimated and the other parameters are fixed. In this procedure, the observed delays may include delay ambiguities, which are certain amounts of time multiplied by integers. The ambiguities are the results of the bandwidth synthesis processing, and the minimum step of ambiguity is defined by the inverse of the greatest common divisor of frequency spacings of the local frequencies of observation channels, which is 100 nanoseconds for both the X- and S-band frequency assignments in Table 2.3. The ambiguities are resolved using the residuals of delays after the least squares adjustment. In the second step, clock offsets at a time interval of 1 hour and site coordinates of all stations except for a reference station are estimated by the routine VLBEST. Observed delays having large residuals are flagged and removed from the following analysis by the routine MRKOBS. If the residual is greater than three times the root mean squared (rms) of the residual delays and also greater than 200 picoseconds (ps), it is regarded as a bad datum. This step is iterated until there are no more actual data to be removed. In the last step, the wet tropospheric zenith delays at a time interval of 3 hours are added to the parameters to be estimated, and the final results are obtained. The quality of the results is evaluated by the final rms of the delays. If the rms residual is smaller than a certain criterion (e.g. 100 ps), the results are regarded as reliable and are made accessible via WWW and anonymous ftp (file transfer protocol) over the Internet. If the residual rms exceeds the criterion, an alarm message is sent to pre-registered e-mail addresses. In this case, the database is analyzed manually and the results are finally publicized if reliable ones are obtained.

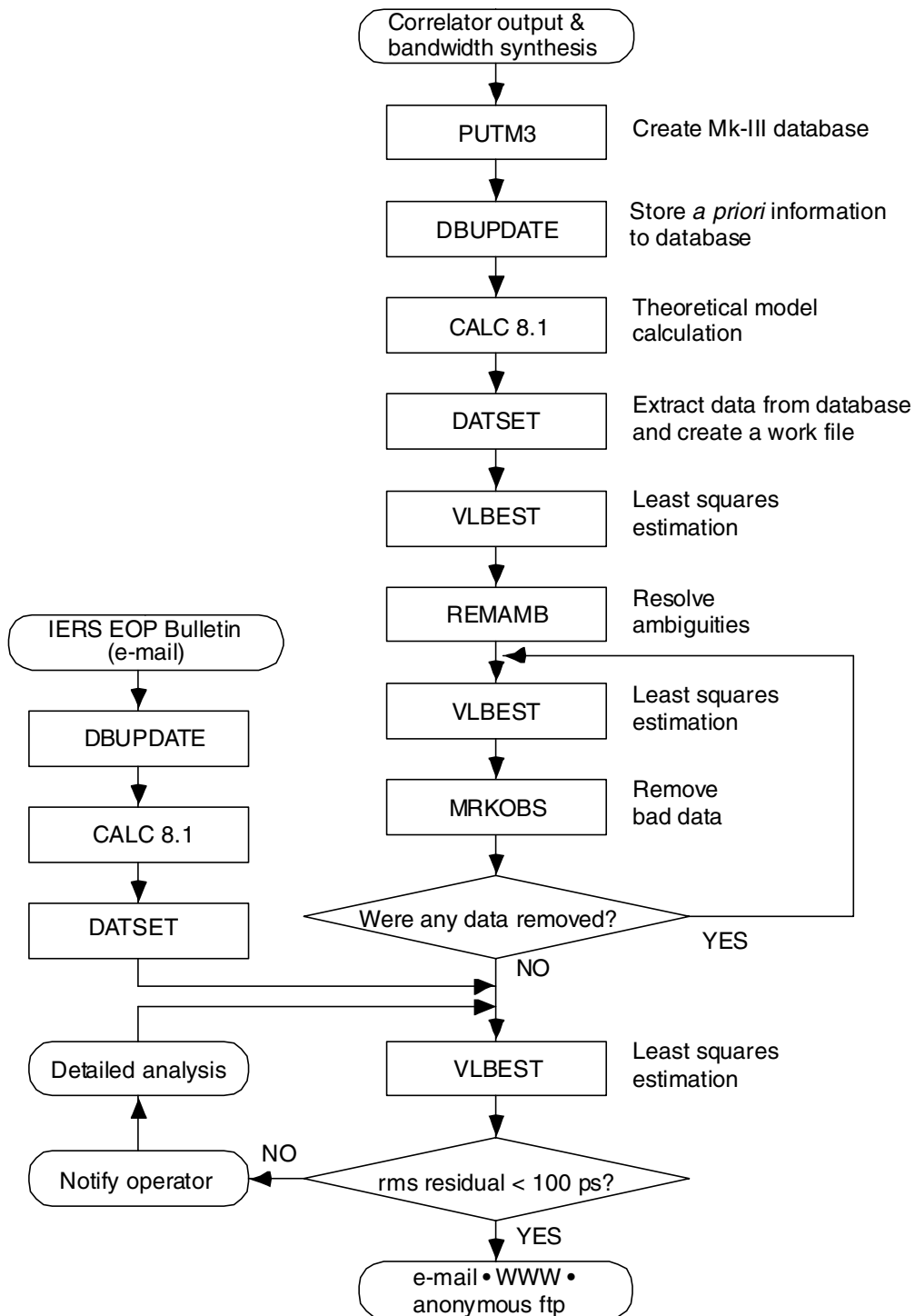


Figure 3.2 Schematic data flow and block diagram of the automated VLBI data analysis.

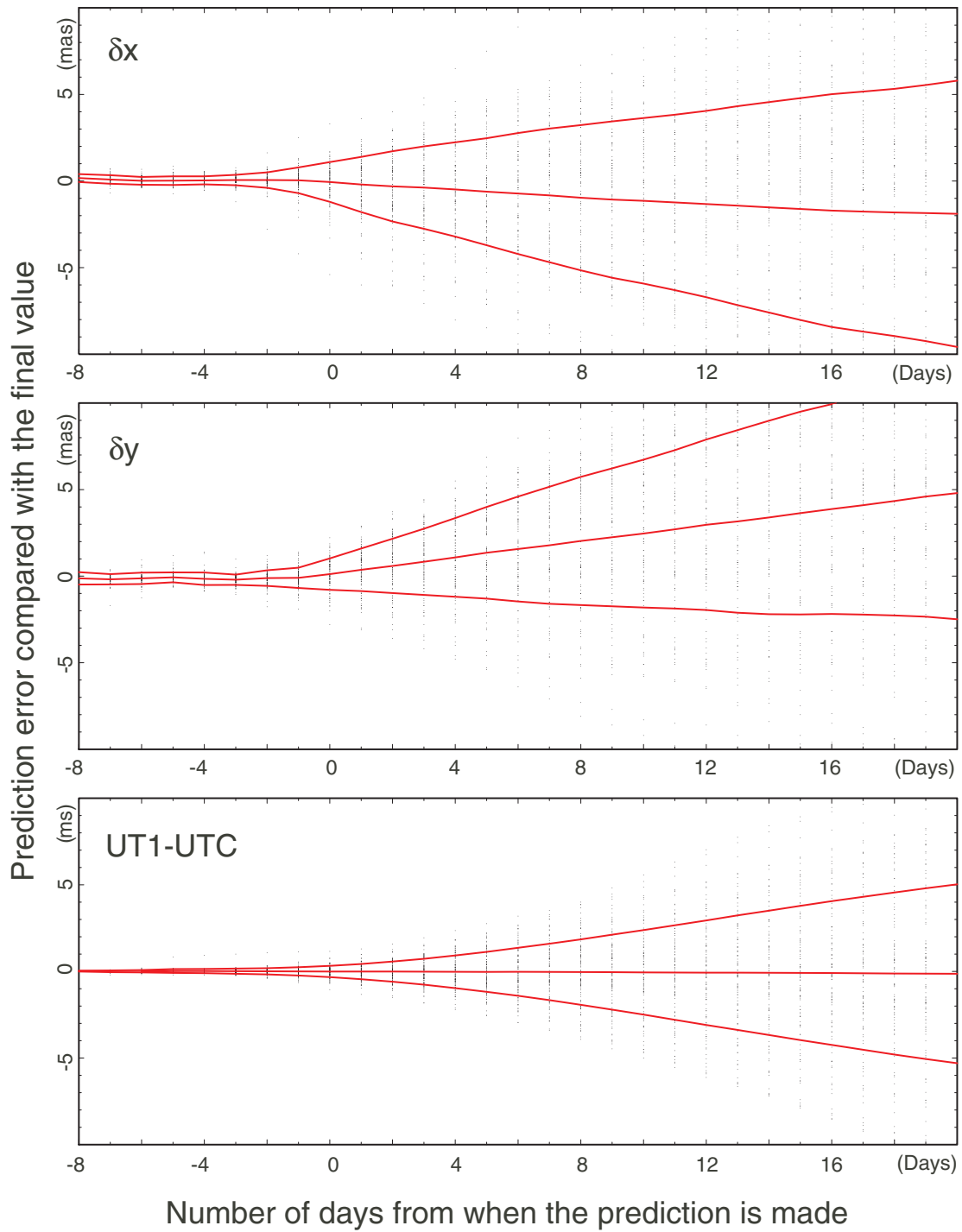


Figure 3.3 Offsets of the three EOP values published in the IERS Bulletin-A from the final values appeared in the IERS Bulletin-B in the period between January 1996 and August 1997.

3.1.3 Updating Data Analysis Results

In addition to the normal data analysis procedure, results are updated when any of the *a priori* information is improved. The most frequent case of this is when the IERS issues a bulletin. IERS is responsible for providing up-to-date series of parameters related with Earth's rotation and issues Bulletin-A twice a week and Bulletin-B once a month. At the time of initial data analysis, only the predicted values of δx , δy and UT1-UTC are available as *a priori* information. No predictions are provided for the nutation offsets, so these values should be obtained using empirical model. The values of these parameters are improved in the bulletins issued after the experiment. The bulletins are received by e-mail and are processed automatically by the data analysis software. All the databases for which *a priori* information is improved are updated with the improved *a priori* information by the routine DBUPDATE. These databases are then processed by the routine CALC, and finally the parameters are reanalyzed by the routines DATSET and VLBEST.

The uncertainties of the predicted EOP are estimated as 3.8 mas (mas: milli arc seconds) for δx and δy , and 1.5 ms for UT1-UTC for a prediction time of 10 days [IERS, 1995]. In Figure 3.3, the actual offsets of the three EOP published in the IERS Bulletin-A issued from January 1996 through August 1997 are compared with the final values that appeared in the IERS Bulletin-B. The actual prediction errors in the IERS Bulletin-A were worse than the values published in the IERS documents. From the comparison, the rms prediction variations of the δx and δy were evaluated as 5.1 mas (δx) and 4.3 mas (δy) at a prediction time of 10 days, and 3.1 mas (δx) and 2.7 mas (δy) at a prediction time of five days, whereas the rms prediction variations of the UT1-UTC were evaluated as 2.4 and 1.2 ms at a prediction time of 10 and 5 days, respectively. In the KSP VLBI initial data analysis, the predicted values of the EOP in the latest IERS Bulletin-A are used and the prediction time increases to 5 days in the worst case. This means that the three-dimensional site positions estimated from the initial data analysis are affected by the prediction errors. The 4.3 mas of the Earth's rotation pole position errors and the 1.2 ms of UT1-UTC error correspond to site position estimation errors of 2.4 and 9.6 mm in the horizontal and vertical components, respectively, for a baseline 110 km, which is roughly the distance between Kashima and Koganei stations. The discussions above are based on the rms prediction variations of the EOP, so the actual

site position errors may sometimes be larger.

Therefore, the data analysis should be repeated when the new IERS bulletin arrives and more accurate EOP become available. When a new IERS bulletin arrives by e-mail, all the databases containing EOP for which new values are now available are reanalyzed by the automated data analysis system. The errors in the parameters before the bulletin issue date are small and the site position errors due to them can be ignored.

3.1.4 Discussions

Both the VLBI observation control system and the VLBI data analysis system for the KSP have been designed for automation and robustness through the use of redundancy. The unique features of the KSP VLBI system have resulted in regular geodetic VLBI experiments with four VLBI stations with a time interval of one or two days. Results from the experiments are produced quickly after the experiment. In the tape-based VLBI mode, the results can be obtained within two days from the last observation in the experiment, whereas the time required between the last observation and the data analysis was reduced to a few minutes in the real-time VLBI mode. From 23.5 hours of experiments, the horizontal and vertical position uncertainties were about 2 and 9 mm, respectively, in a sense of internal estimation error evaluated by one sigma standard deviation.

To improve the estimation accuracy, the key is to increase the number of successful observations as well as to improve the theoretical models. The number of observations in an experiment can be increased by reducing the observation time for each radio source. Data synchronization can be performed while the antenna is slewing to change from the previous radio source to the next one. The number of observations in an experiment might also be increased significantly if the synchronization time in the cross correlation processing is shortened by a fine tuning of the data synchronization algorithm. The observation time can be shortened for strong radio sources if the minimum integration time is decreased from the present value of 50 seconds. If the minimum integration time is set too short, however, interferometric fringes may not rotate enough and the obtained delays may have errors that cannot be ignored. Therefore, the minimum integration time should be carefully investigated. Although only the group-delay data are used at present, the usage of the phase-delay data has a potential to

improve the precision of the VLBI measurements [Herring and Pearlman, 1993]. The possibility of the phase delay measurements will be investigated in the near future by using the KSP VLBI network.

The availability of the VLBI data obtained from the regular KSP experiments will be greatly improved if the results are generated in SINEX (Solution Independent Exchange) format, which will enable these results to be combined with other geodetic measurements including the GPS and SLR. A detailed comparison of the VLBI results with results from GPS and SLR measurements is one of the major purposes of the KSP. The implementation of the automated SLR and GPS data analysis system is on the way and soon the comparison will become possible.

3.2 K5 Data Processing System

3.2.1 K5 Software Correlator Programs

To process the data sampled and obtained with the K5 observation system, software correlation processing programs are under developments on conventional PC systems. Currently the correlation processing programs process two data files recorded beforehand and the near-real-time VLBI data processing is possible. However, in the future, we are planning to develop a set of programs to transmit the sampled data from an observing site to a correlation site during observations and process the received data at the correlation site for real-time VLBI observations. The concept of the software correlation used to be utilized in the very early stage of the history of the VLBI. In 1960's, the observed signals at the radio telescopes were recorded on the magnetic tapes and the data were transferred to a main frame computer system and the cross correlation was calculated by software correlation programs [Bare *et al.*, 1967]. The K5 software correlation programs are based on the CCC (Cross Correlation in a Computer) program developed for the K3 VLBI system [Kondo *et al.*, 1991]. In the past, the software correlation used to take very long time to process the wide-band observation data. However, the recent rapid growth of the PC systems is gradually making the software correlation feasible for operational VLBI data processing. By using the recent PC systems running on Unix operating systems and the high speed local area networks, multiple PC systems can be used together for the distributed processing. Unlike the

hardware correlators, it is easy to expand the processing capacity by simply increasing the number of PC systems. The software program is also very flexible and it can be easily modified if special correlation condition is required. For example, if extremely fine frequency resolution is required, the lag length can be expanded by modifying the software programs whereas such a modification is very difficult with hardware correlators.

As the K5 data processing system, a set of software programs have been developed to process the observed data files by the K5 observation systems. At first, an observation schedule file and *a priori* clock difference information are used to calculate time delays and their rates of change for every scans and every combinations of observing antenna pairs included in the schedule file. Then the coarse delay resolution functions of a selected scan are calculated for all of the baselines. By using the results, accurate clock offsets of observing sites are determined and the *a priori* information is improved by using the determined clock offsets. After these preparation procedures, correlation processing is performed for every scans and all baselines by using multiple PC systems. For the distributed processing with many PC systems, a simple server and client mechanism shown in Figure 3.4 has been developed. On the server system, a master control file is maintained and the file holds all the information necessary to control the distributed processing. By reading the master control file, the server system can assign a set of data files with which the client systems can process. Each client system obtains the data files and necessary information from the server system and starts to process the data. When the processing is completed at the client system, the client system places the results to a specific place and then requests the server system for the next data files. By using this simple mechanism, all the data files can be processed effectively using available computing resources of the client PC systems. Although the performance of each PC system may differ, each client PC systems can process the data files according to the available performance. Status of the correlation processing can be monitored by any WWW browsers connected to the local area network as shown in Figure 3.5.

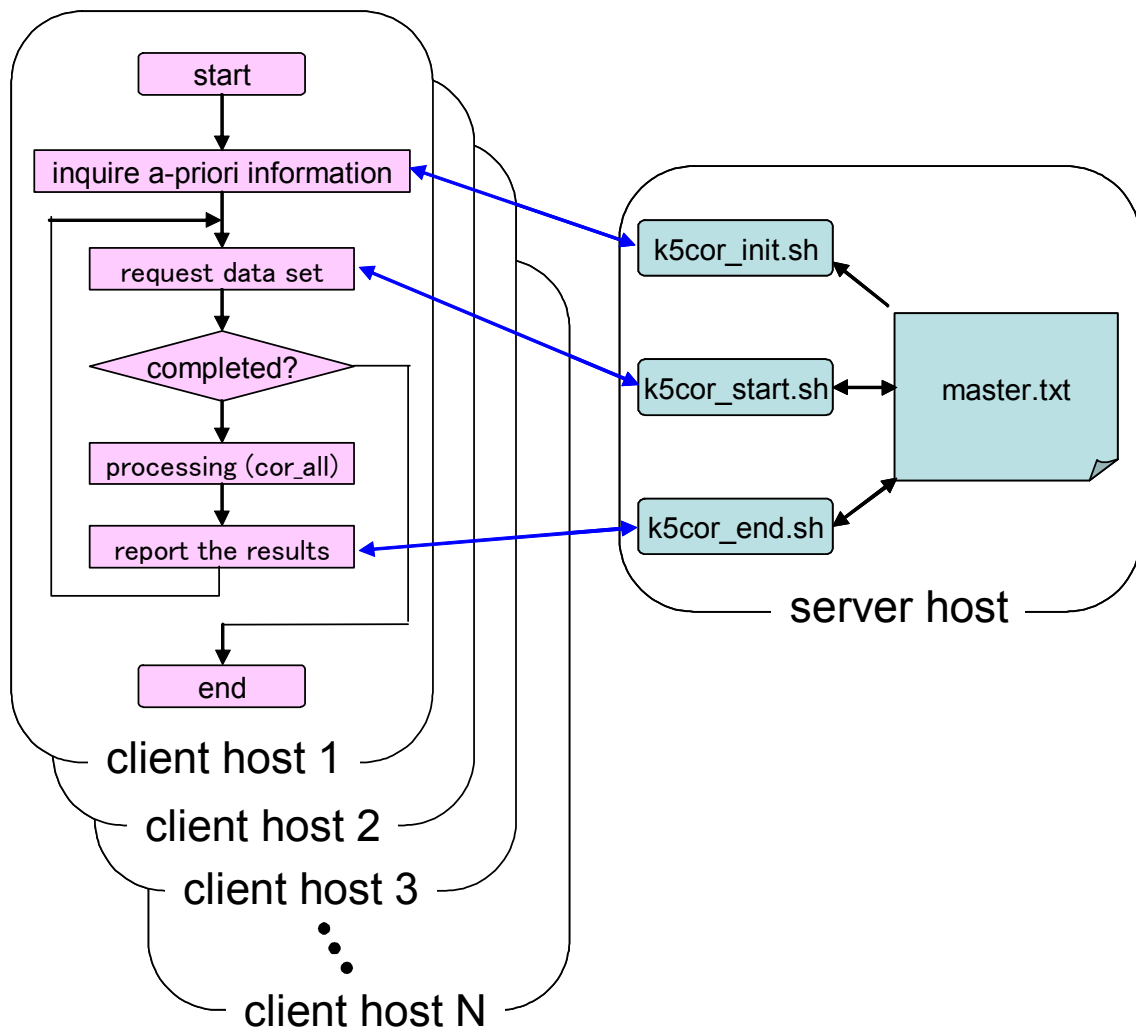


Figure 3.4 A schematic diagram of the server and client mechanism developed for the distributed cross correlation processing.

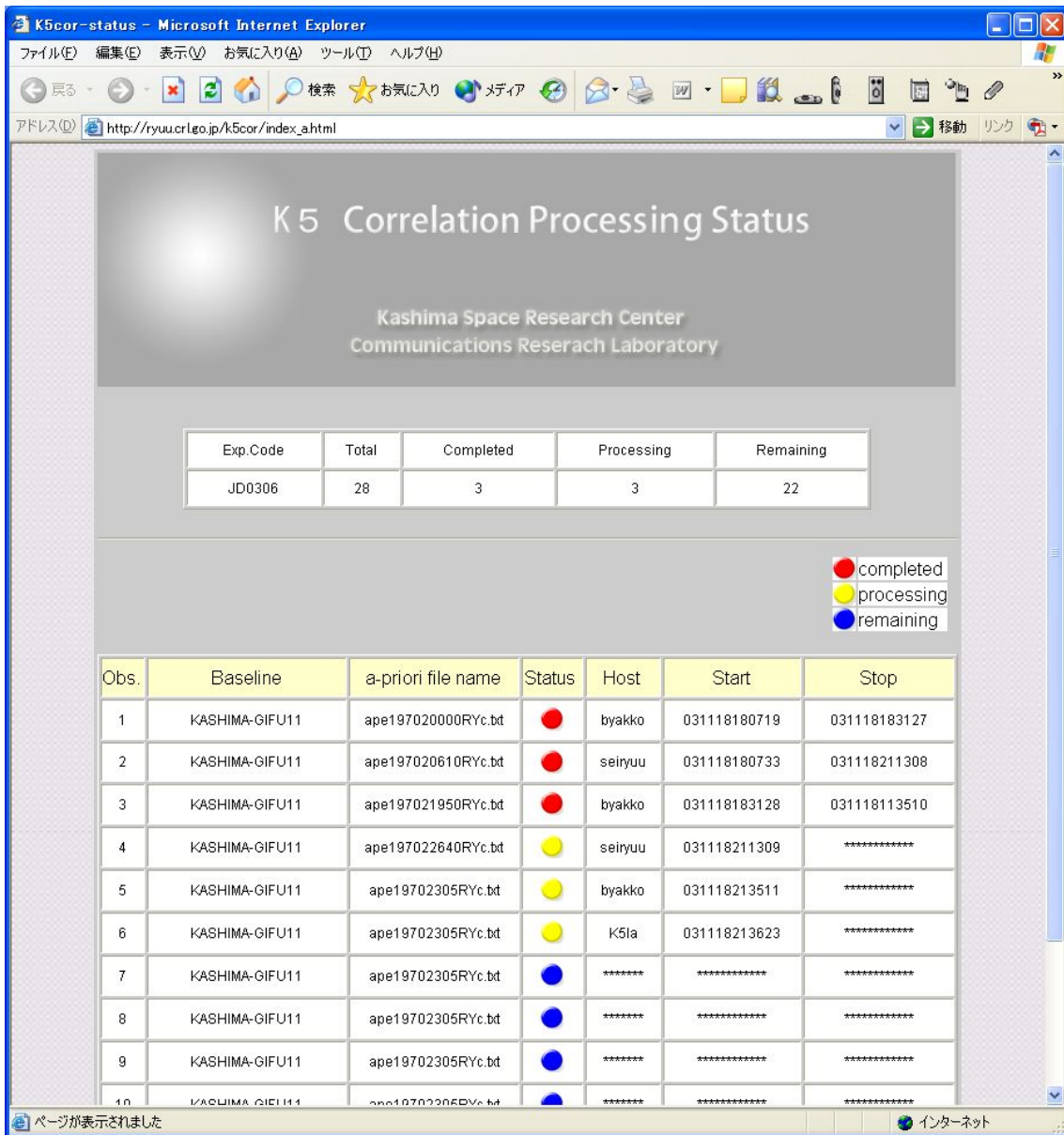


Figure 3.5 A WWW browser screen for monitoring distributed processing status.

3.2.2 Test Experiment with Kashima-Koganei Baseline

After completing two prototype K5 VLBI data acquisition terminals, 24 hours of geodetic e-VLBI experiment was performed using two 11-m antennas at Kashima and Koganei from January 31 to February 1, 2003. Eight channels were assigned to both X-band and S-band and the total data rate was 64 Mbps. Observed data were stored in the internal hard disks as the data files. The data files were read by the software correlation program and the cross correlation processing was performed after all the observations finished. Then the bandwidth synthesis processing was performed and the obtained data were analyzed by CALC and SOLVE software developed by Goddard Space Flight Center of National Aeronautics and Space Administration. During the observations, tape-based K4 data acquisition systems were used at both sites in parallel to compare the results. The data obtained with the K4 systems were processed with the K4 correlator at Kashima and analyzed similarly with the data obtained with the K5 systems. The results are compared in Figure 3.6 and Table 3.1. Figure 3.6 shows the difference in group delay and delay rate obtained by the K4 VLBI system and the K5 VLBI system. The constant offset of the group delay shown in the figure is considered to be caused by the different lengths of cables and by the timing of synchronization to the 1 pulse-per-second signals. On the other hand, the constant offset is absorbed as a part of the clock difference estimated through the data analysis processing and therefore it does not cause any problem in the data analysis. The RMS of the difference is calculated as 72.7 psec for delay and 118 fsec/sec for delay rate, and it can be concluded that the K4 and K5 systems are consistent with each other. Table 3.1 shows the estimated results from the data analysis. From these comparisons, it can be concluded that the estimated baseline lengths are consistent with each other within two times the estimated uncertainties. In addition, the comparison of the RMS residuals of delay and delay rates suggests the performance of the K5 systems is better than the K4 systems. The part of the reason of the improvement can be considered that the phase calculation of the phase calibration signals by the software correlation processing uses precise formula whereas the K4 hardware correlator uses a three level approximation for sine and cosine functions for faster processing and to make the design of the hardware correlator very simple.

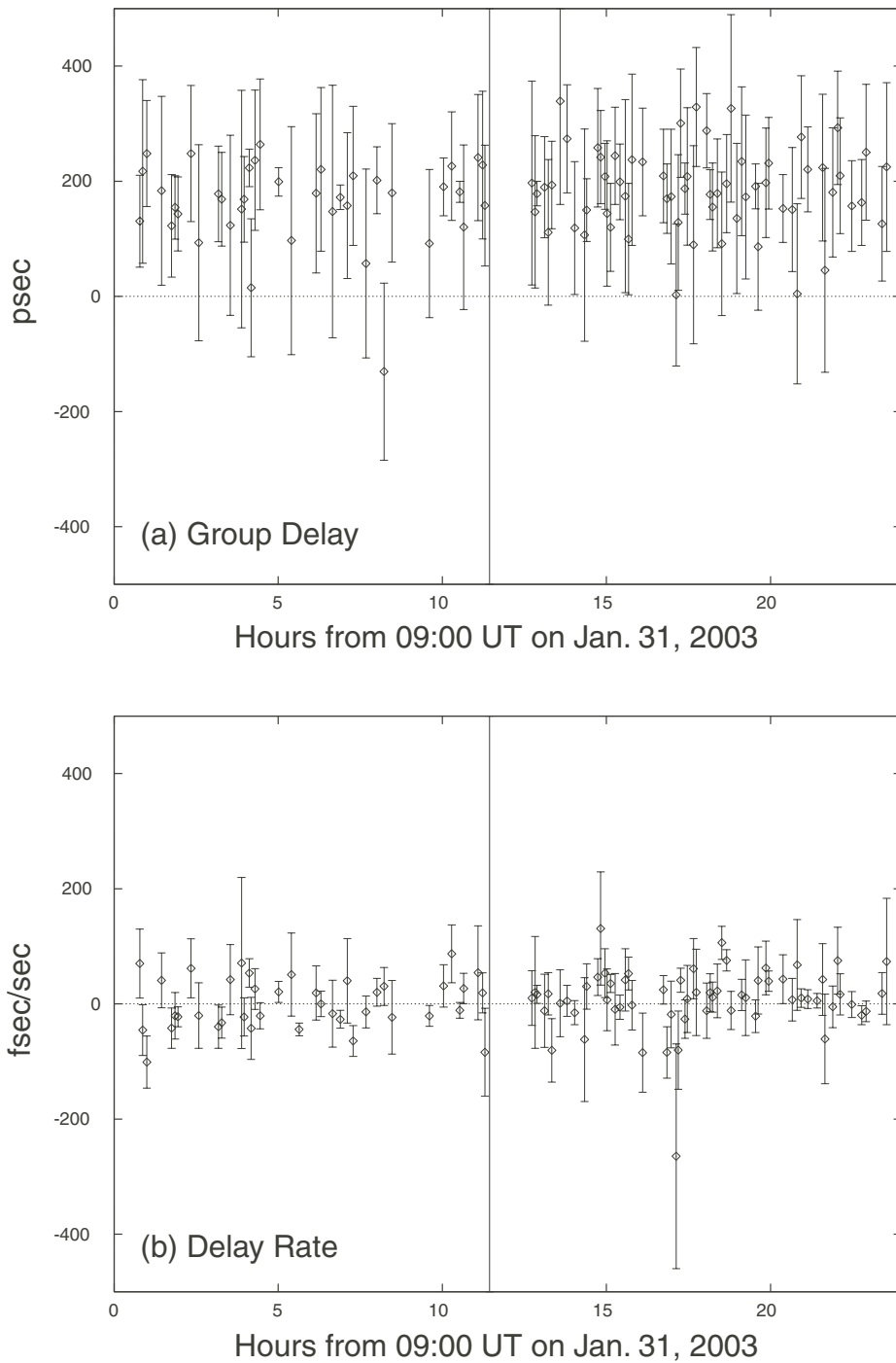


Figure 3.6 Difference of (a) group delay and (b) delay rate obtained from K4 and K5 systems. Horizontal axis is the time of the scan in hours from the beginning of the session while the vertical axis is the difference of group delay and delay rate. The error bars are one-sigma errors evaluated from $(s_{K4}^2 + s_{K5}^2)^{1/2}$ where s_{K4}^2 and s_{K5}^2 are standard deviations of the data estimated from K4 and K5 systems, respectively.

Table 3.1 Comparison of baseline lengths estimated from the data obtained with K4 and K5 systems.

	No. of valid data	Baseline Length (mm)	RMS Residual	
			Delay (psec)	Rate (fsec/sec)
K4	112	109099657.0 ± 6.7	76	136
K5	159	109099641.2 ± 3.2	33	92

3.2.3 Test Experiment with Multiple Baselines

After the first test geodetic VLBI experiment described in the previous sub-section, an opportunity of a domestic regular geodetic VLBI experiment performed by GSI was used for the evaluation of the K5 VLBI system. The experiment JD0306 was performed for 24 hours from July 16, 2003. As a regular domestic experiment, four VLBI stations operated by GSI at Tsukuba (32-m), Shintotsukawa (3.8-m), Chichijima (10-m), and Aira (10-m) participated with the K4 VLBI systems. At Tsukuba station, the K5 VLBI system was used in addition to the K4 VLBI system. By using the same observing schedule, Kashima (11-m), Tomakomai (11-m), Gifu (11-m) participated in the experiment by using K4 VLBI system and K5 VLBI system in tandem. In addition, at Yamaguchi (32-m) station, K5 VLBI system with two PC units was used to perform observations only in X-band with 8 channels. At three stations (Kashima, Tomakomai, and Tsukuba), the VSSP systems were used while PC systems configured with IP-VLBI boards were used at Gifu and Yamaguchi stations. Table 3.2 shows the comparison between results obtained from K4 VLBI system and K5 VLBI system for six baselines. Since the K5 VLBI system at Kashima and Gifu stations stopped recording for about six hours and 12 hours respectively during the observations, the number of valid data for baselines including Kashima and Gifu stations are fewer than the data from the K4 VLBI system. The comparison suggests that the estimated error obtained from both systems are comparable considering the number of available data and the estimated baseline lengths are consistent with each other considering the estimated error.

In Table 3.3, preliminary results of estimated coordinates of the Yamaguchi

32-m station based on the ITRF97 reference frame [Boucher *et al.*, 1999] are presented. In the data analysis, site coordinates of the Tsukuba 32-m station was used as the reference and the X-band group delay data for Tsukuba-Yamaguchi baseline were used. Since ionospheric delay correction can not be performed by using only one frequency band (X-band) taken at Yamaguchi station, it has to be noted that there might be a systematic error in the estimated coordinates.

Table 3.2 Comparison of baseline lengths estimated from the data obtained with K4 and K5 systems.

Baseline	System	No. of valid data	Baseline Length (mm)	RMS Residual	
				Delay (psec)	Rate (fsec/sec)
Tsukuba-Kashima	K4	176	53811894.9 ± 2.1	53	158
	K5	130	53811891.6 ± 3.1	81	121
Tsukuba-Gifu	K4	184	311067474.0 ± 2.9	98	189
	K5	55	311067483.3 ± 4.0	58	136
Tsukuba-Tomakomai	K4	124	740526116.3 ± 4.4	103	165
	K5	169	740526119.4 ± 5.1	103	146
Kashima-Gifu	K4	174	358799168.6 ± 2.8	72	191
	K5	48	358799174.7 ± 4.5	92	144
Kashima-Tomakomai	K4	171	749810979.9 ± 4.4	115	125
	K5	108	749810985.5 ± 5.5	106	143
Gifu-Tomakomai	K4	154	902668931.2 ± 4.8	135	125
	K5	49	902668930.6 ± 6.1	116	138

Table 3.3 Estimated coordinates of the Yamaguchi 32-m VLBI station.

X :	-3502544258.3 ± 22.1 (mm)
Y :	3950966396.9 ± 25.8 (mm)
Z :	3566381164.9 ± 22.0 (mm)

By using the results of two test geodetic VLBI experiments described in this sub-section and the previous sub-section, the data obtained with the K4 and K5 VLBI systems were compared to ensure that the K5 VLBI system has expected capability and performance similar or better than the K4 VLBI system. As far as the results from the two test experiments are seen, the results from two different systems seem to be considered with each other considering the estimated errors. From these comparisons, it can be concluded that there is no problem in using the K5 VLBI system for precise VLBI observations.

Chapter 4 Motion of the Observing Sites

4.1 Daily and Sub-daily Monitoring of Site Motions in the KSP

From Figure 4.1 through Figure 4.6, the estimated lengths of the baselines between four KSP VLBI stations are plotted. Figures 4.7, 4.8, and 4.9 show the three dimensional displacements of Koganei, Miura, and Tateyama stations, respectively. The formal error of the estimation is shown by a vertical bar in both figures. The variations in baseline length and three components of site position are fitted by linear lines and the best fit lines are shown by straight solid lines. The reduced chi-squared value of the fit for the baseline length data in the Figure 4.7 is 3.0 and the weighted rms of residuals is 3.1 mm. The values for the other baselines and horizontal components of site positions are similar whereas the weighted rms of residuals for vertical components of site positions is larger (17.6 mm for Koganei station for example). The fact that the reduced chi-squared value is significantly greater than 1.0 indicates that either all the formal errors were underestimated or there may have been a systematic error with seasonal variation. In the figures, one can also see evidence of gradual improvements in data quality with time. The results after September 30, 1997 are remarkable, reflecting the extended duration of each experiment. The formal errors in baseline length estimates decreased to about 1 mm and, if only the data after September 30, 1997 were used, the weighted rms residual would be about 2 mm. Estimated three-dimensional site positions for the same period yielded the weighted rms residual as about 2 mm for the horizontal components and 9 mm for the vertical component.

Table 4.1 tabulates the lengths of six baselines estimated for the epoch of September 1, 1996, and their rates of change estimated from all the data by least squares estimation. Both the baseline lengths and their rates of change have been precisely determined from more than three years of experiments. These results, as well as the three-dimensional station positions, are updated every time either an initial data analysis is done or a reanalysis is done using updated EOP, and they are made publicly available from the Internet via WWW and ftp servers. The correlated amplitudes of observed radio sources are also accessible through the Internet and can be utilized for astronomical purposes.

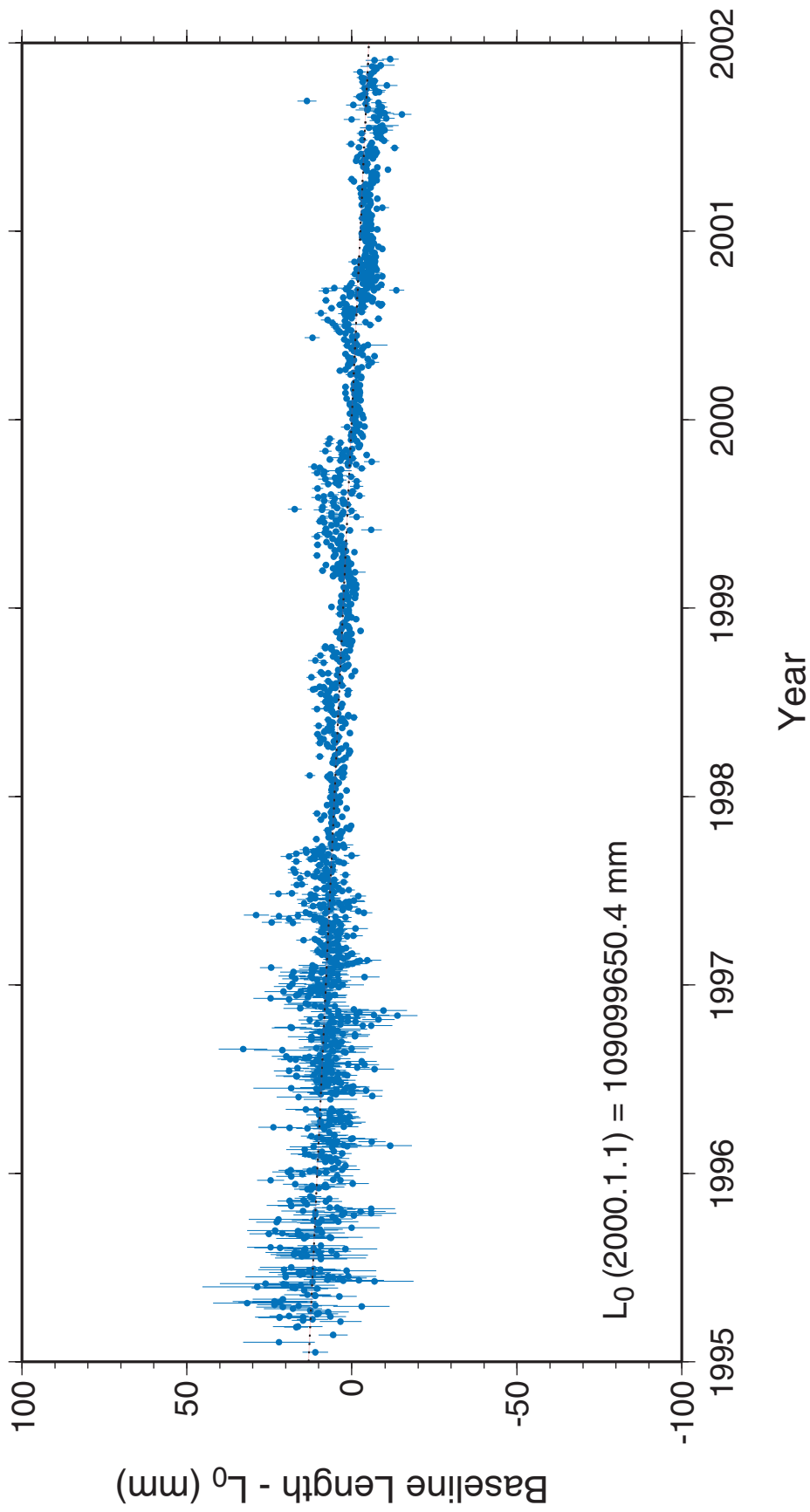


Figure 4.1 Length of the baseline between Kashima and Koganei stations estimated from the KSP VLBI experiments. Estimated uncertainties in the estimates are shown by the one-sigma formal error. The epoch value of the baseline length L_0 and the rate of change were estimated from the data before June 2000 by the least squares estimation and L_0 was subtracted from each data.

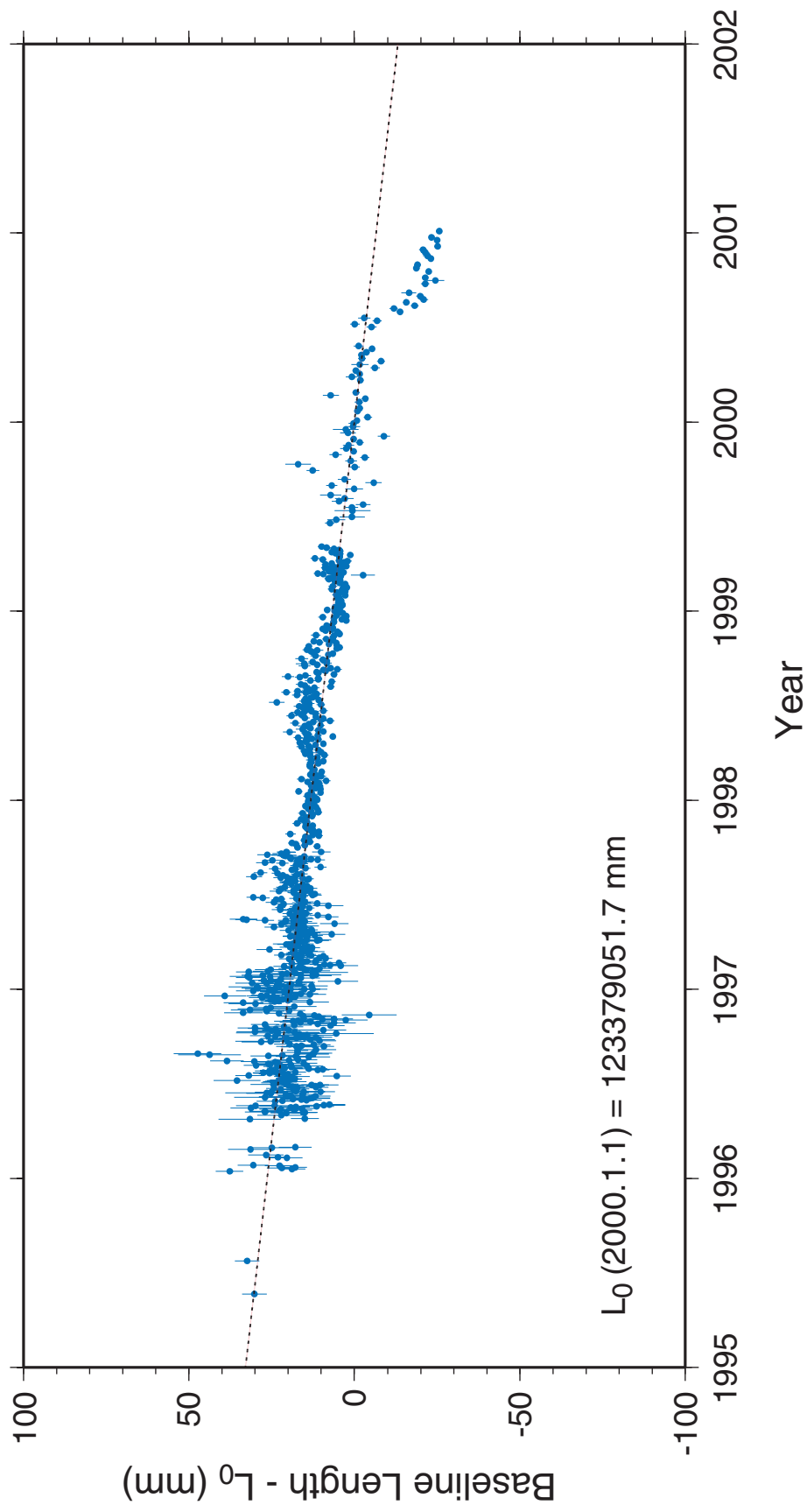


Figure 4.2 Length of the baseline between Kashima and Miura stations.

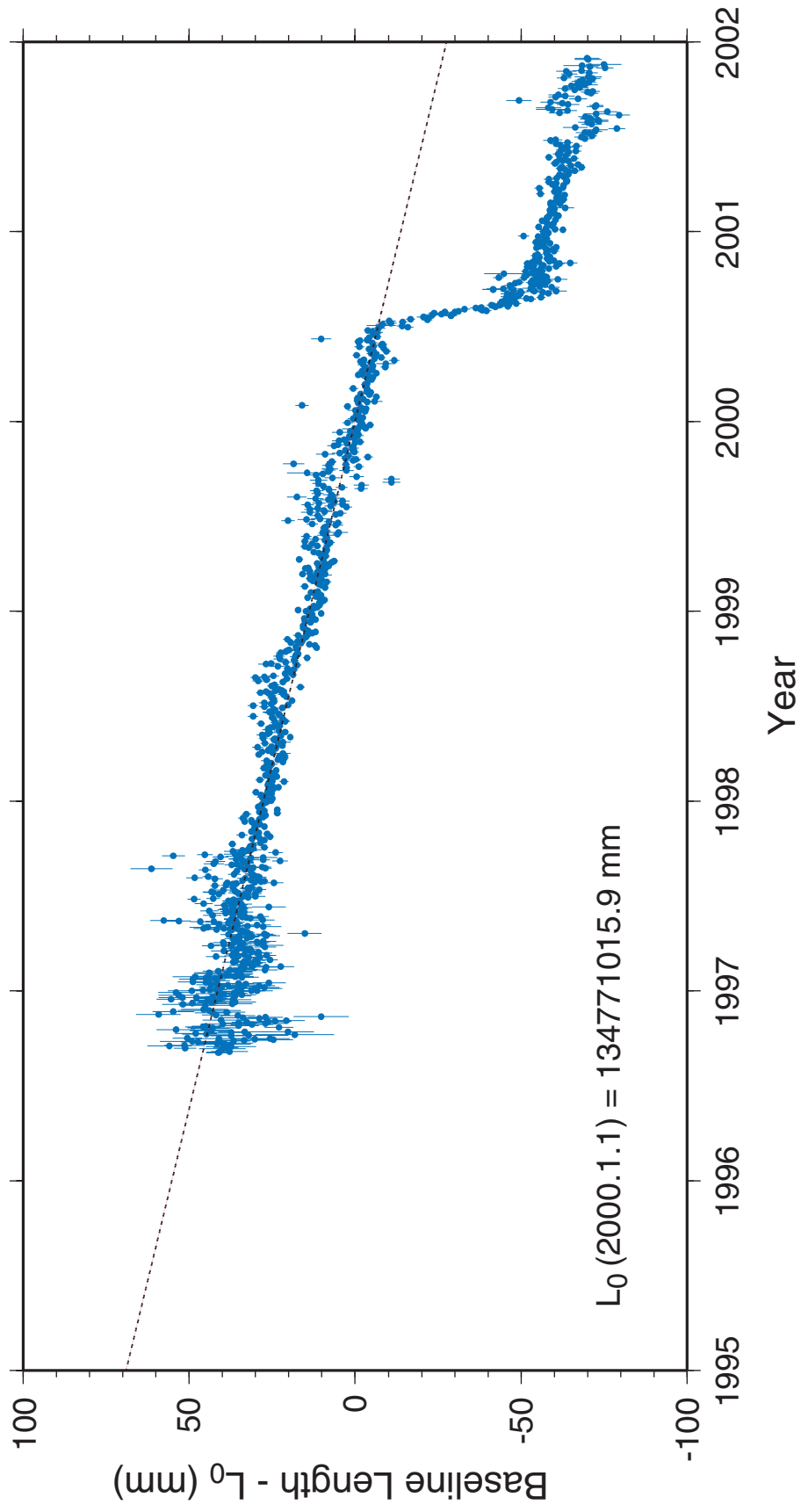


Figure 4.3 Length of the baseline between Kashima and Tateyama stations.

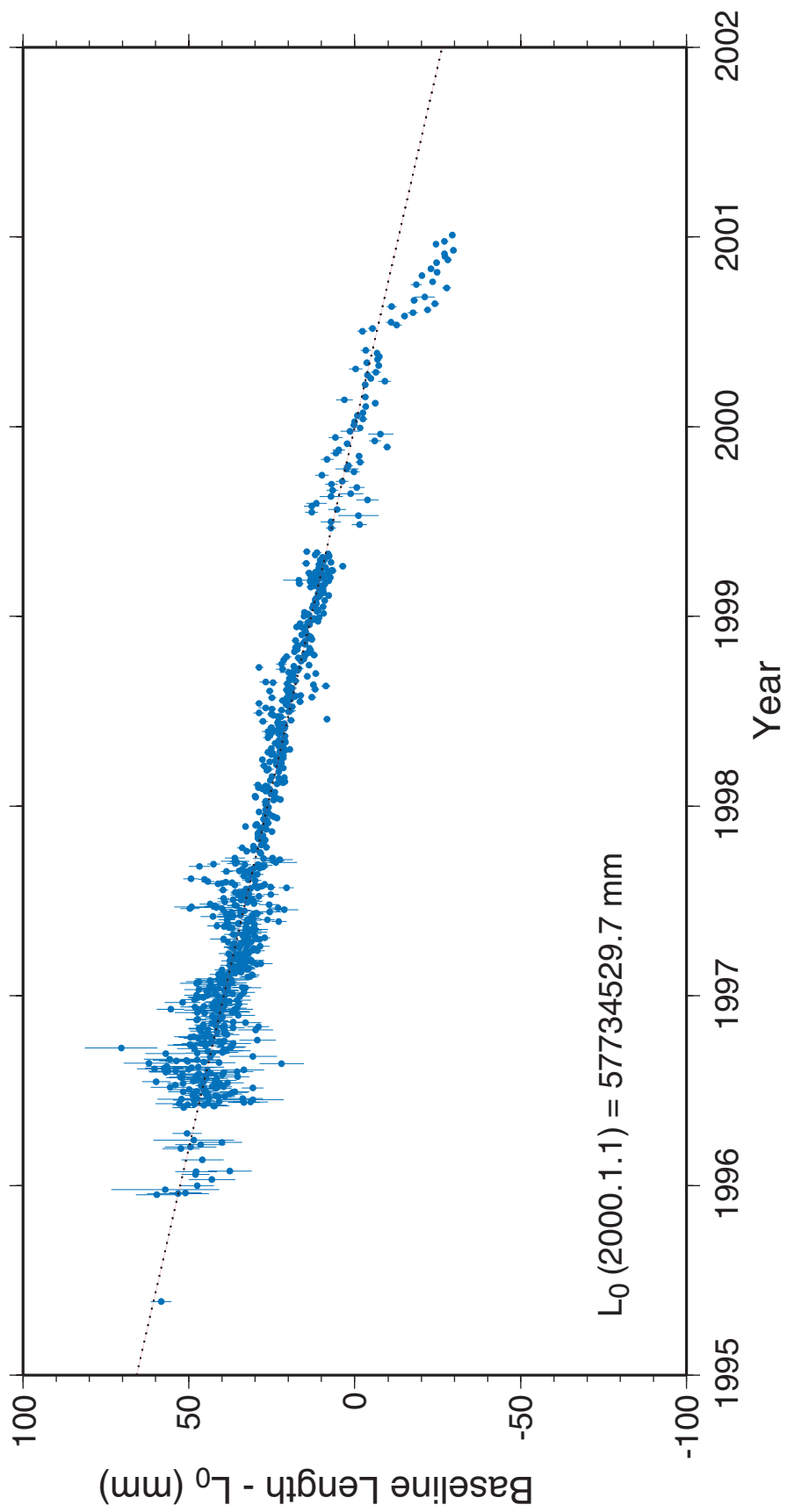


Figure 4.4 Length of the baseline between Koganei and Miura stations.

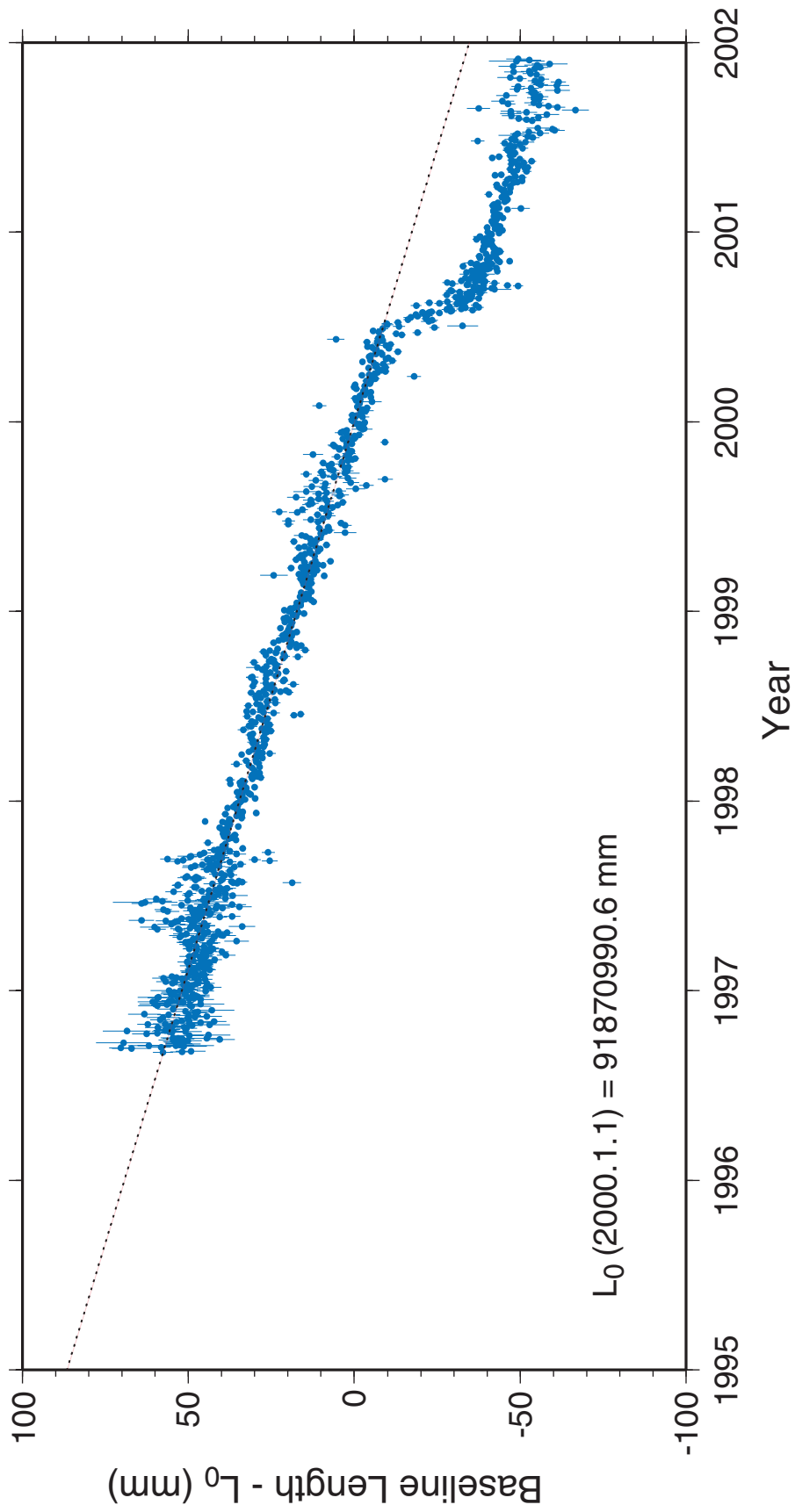


Figure 4.5 Length of the baseline between Koganei and Tateyama stations.

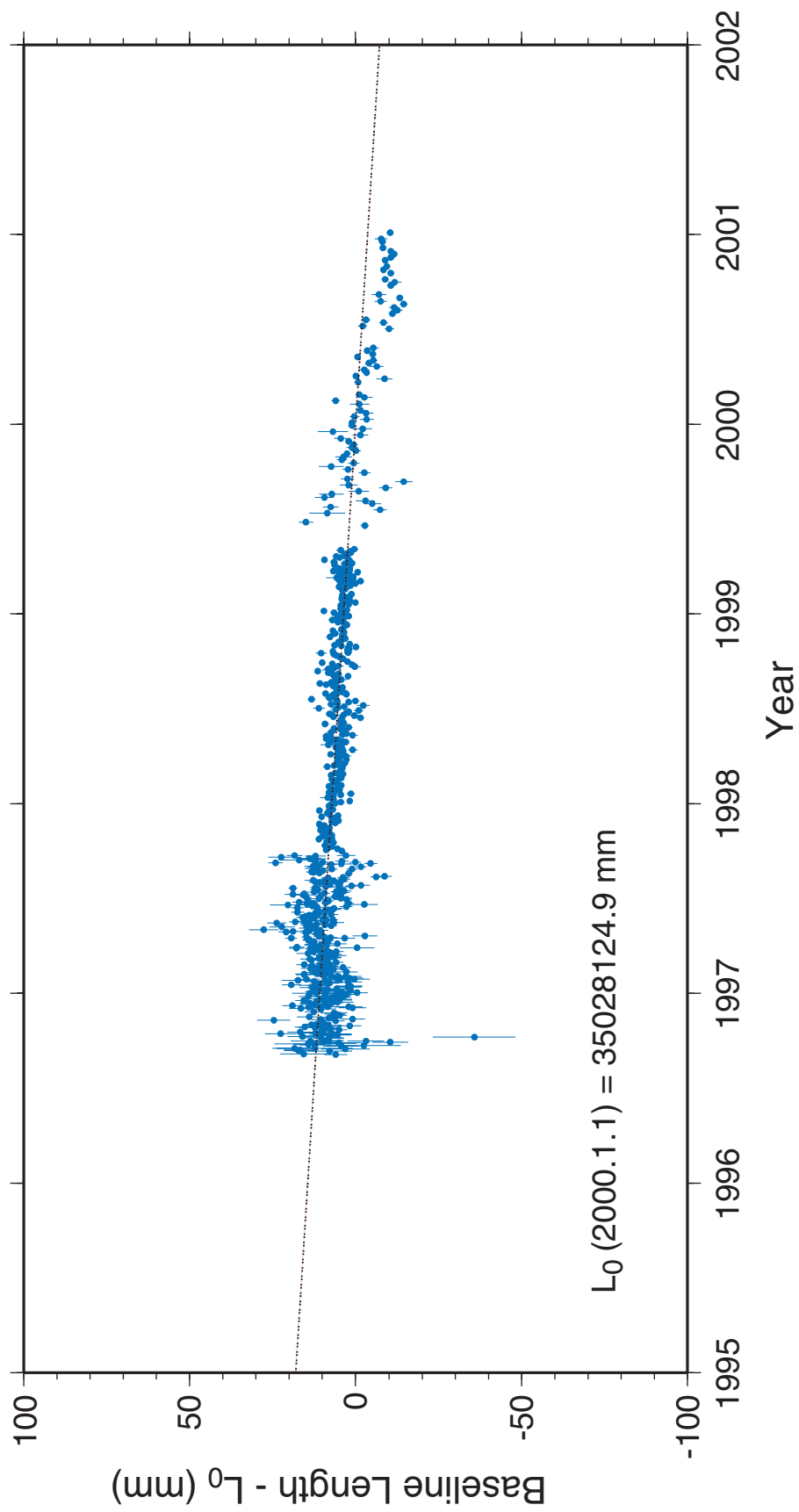


Figure 4.6 Length of the baseline between Miura and Tateyama.

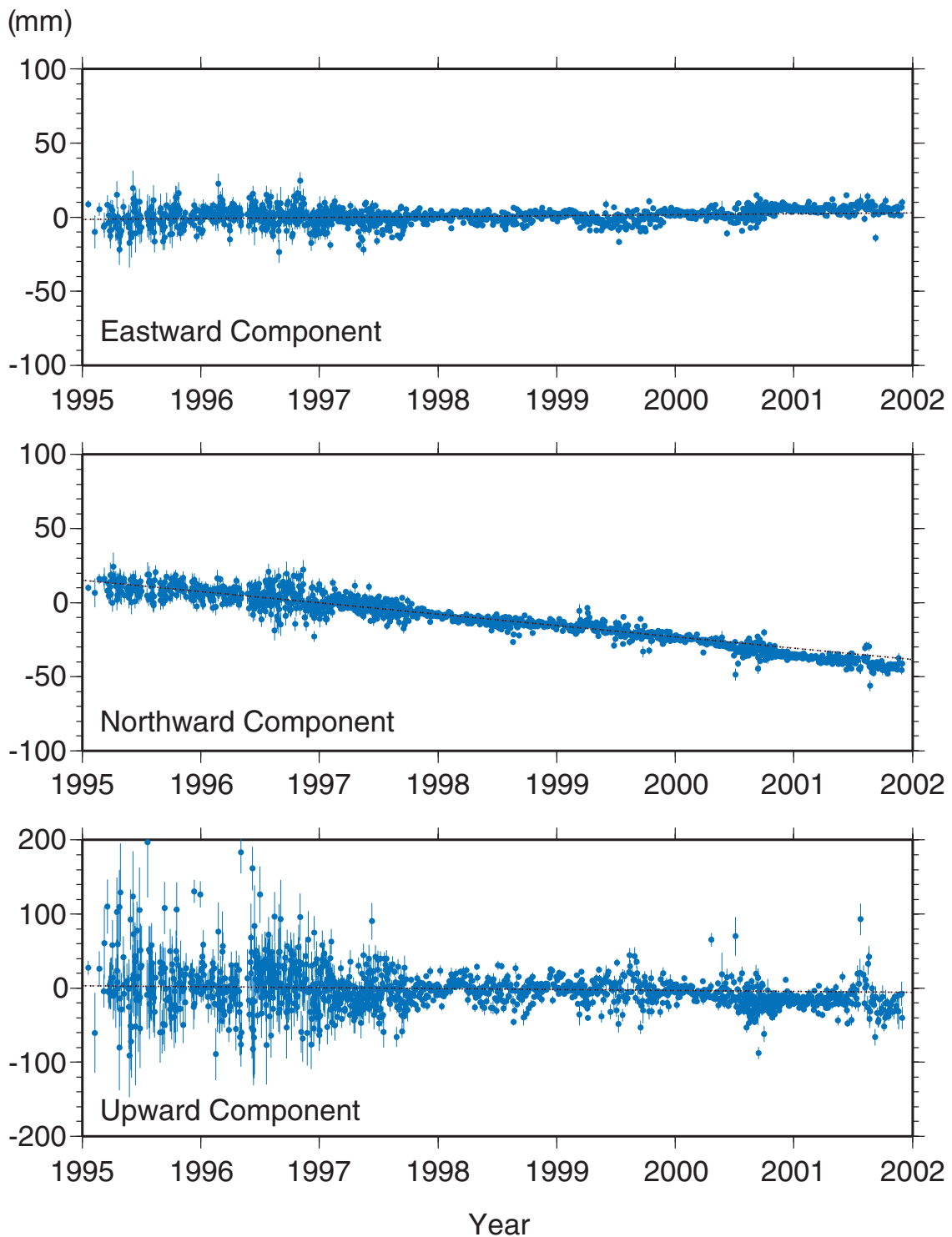


Figure 4.7 Site position of the Koganei station in the local cartesian coordinate system. Estimated uncertainties in the estimates are shown by the one-sigma formal error. A straight line in each figure is showing the best-fit line to the estimated site position before June 2000.

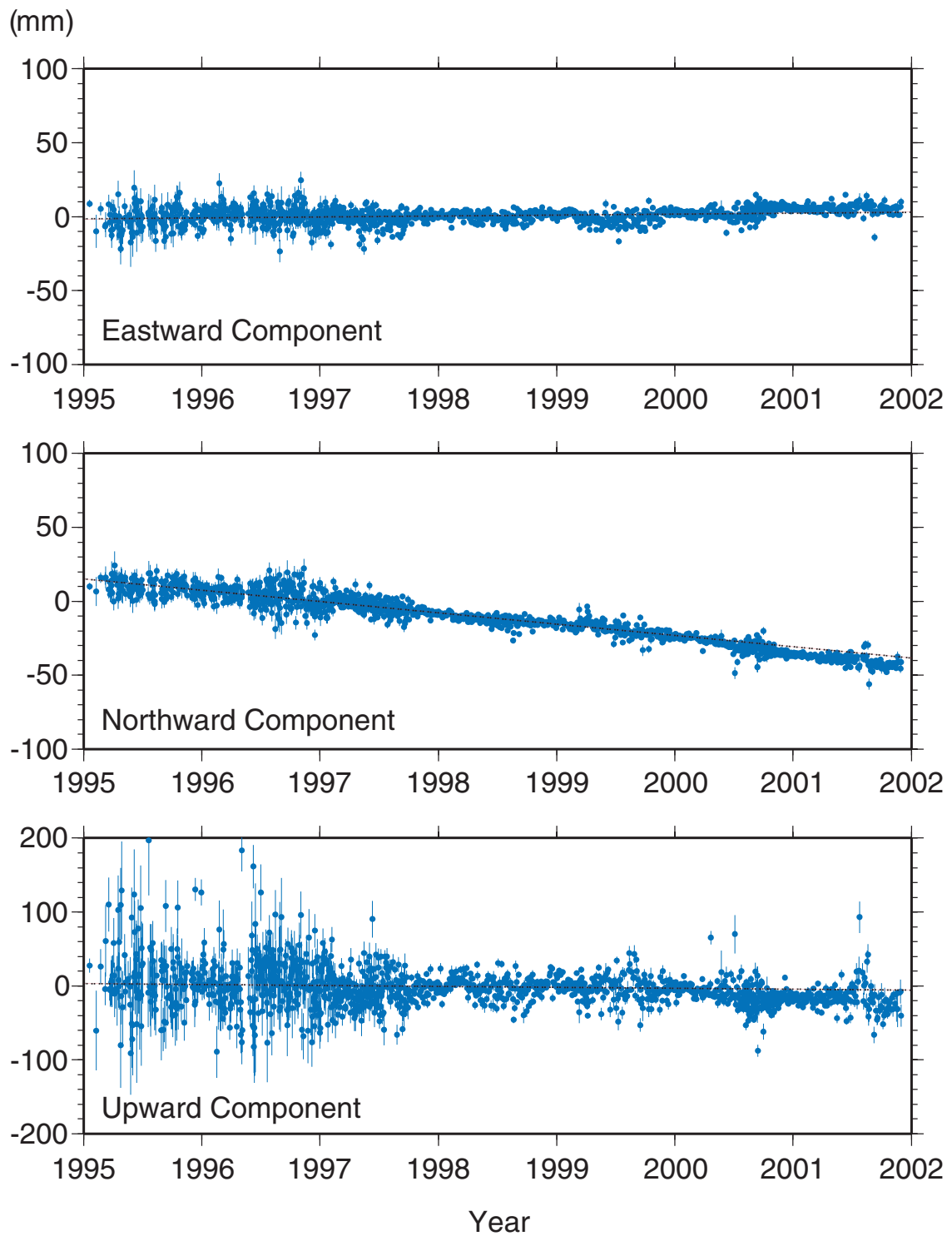


Figure 4.8 Site position of the Miura station in the local cartesian coordinate system.

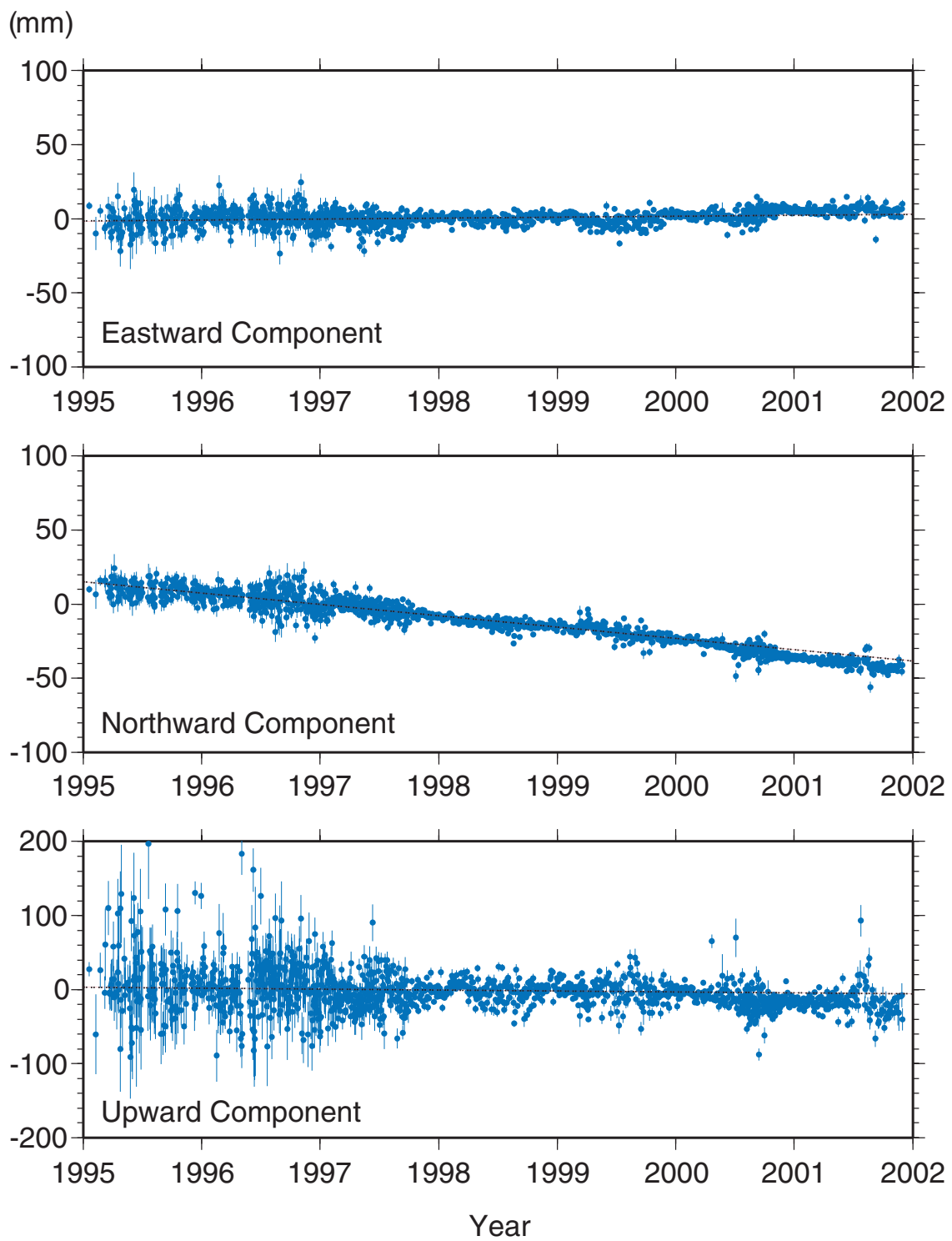


Figure 4.9 Site position of the Tateyama station in the local cartesian coordinate system.

Table 4.1 Baseline lengths L_0 on the epoch of January 1, 2000 and their rates of change estimated for six baselines by the least squares estimation.

Baseline	Baseline Length L_0 epoch : Jan. 1, 2000 (mm)	Rates of Change (mm/year)
Kashima-Koganei	109099650.39 ± 0.06	-2.61 ± 0.04
Kashima-Miura	123379051.67 ± 0.11	-6.60 ± 0.06
Kashima-Tateyama	134771015.90 ± 0.08	-13.79 ± 0.05
Koganei-Miura	57734529.69 ± 0.10	-13.17 ± 0.06
Koganei-Tateyama	91870990.58 ± 0.07	-17.32 ± 0.05
Miura-Tateyama	35028124.86 ± 0.11	-3.59 ± 0.06

4.2 Wide Area Deformation Due to Volcanic Activities

Site positions of the three VLBI stations at Koganei, Miura, and Tateyama are estimated with respect to the site position of the Kashima VLBI station by performing geodetic VLBI experiments regularly under the KSP. Until recently, steady motions of the three stations were observed with respect to the Kashima station, and these motions were well explained by the effects of the relative motions of the Pacific Plate and the Philippine Sea Plate with respect to the North American Plate. However, a remarkable change of the Tateyama site position was noticed in the middle of July 2000. Immediately after the unusual motion of the Tateyama station was recognized, the frequency of the real-time VLBI experiments with three stations at Kashima, Koganei, and Tateyama were doubled to the every day basis from the regular frequency of once every two days. Since the high speed ATM (asynchronous transfer mode) digital network to the Miura station became unavailable from the beginning of May 1999, the VLBI experiments including the Miura station is now performed only by the conventional tape-based VLBI observations, and the frequency of the all four sites are performed once every six days. Because the frequency of the VLBI experiments with the Miura station is very low, it took a while to obtain convincing results but the extraordinary site displacement is also apparent at Miura station. Figure 4.10 shows the baseline lengths of the Kashima-Tateyama baseline.

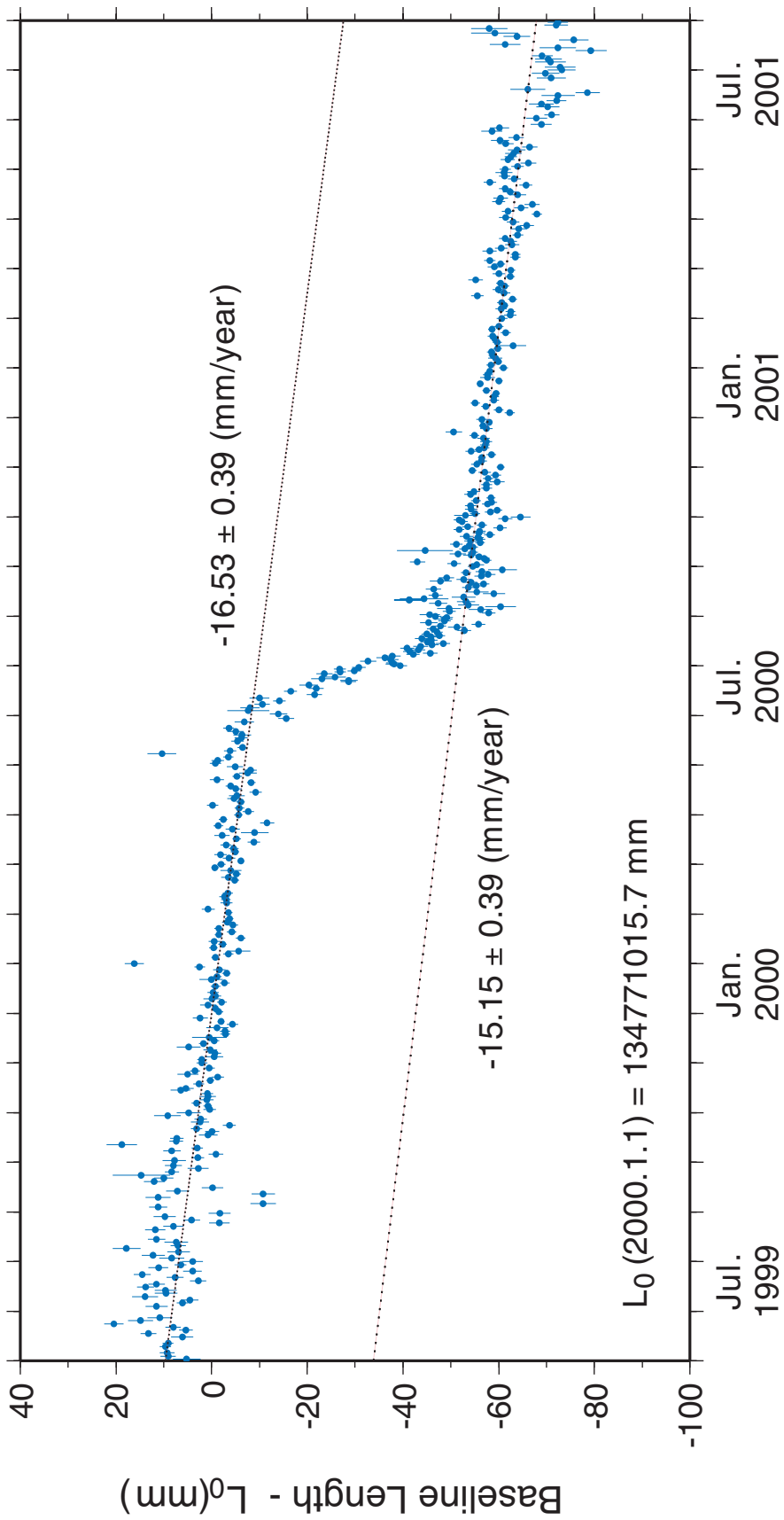


Figure 4.10 Baseline length between Kashima and Tateyama stations for the period between June 1999 and August 2001. Dotted straight lines are the linear fits for two periods before June 1, 2000 and after September 1, 2000.

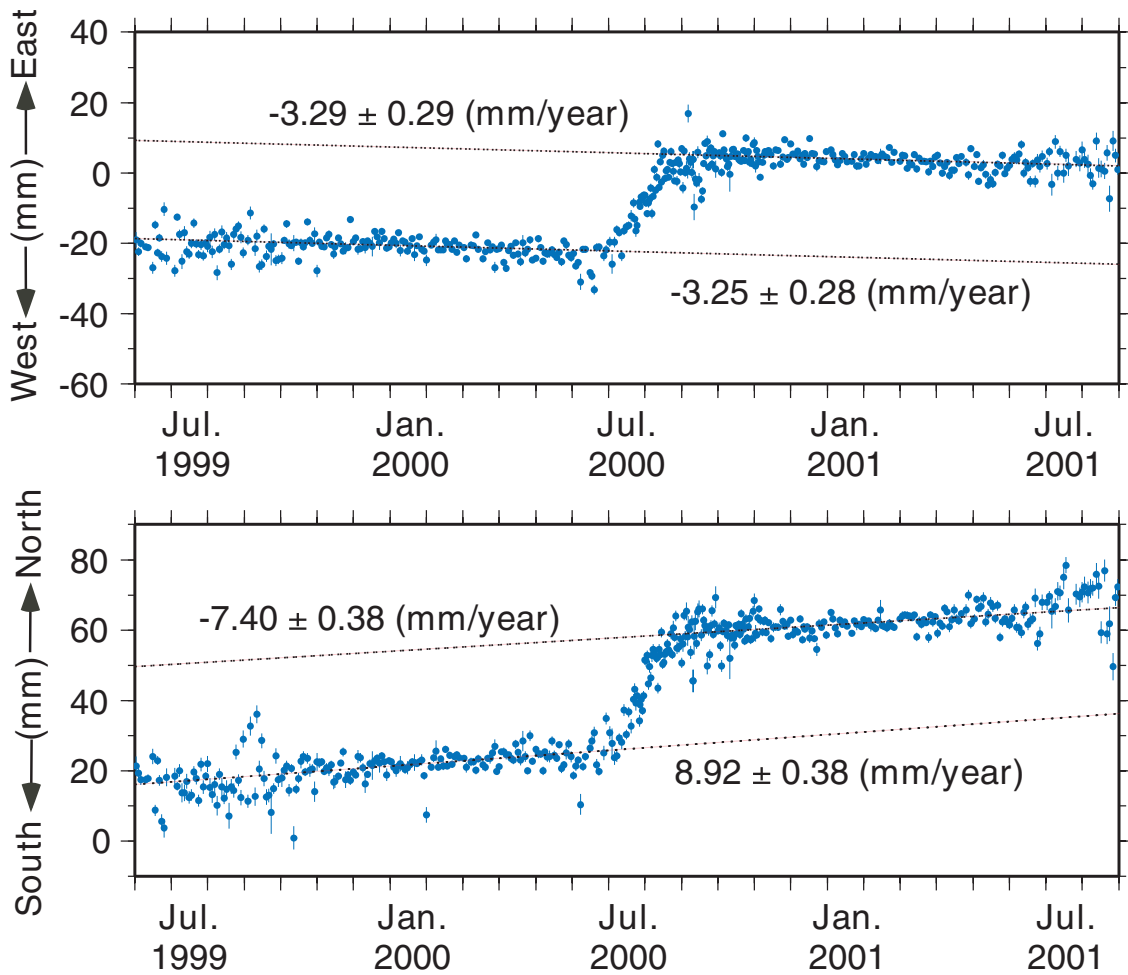


Figure 4.11 Displacement of Tateyama station in the horizontal plane. Dotted straight lines are the linear fits for two periods before June 1, 2000 and after September 1, 2000.

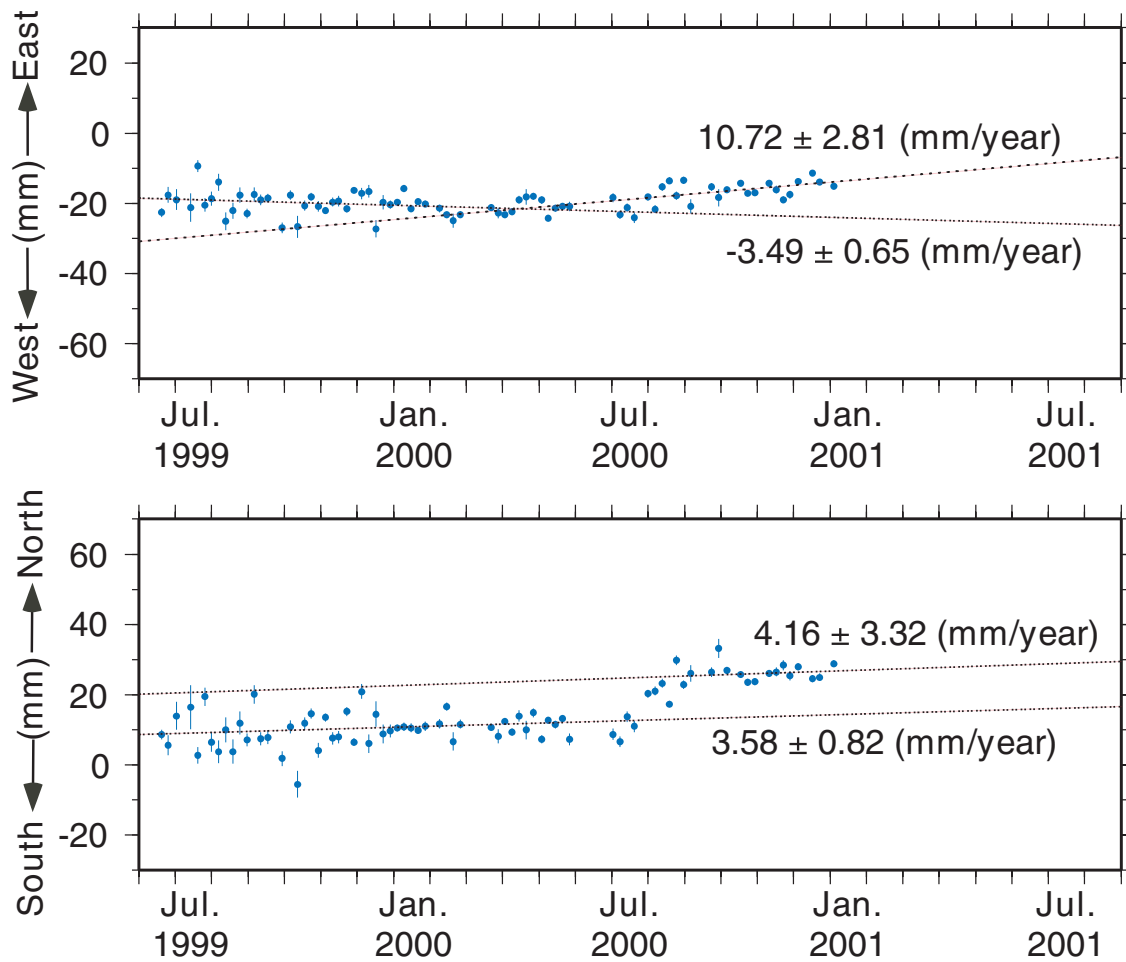


Figure 4.12 Displacement of Miura station in the horizontal plane.

It is apparent that the extraordinary change of the baseline lengths began at some time between the end of June and the beginning of July. Similarly, large displacements of the GPS observation sites in the area near the Izu islands have been found in the results of the continuous GPS monitoring network operated by the Geographical Survey Institute. These results indicate that a wide area crustal deformation occurred in the area. Almost at the same time when the deformation began, seismic activities in the area of the Izu Islands and volcanic activities at Miyakejima Island began. The epicenter of the earthquake swarm moved from the west side of the Miyakejima Island to the area east of the Kozushima Island. The volcanic activities at the Miyakejima Island started on 26 June 2000 and have been continued until present. A few eruptions occurred during the period and emissions of the volcanic gases are still continuing. On the other hand, the earthquake swarm continued for about two months and it became quiet. The cause of the earthquake swarm is explained by an intrusion of a dyke in the area. By considering a dyke model, both the earthquake swarm and the crustal deformation can be explained. The motion of the epicenter from the Miyakejima Island to the eastern off of the Kozushima Island is explained by a model which assumes that a huge amount of magma under the Miyakejima Volcano moved to the east of the Kozushima Island. The model is consistent with the actual phenomena of the collapse of the summit of the Oyama Mountain which is the volcano of the Miyakejima Island. Tateyama and Miura are located about 50 km northeast of the epicenter of the earthquake swarm and the motions of these sites provide useful condition to constrain various parameters of the dyke model. In Figures 4.10, 4.11, and 4.12, the linear fits before and after the event are shown by straight lines and the estimated rates of change are also shown. The rates can be considered to be almost same before and after the event for the baseline length of Kashima-Tateyama baseline and site position of Tateyama station, whereas the rates of site position for Miura are significantly different before and after the event. These results are suggesting the deformation was almost settled by September 2002, but the relaxation process might be remaining for a while.

Figure 4.13 shows the site velocities of the Keystone VLBI sites observed before extraordinary site motions began while Figure 4.14 shows the site displacements observed during the period between the end of June 2000 and the middle of September 2000. Figure 4.15 shows the deformation pattern expected from a combination model with a dyke and a strike slip fault. The model was constructed from the distribution of

the epicenter of the earthquake swarm and the crustal deformation observed by the GPS and VLBI measurements. The dyke is assumed to be 5m thick with a depth of 3 km and dimensions of 20 km (horizontal) and 12 km (vertical). The fault is assumed to have a slip of 4 m with a depth of 3 km and dimensions of 5.9 km (horizontal) and 10 km (vertical).

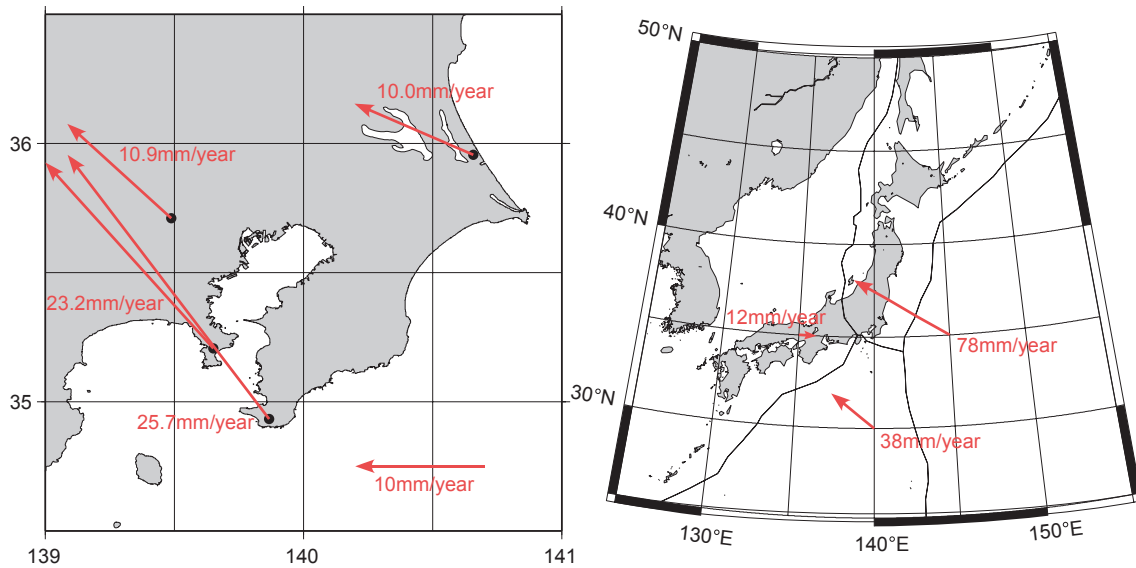


Figure 4.13 Horizontal site velocities of four VLBI stations of the KSP VLBI Network at Kashima, Koganei, Miura, and Tateyama with respect to the North American Plate (left). Plate motion velocities around Japan with respect to the North American Plate using Nuvel-1A and Seno plate motion models (right).

As shown in Figure 4.15, the model used in the figure well explains the 5cm and 3cm site displacements at Tateyama and Miura stations. The distances from the area where the earthquake swarm concentrate to Tateyama and Miura stations are about 100km and 120km, respectively. The fact that the effect of the crustal deformation extended to such long distances indicates that the depth of the dyke is quite deep. This way, the precise site displacements measured by the geodetic VLBI measurements at Tateyama and Miura provide crucial information which can constrain the parameters of the geophysical model.

Although it was planned to terminate the operations of Tateyama and Miura stations by the end of the year 2000, many efforts were paid to continue the operation at least at Tateyama station. Because of these efforts, it was determined to continue

real-time VLBI operations with three stations at Kashima, Koganei, and Tateyama until the end of 2001.

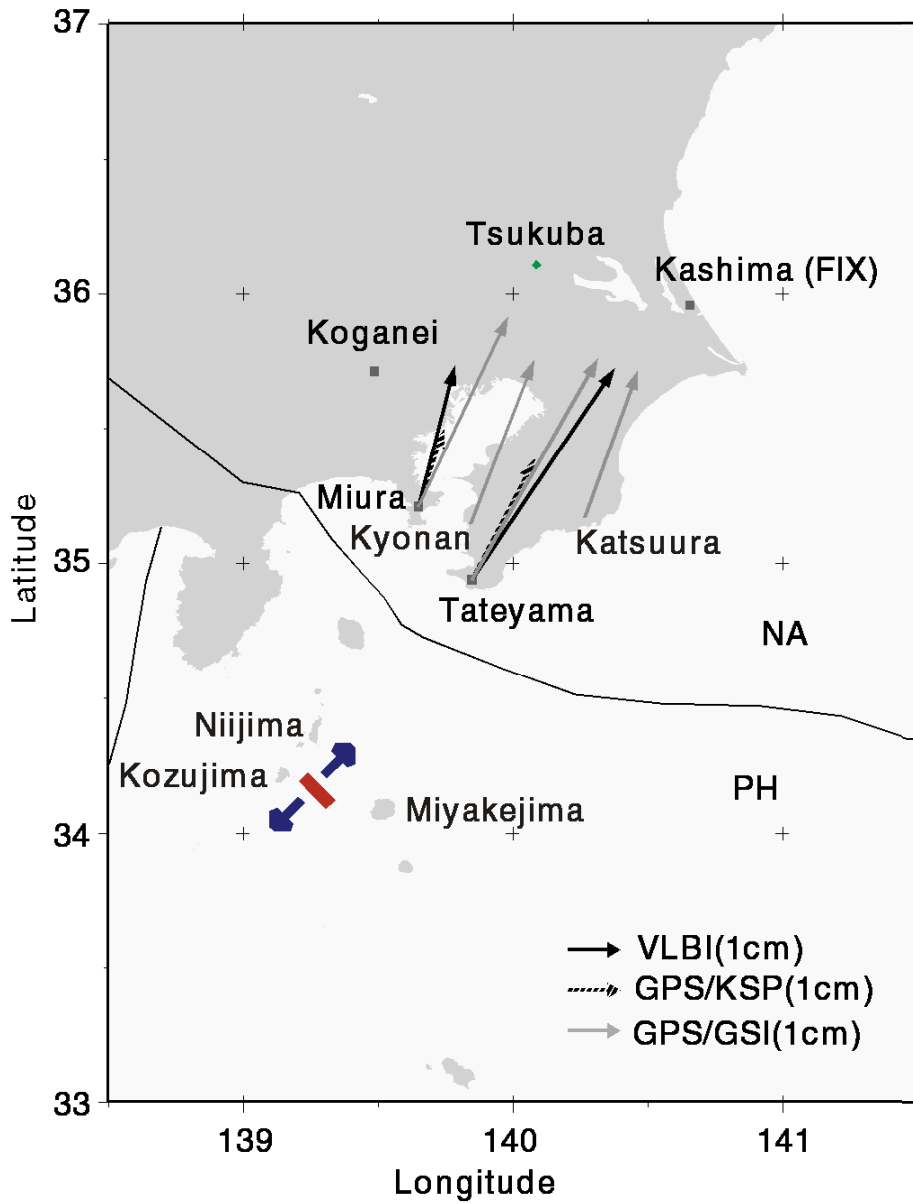


Figure 4.14 Site displacements at Tateyama and Miura sites observed during the three months from the end of June 2000 detected by the KSP VLBI network and a model which can explain the observed crustal deformation.

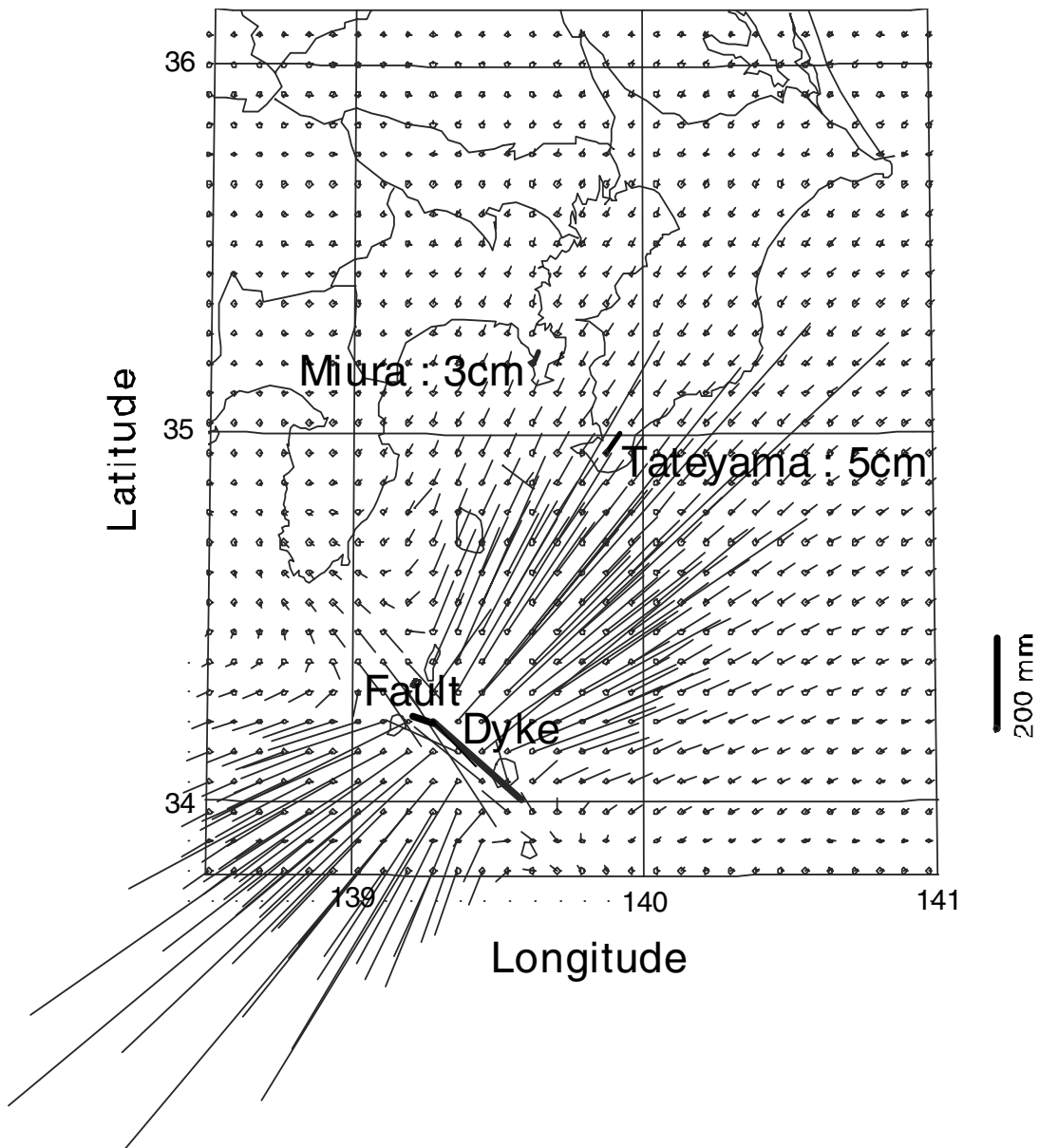


Figure 4.15 A proposed geophysical model with a dyke and a strike slip fault which can explain the observed crustal deformation. The dyke is assumed to be 5m thick with a depth of 3km and dimensions of 20km (horizontal) and 12km (vertical). The fault is assumed to have a slip of 4m with a depth of 3km and dimensions of 5.9km (horizontal) and 10km (vertical). The model parameters were taken from a model proposed by the group of Nagoya University. The displacements were calculated by the software MICAP-G developed by the Meteorological Research Institute.

Chapter 5 Flux Density Variation of Radio Sources

5.1 Background

Compact and strong radio sources were repeatedly observed in regular geodetic very long baseline interferometry experiments under the KSP. The flux densities of these sources in the S and X bands were estimated from a set of correlated amplitudes obtained through the correlation processing of the observed data. From ~5 years of the observed data, irregular variations in the flux densities were detected for several radio sources using the source 2134+004 as the calibrator. The results showed the monitoring of flux density variations by means of very long baseline interferometry is feasible. Since the correlation processing of the observed data are performed real-time using a high-speed digital communication technique, this method gives a capability to monitor flux density variations of quasars and BL-Lac types of extragalactic radio sources.

Variations in the flux densities of extragalactic radio sources have been studied for various sources and in various frequency bands. It is known that some of the quasars and BL-Lac types of extragalactic sources show rapid variability, and these sources are categorized as blazars. Observations of blazars during the outbursts in many wavelengths ranging from radio to X ray can give us useful information to investigate physical properties of the phenomena, [e.g., *Sincell*, 1997; *Türler et al.*, 1999]. Extremely scattering events were also monitored at S band and X band by using a connected element interferometer for ~8 years from 1979 [*Fiedler et al.*, 1987; *Waltman et al.*, 1991]. In this paper, we present a method to monitor the variability in the microwave region by using geodetic very long baseline interferometry (VLBI) observation data. The VLBI technique has been used in the various field of geodesy, astrometry, and astronomy for a few decades, and VLBI observations are frequently performed with many varieties of configurations and purposes at present. However, the monitoring of microwave variability by means of the VLBI technique had not been realistic because the configurations of the VLBI observations change and the characteristics of the receiving systems in a configuration are usually very different. On the other hand, the antennas and related facilities are identical at four observation stations in a VLBI observation network used in this study, and the same set of radio

sources are repeatedly observed by the network. By using the observation data obtained with the network, reliable monitoring of the microwave variability of compact radio sources has been realized. The method used to estimate flux densities of the observed radio sources and the results will be described in this paper. Part of the monitored sources are included in the defining and candidate sources for the International Celestial Reference Frame (ICRF) [Ma *et al.*, 1998], and monitoring the physical behavior of such sources is very important to maintain the quality and reliability of the ICRF.

A VLBI observation network has been established around Tokyo, Japan, as part of the KSP [Yoshino, 1999]. The network consists of four observation sites located in Koganei, Kashima, Miura, and Tateyama. The lengths of the six baselines range from 35 to 135 km. The two main purposes of the KSP VLBI network are to precisely measure relative site positions and to monitor their variations with a minimum delay of processing time. To achieve these purposes, the observation and data analysis system have been fully automated, and a real-time VLBI system has been developed. Consequently, frequent VLBI observations became possible, and the necessary time to obtain results has been minimized [Koyama, 1998]. In a typical case, all the processing of the data analysis is complete in ~12 min after the last observation in the session, and the results are placed in the publicly accessible server from the Internet.

In a VLBI observation, radio signals from a common radio source are received in two frequency bands (i.e., S and X bands) at two or more observation sites. The time delays between signals received at the two sites and their rates of change are obtained through data correlation and bandwidth synthesis processing. These quantities are then used to estimate various parameters, including the coordinates of the observing sites. These are the major products from the geodetic VLBI experiments. At the same time, correlated amplitudes are also obtained as by-products of correlation processing. These correlated amplitudes can be used to monitor variations in the radiation intensity of radio sources.

At present, >500 observations are performed in a standard KSP VLBI experiment, and a precise time delay is obtained for six pairs of sites from each observation after the correlation processing. Various parameters, including site coordinates, clock offsets, and wet atmospheric zenith delays, are estimated from a set of time delay measurements for all baselines and observations after data correlation processing. The correlation processing is performed real time using high-speed digital

communication links, and the final results are obtained immediately after completing all the observations. Such experiments are performed every other day since the end of September 1997. Until the end of September 1997, the high-speed digital links between the observation stations were not available, and the VLBI experiments were performed 6 hours every day using VLBI data recorders. All the experiments performed between March 1996 and August 2000 were included in this study.

5.2 Observations

The first VLBI experiment with the KSP VLBI network was performed on August 30, 1994, by using two observation sites at Kashima and Koganei. The first VLBI experiment using the third site at Miura was performed on May 22, 1995, and the regular VLBI experiments began in March 1996 with these three stations when a tape-based VLBI correlator commenced operation. The first experiment using the fourth site at Tateyama was performed on September 3, 1996, and the regular VLBI experiments with the four stations began since then.

KSP VLBI observations are performed by receiving radio signals from compact celestial radio sources using 11-m fully steerable cassegrain antennas at four observation sites. These antennas are equipped with S band (2100-2500 MHz) and X band (7700-8600 MHz) receivers. Propagation time delays and their rates of change in the X band are the primary observable in the geodetic data analysis, and the S band data are used to evaluate ionospheric propagation effects on the time delays.

Received right-hand circular polarization signals in the S and X bands are converted to intermediate frequency (IF) signals from 500 to 1000 MHz. Sixteen frequency channels (6 in the S band and 10 in the X band) are allocated within the received signal ranges, and base-band signals with 32 MHz of bandwidth are produced with image rejection mixer units. Frequencies of the observation channels were determined by optimizing the delay resolution function, which is produced by the bandwidth synthesis technique. The average of the frequencies of observation channels is 2275 MHz for S band and 8137 MHz for X band.

Base-band signals are sampled at a rate of 64 MHz, and a low-pass digital filter algorithm is applied to the sampled data. The total data, at rates of 64 or 256 Mbps, are then either recorded by a data recorder or transferred to a correlator facility at Koganei

through optical fibers in the asynchronous transfer mode (ATM). After this process is complete, correlated amplitudes are obtained. The obtained correlated amplitudes are proportional to the flux density of sources as given in the equation (2.1) and can be used to monitor the variations of the microwave radiation intensities. Typically, ~580 observations are performed in consecutive 23.5 hours, and each radio source is repeatedly observed for 20-40 times within the same time period. The duration of each observation is determined to the time length between 60 and 360 s, depending on the flux densities of the radio source to be observed. The observed radio sources are listed in the Table 5.1. The coordinates and the type of radio sources listed in the table are from Ma and Feissel [1997]. The sizes in S and X bands were evaluated from contour maps of the radio sources given by Charlot [1994], Fey et al. [1996], and Fey and Charlot [1997] and in the calibrator source catalog used by the very long baseline array

Table 5.1 Compact Radio Sources Observed by the KSP VLBI Network in Regular Geodetic VLBI Experiments.

Name	Right Ascension	Declination	Size (mas)		Type
			X band	S band	
0059+581	01 ^h 02 ^m 46 ^s	+58°24'11"	7	28	
3C84	03 ^h 19 ^m 48 ^s	+41°30'42"	30	29	galaxy
0420-014	04 ^h 23 ^m 16 ^s	-01°20'33"	9	42	quasar
0552+398	05 ^h 55 ^m 31 ^s	+39°48'49"	6	20	quasar
0727-115	07 ^h 30 ^m 19 ^s	-11°41'13"	12	47	quasar
4C39.25	09 ^h 27 ^m 03 ^s	+39°02'21"	6	18	quasar
3C273B	12 ^h 29 ^m 07 ^s	+02°03'09"	11	33	quasar
3C279	12 ^h 56 ^m 11 ^s	-05°47'22"	16	71	quasar
1308+326	13 ^h 10 ^m 29 ^s	+32°20'44"	11	25	quasar
1334-127	13 ^h 37 ^m 40 ^s	-12°57'25"	10	27	quasar
3C345	16 ^h 42 ^m 59 ^s	+39°48'37"	12	67	quasar
NRAO530	17 ^h 33 ^m 03 ^s	-13°04'50"	10	62	quasar
1921-293	19 ^h 24 ^m 51 ^s	-29°14'30"	14	38	BL Lac
2134+004	21 ^h 36 ^m 39 ^s	+00°41'54"	8	22	quasar
2145+067	21 ^h 48 ^m 06 ^s	+06°57'39"	12	94	quasar
3C454.3	22 ^h 53 ^m 58 ^s	+16°08'54"	20	26	quasar

of National Radio Astronomy Observatory. The majority of the sources are categorized as quasars, and two BL-Lac objects and one radio galaxy are included in the target radio sources. Eight radio sources (i.e., 3C84, 0420-014, 3C273B, 3C279, 1308+326, 3C345, NRAO530, and 3C454.3) are the blazars. Two sources (i.e., 1308+326 and 2145+067) are included in the defining source in the latest ICRF, and one source (i.e., 0552+398) is included in the candidate source in the ICRF.

5.3 Flux Density Estimation Method

In the processing of the VLBI observation data, the correlator produces correlated amplitudes in addition to the delays and delay rates which are the main observables used in the geodetic VLBI data analysis. In the KSP VLBI data processing system the postcorrelation software makes necessary corrections for various loss factors, such as one-bit sampling and three-level approximation in the fringe rotation algorithm. The correlated amplitudes are proportional to the flux densities of the observed radio sources. To use the correlated amplitudes for the evaluation of the flux densities of the observed sources, however, the noise generated in the receiving system and that transmitted from the atmosphere must also be evaluated. By expressing the power of noise in temperature, the correlated amplitude ρ can be evaluated by using the following equations.

$$\rho = \text{sqrt}(T_{\text{src},1}' T_{\text{src},2}') / \text{sqrt} \{ (T_{\text{sys},1} + T_{\text{src},1}') (T_{\text{sys},2} + T_{\text{src},2}') \} \quad (5.1)$$

$$T_{\text{src},i}' = T_{\text{src},i} e^{-\tau_i}, \quad (i=1,2) \quad (5.2)$$

$$T_{\text{sys},i} = T_{\text{ant},i} + T_{\text{atm},i}(1-e^{-\tau_i}), \quad (i=1,2) \quad (5.3)$$

In equations (5.1)-(5.3), τ_i is the optical depth of the atmosphere and $e^{-\tau_i}$ is the absorption factor due to the atmosphere at the i -th site. This factor and the physical temperature of the atmosphere at the i -th site $T_{\text{atm},i}$ are related to the contribution from the atmosphere to the system noise as in (5.3). $T_{\text{ant},i}$ in (5.3) is the antenna noise temperature of the i -th site, which includes the power of the noise generated in the receiving system and the power of the noise associated with background radiations. This background radiation is mainly from the antenna structure and the ground. $T_{\text{sys},i}$ is called the system noise temperature and is the sum of the antenna noise temperature $T_{\text{ant},i}$ and

the contribution from the atmosphere. $T_{src,i}$ is the increase in noise power due to the observed source, expressed by an equivalent temperature. If the source has an extended structure that cannot be ignored compared to the fringe spacing, $T_{src,i}$ must be multiplied by a visibility factor between 1 and 0. However, the minimum fringe spacing of the KSP VLBI network is ~ 0.053 arc sec for the X band and ~ 0.18 arc sec for S band. Therefore the sizes of all the sources in the Table 5.1 are small enough to assume that the visibility factor is 1.

By assuming a simple uniform distribution model for the atmosphere, τ_i can be expressed as $ah / \sin \theta$, $\theta = (\theta_1 + \theta_2)/2$, where h is the height of the atmosphere model and θ_i is the elevation angle of the source at the i -th site. The coefficient a is a factor which is proportional to the opacity of the atmosphere. In this model the atmosphere is assumed to be uniform from the ground to the height h . In addition, the atmospheric condition at two observation sites is assumed to be the same, and the average of the two elevation angles at two sites is used to evaluate the elevation angle of the observed source. Since the geographical locations of the observation sites in the KSP network are close, the difference of the elevation angles can be ignored. Finally, the following equation can be derived by approximating $e^{-\tau_i}$ with $1 + \tau_i$ because τ_i is considered to be very small.

$$1 / \rho - 1 = \text{sqrt}(T_{ant,1} T_{ant,2}) / \text{sqrt}(T_{src,1} T_{src,2}) (1 + ah(1+b) / \sin\theta). \quad (5.4)$$

In (5.4), $\text{sqrt}(T_{atm,1} T_{atm,2}) / \text{sqrt}(T_{ant,1} T_{ant,2})$ was replaced with b . By using a set of correlated amplitudes ρ at various elevation angles the values of $ah(1+b)$ and $\text{sqrt}(T_{ant,1} T_{ant,2}) / \text{sqrt}(T_{src,1} T_{src,2})$ can be evaluated by using the least squares estimation. Figure 5.1 shows an example of the results obtained with a baseline between two stations at Kashima and Miura during an experiment performed on March 22, 2000. In Figure 5.1 the vertical axis is from the left side of (5.4) and the horizontal axis is $1 / \sin\theta$. The results for three radio sources of 3C273B, 3C279, and 1334-127 are shown as a typical example. The dotted lines are the least squares fits for these data. As expected from (5.4), the observed data are closely distributed along each line very well. This example demonstrates that T_{ant} , T_{src} , a , h , and b did not change significantly during the experiment, and the simple atmosphere model offered a good approximation. If the gain of the antenna significantly changes with the elevation angle, for example, the data

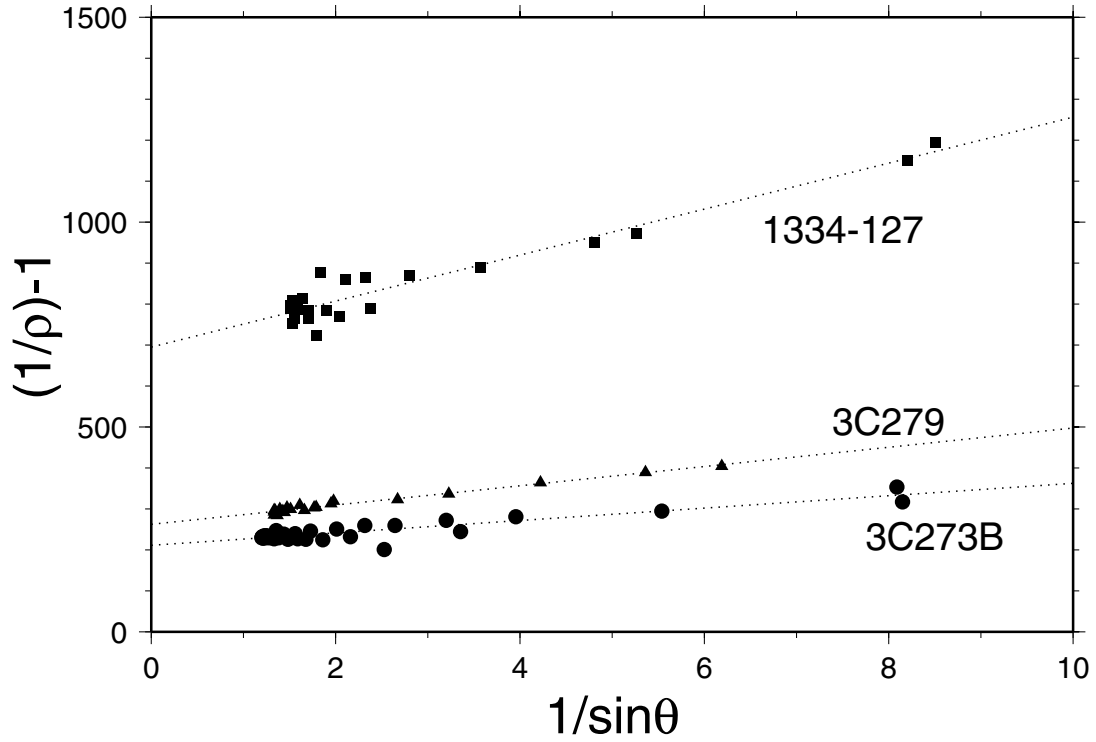


Figure 5.1 Geographical locations of the four observation sites in the KSP VLBI network observation sites. The names of the sites are Kashima, Koganei, Miura, and Tateyama.

points in the Figure 5.1 would not align along a straight line. The points where the lines and vertical axis intersect give approximate values for $\sqrt{T_{\text{ant},1} T_{\text{ant},2}} / \sqrt{T_{\text{src},1} T_{\text{src},2}}$. The expression $ah(1+b)$ can be evaluated by dividing the slope of the line by the estimated value of $\sqrt{T_{\text{ant},1} T_{\text{ant},2}} / \sqrt{T_{\text{src},1} T_{\text{src},2}}$.

Once the values of $\sqrt{T_{\text{ant},1} T_{\text{ant},2}} / \sqrt{T_{\text{src},1} T_{\text{src},2}}$ and $ah(1+b)$ are estimated, the flux density of the source can be obtained by the following equation.

$$S_{\text{src}} = \sqrt{S_{\text{ant},1} S_{\text{ant},2}} / \sqrt{\{ (T_{\text{ant},1} T_{\text{ant},2}) / (T_{\text{src},1} T_{\text{src},2}) \}} \quad (5.5)$$

In (5.5), S_{src} is the flux density of the source, and $S_{\text{ant},i}$ is the equivalent flux density of the antenna noise at the i -th site. The equivalent flux density of the antenna noise $S_{\text{ant},i}$ can be evaluated by observing a calibration radio source at various elevation angles. If the signal power of the receiver output is measured while the calibration radio source is tracked by the antenna P_{on} and while the antenna beam is offset from the source P_{off} , the

$S_{ant,i}$ is given by the following equations.

$$P_{on} / P_{off} = S_{ant,i} + S_{atm}(1 - e^{-\tau}) + S_{cal}e^{-\tau} / S_{ant,i} + S_{atm}(1 - e^{-\tau}) \quad (5.6)$$

$$S_{cal} / (P_{on}/P_{off} - 1) = S_{ant,i} + ah / \sin\theta (S_{ant,i} + S_{atm}) \quad (5.7)$$

In (5.6) and (5.7) S_{atm} is the equivalent flux density for the thermal noise power due to the atmosphere, and S_{cal} is the flux density of the observed calibration radio source. Calibration observations were performed by tracking Cas-A. The S_{cal} of Cas-A at S and X bands were taken from the results reported by Wait [Wait, 1983]. The size factor corrections were applied to obtain the values of S_{cal} . The values of $S_{ant,i}$ were estimated by the least squares estimation. The results evaluated from observations toward Cas-A in S and X bands on March 27, 2000 are given in Table 2.1. In the estimations, the power of the antenna noise was assumed to be constant over all elevation angles, and the atmospheric conditions toward different horizontal directions have to be uniform. Once the $S_{ant,i}$ values are evaluated, these values are independent from the variations of the atmospheric conditions due to weather and seasons.

Figure 5.2 shows the estimated flux densities of 3C273B and 2134+004 at X band and S band by using the $S_{ant,i}$ given in the Table 2.1 and the least squares estimations based on (5.4) and (5.5). Results obtained from experiments performed between March 1996 and August 2000 are shown. The high-speed ATM data line became unavailable in March 2000, and number of data after that time is limited because the experiment frequency with the Miura station was decreased from once every 2 days to once every 6 days. An estimated data point was removed if the root-mean-square of the residual after the least squares estimate was too large or if the value $ah(1+b)$ became negative. Figure 5.2 shows that the estimation of the flux density is fairly stable, but the number of successful estimations was small. Figure 5.2 also shows that the flux densities of the 2134+004 are quite stable both at S and X band, while a slow change in the X band flux density is visible for the 3C273B. Earlier monitoring of the 2134+004 also shows stable behavior at two frequency bands, and the flux densities of the source were given as 8.2 and 8.6 Jy ($1 \text{ Jy} = 10^{-26} \text{ Wm}^{-2} \text{ Hz}^{-1}$) at S and X-band, respectively [Fiedler et al., 1987]. Because we could confirm that the 2134+004 does not show significant variations in its flux density, 2134+004 can be used as the calibrator to estimate the flux densities of other sources.

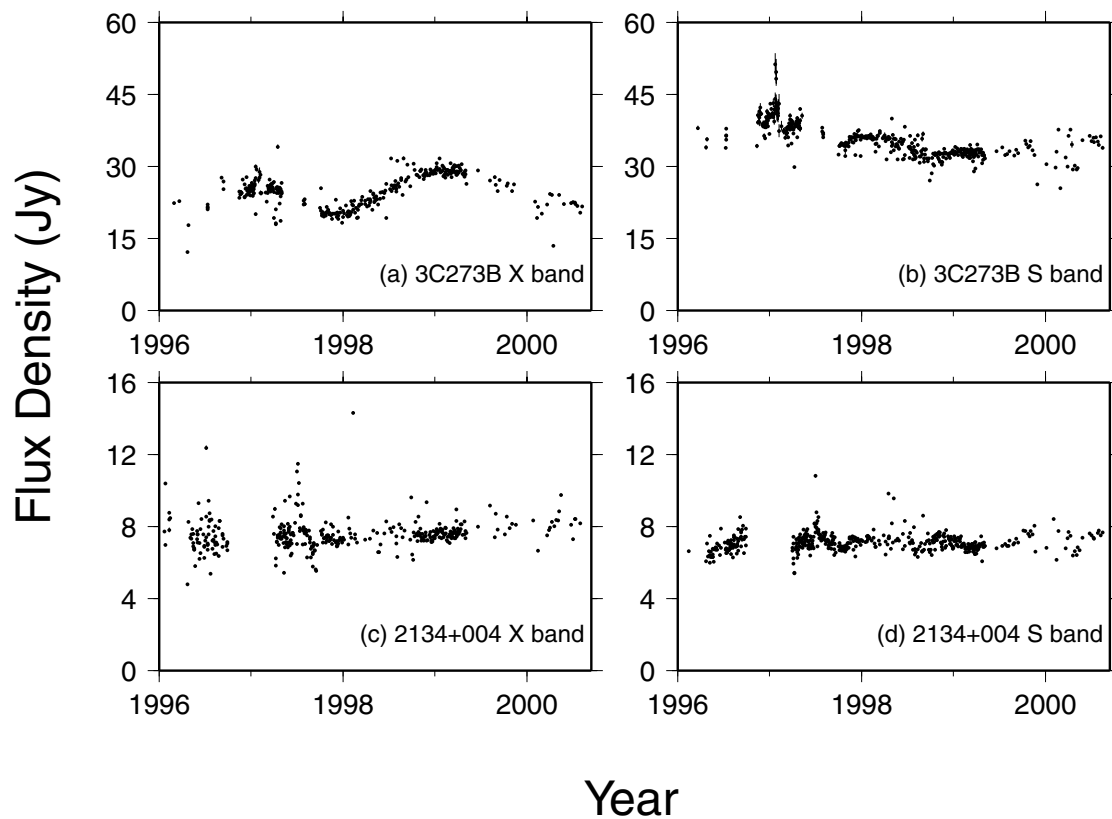


Figure 5.2 Relationship between correlated amplitudes ρ and elevation angles θ shown for three radio sources, e.g., 3C273B (circles), 3C279 (triangles), and 1334-127 (squares). The elevation angles were evaluated by the mean of two elevation angles at two stations. The correlation amplitudes are the results obtained with the baseline between observation sites at Kashima and Miura in X band during an experiment performed for ~ 22.3 hours from 0200 UT on March 22, 2000. The vertical axis is $(1/\rho)-1$ and the horizontal axis is $1/\sin\theta$. The three dotted lines are the least squares fits to the observed data.

Figure 5.3 shows the values of $ah(1+b)$ estimated with the 3C273B. Since the value changes according to the atmospheric condition, the estimated results show large dispersion. It can be seen that the dispersion of the $ah(1+b)$ is larger in X band than in S band. The same estimations were performed for the baseline between two stations at Kashima and Tateyama. The mean values and the deviation of $ah(1+b)$ are then used to evaluate the correlated amplitude of the source without the effect of the atmosphere. The corrected correlated amplitude of the target source is compared with the corrected correlated amplitude of 2134+004, and the flux density of the target source is

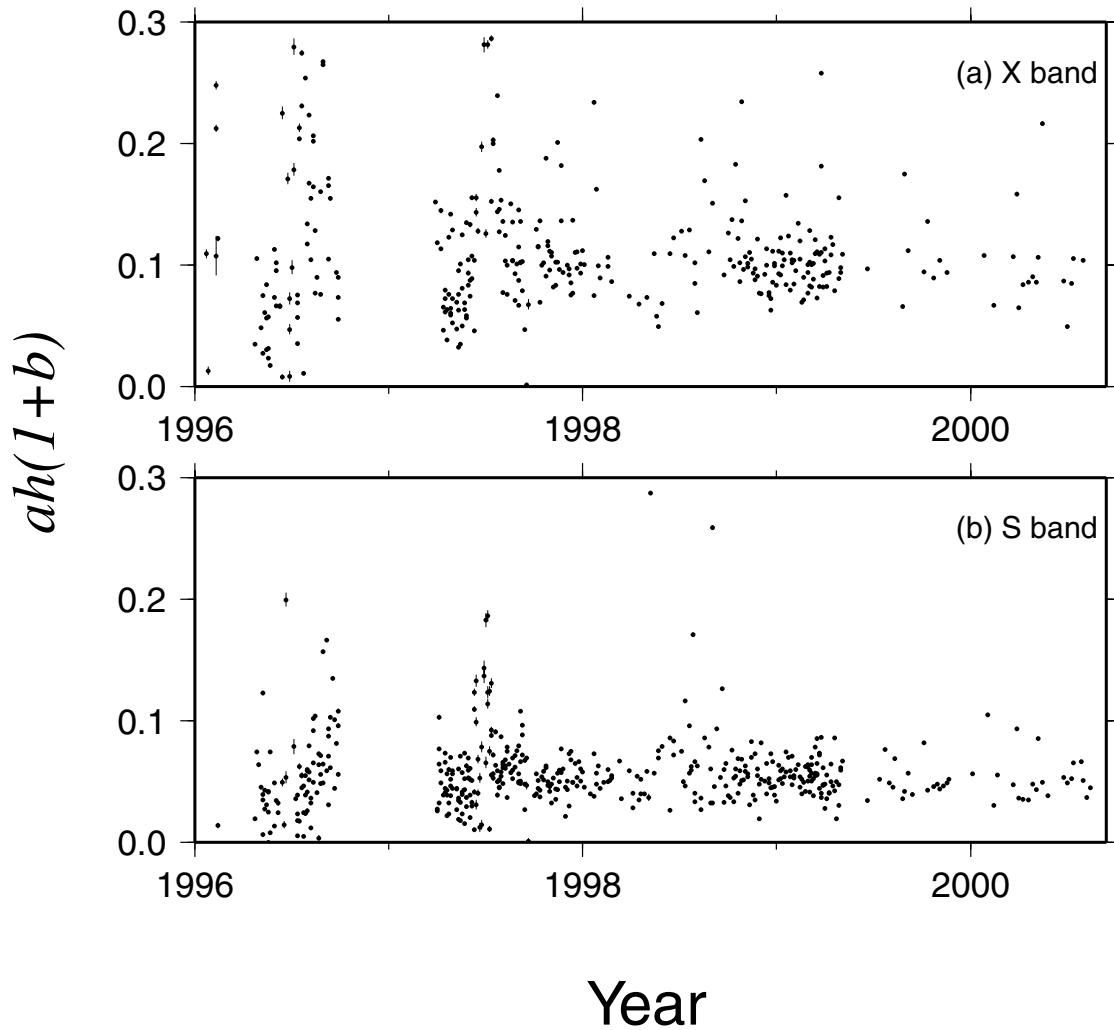


Figure 5.3 Flux densities of 3C273B and 2134+004 at X band and S band estimated by using (5.4) and (5.5). The correlated amplitudes obtained with the baseline between Kashima and Miura stations were used for the estimation. The error bars are $\pm 1\sigma$ uncertainties evaluated by the least squares estimation.

calculated.

5.4 Results and Discussions

Flux densities of 15 observed radio sources listed in Table 5.1 were estimated by using the method described in section 3. For each source, S and X band flux densities were estimated from one experiment. Experiments usually span ~ 6 hours up until the end of September 1997 and ~ 23.5 hours since then. In the estimation, two

baselines of Kashima-Miura and Kashima-Tateyama were used because three stations have clear views to low elevation angles, while the Koganei station is surrounded by tall trees, and the background radiation noise to the antenna is not constant, especially at low elevation angles. Data were selected by using the condition $1 / \sin\theta < 5.0$ ($\theta > 11.5^\circ$) because the variations in the optical depth of the atmosphere become very large in low elevation angle observations. Usually, many values of S_{src} are obtained in a single experiment. The outliers which differed from the average value >3 times the standard deviation were removed recursively until no further outliers could be removed. The mean value of the results was taken for the final estimation of the flux density. The obtained results are shown in Figures 5.4 to 5.18.

As shown in the figures, there are large data gaps before the middle of the 1997. The VLBI observations were performed for ~ 6 hours every day, and the number of observations toward the calibration source, 2134+004, or the target source could become very small. As a result, data are available only when both the calibration source and the target source are observed for enough numbers of time during ~ 6 hours of an experiment. There are also many outliers in Figures 5.4 to 5.18. The outliers occur when there is a problem either in the data of the calibration source or in the data of the target source or if the atmospheric condition changed significantly during an experiment. Nevertheless, the majority of the estimated flux densities show clear trend of the microwave variability of 15 sources at S and X band.

By studying the results given in Figures 5.4 to 5.18 we can see that some of the radio sources do not vary significantly over the 5 years of the time period. For example, estimated flux densities of 0552+398 were quite stable both in the S and X bands. This suggests that the method we used to estimate flux density was valid and that the receiving systems at Kashima, Miura, and Tateyama were stable. On the other hand, the variation of the flux densities of 0059+581, NRAO530, and 1334-127 are quite large compared with the other sources. Since the variation characteristics were unique for each source, the obtained variation seems very reliable. While 0059+581 demonstrated similar variation patterns in the S and X bands, the variation pattern of NRAO530 in the S band was quite different from that in the X band. This suggests that different physical mechanisms exist for the different intensity variations seen in these sources.

We presented a method to monitor microwave flux densities of compact extragalactic radio sources by using correlated data in geodetic VLBI experiments.

Since the KSP VLBI experiments are processed in real time and are performed with a regular basis, our method gives unique and useful information for studies of rapid variability of blazar sources in microwave region. The variations in the flux densities are considered to be associated with changes in the radio source structures, so that the flux density monitoring of ICRF sources is quite important to maintain the reliability of the reference frame too. Although the number of sources observed by the KSP VLBI experiments was quite limited, the same method can be applied to the other geodetic VLBI experiments performed worldwide, and flux density variation of many weak radio sources should be possible by using the same method.

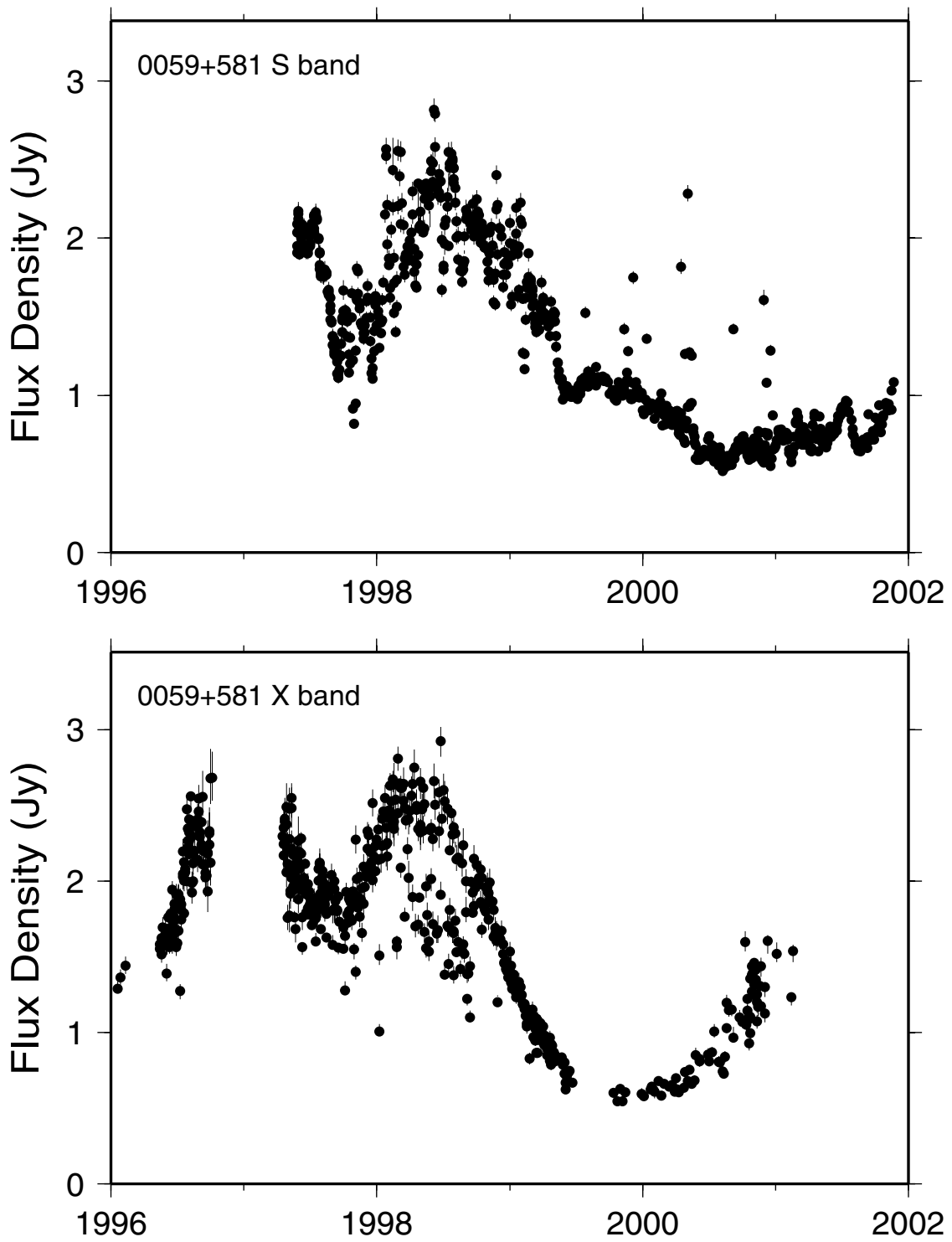


Figure 5.4 Flux densities of the 0059+581 at X band and S band.

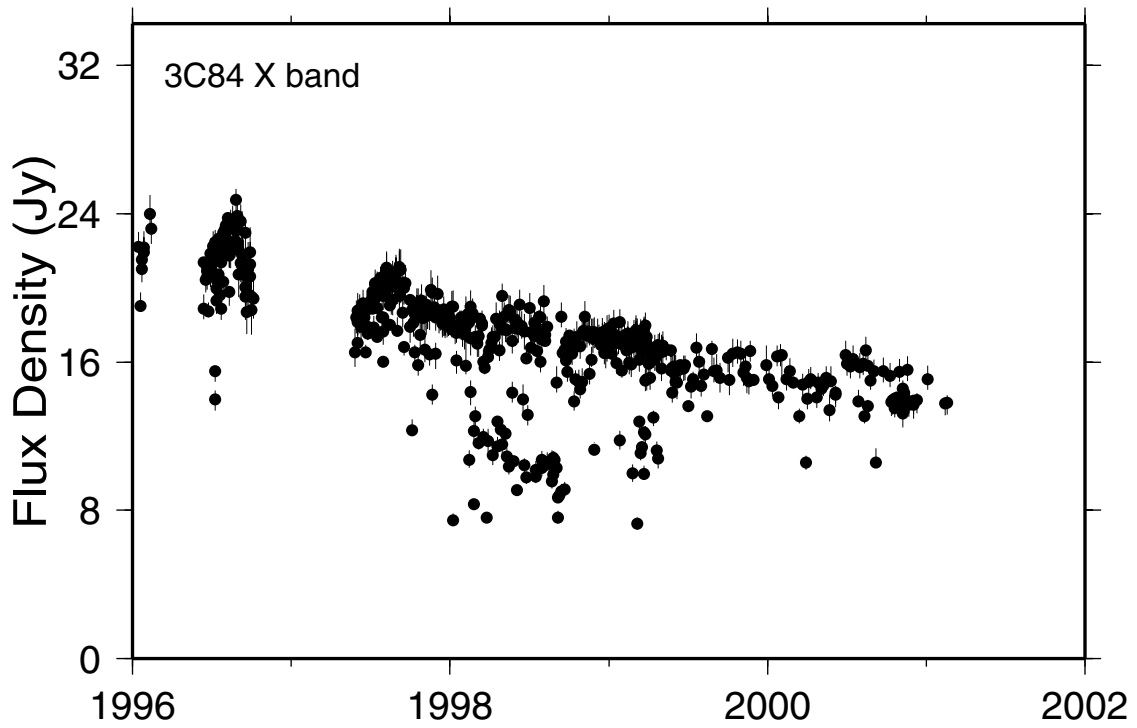
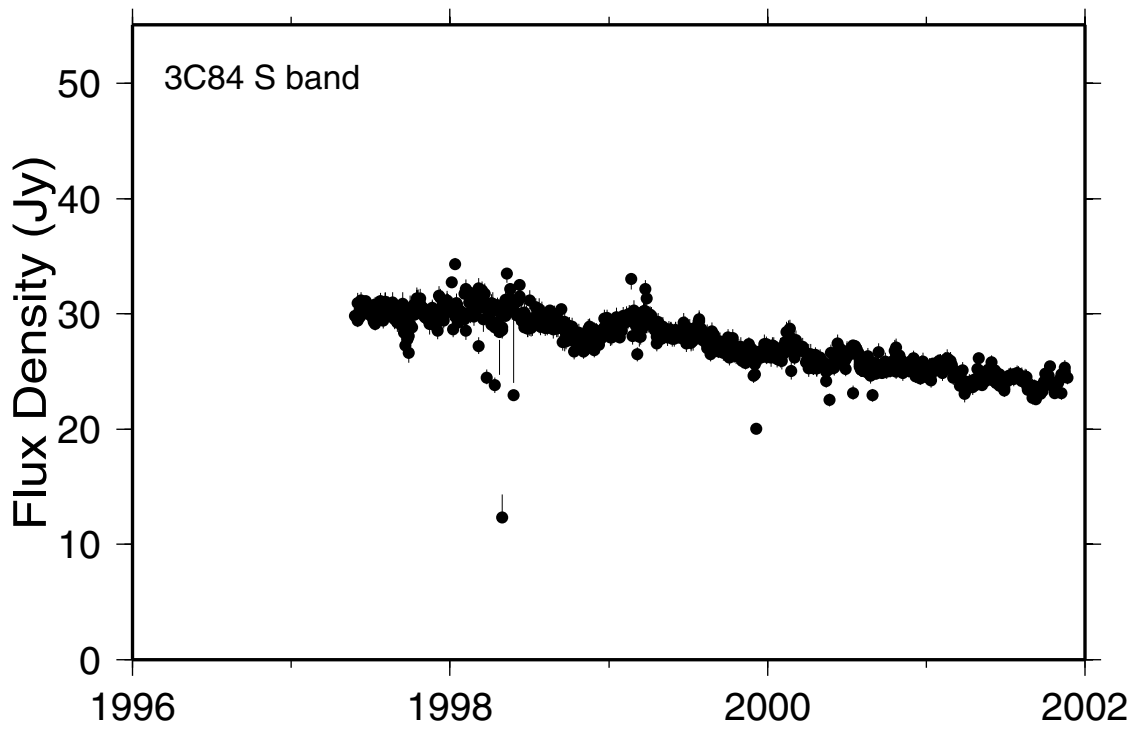


Figure 5.5 Flux densities of the 3C84 at X band and S band.

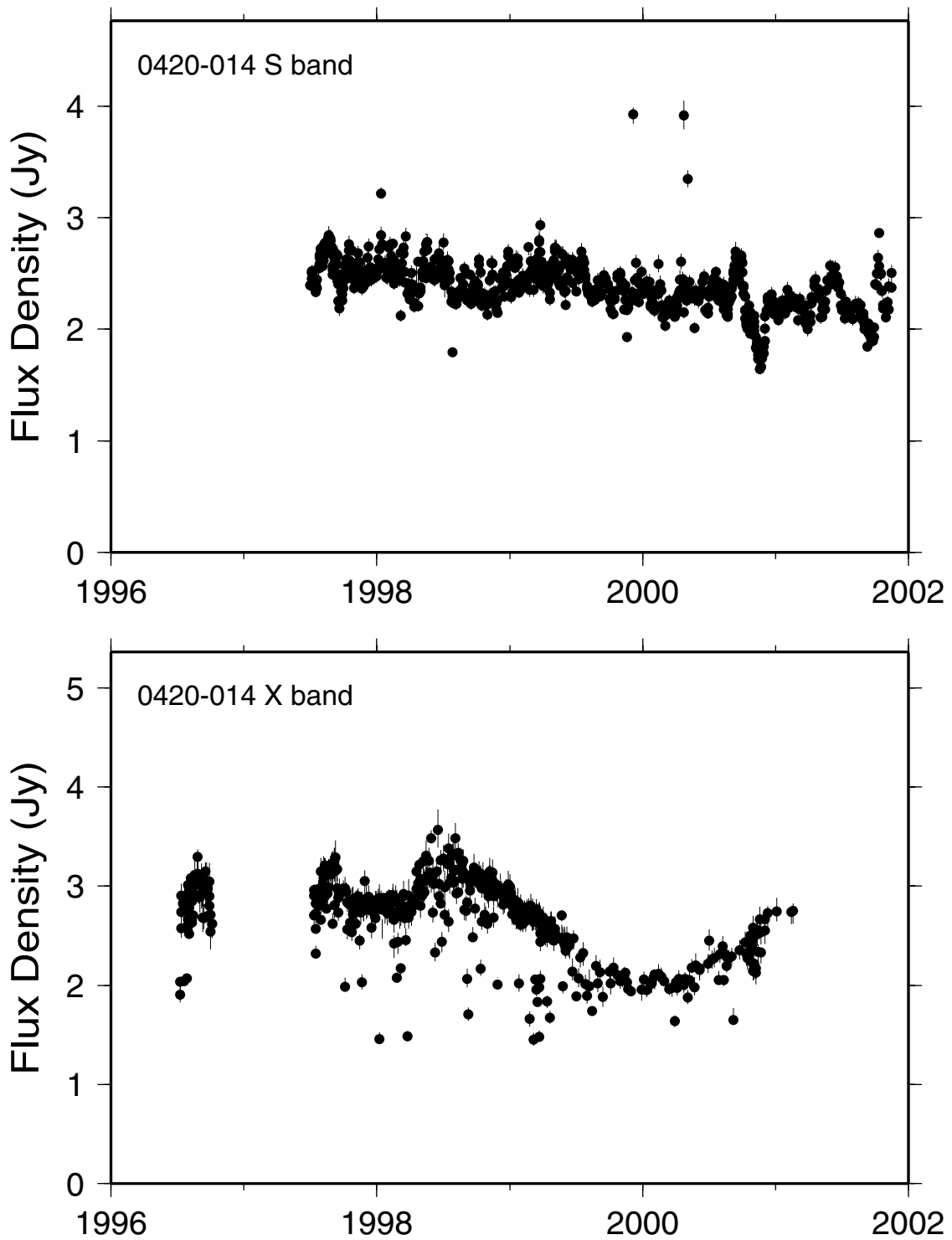


Figure 5.6 Flux densities of the 0420-014 at X band and S band.

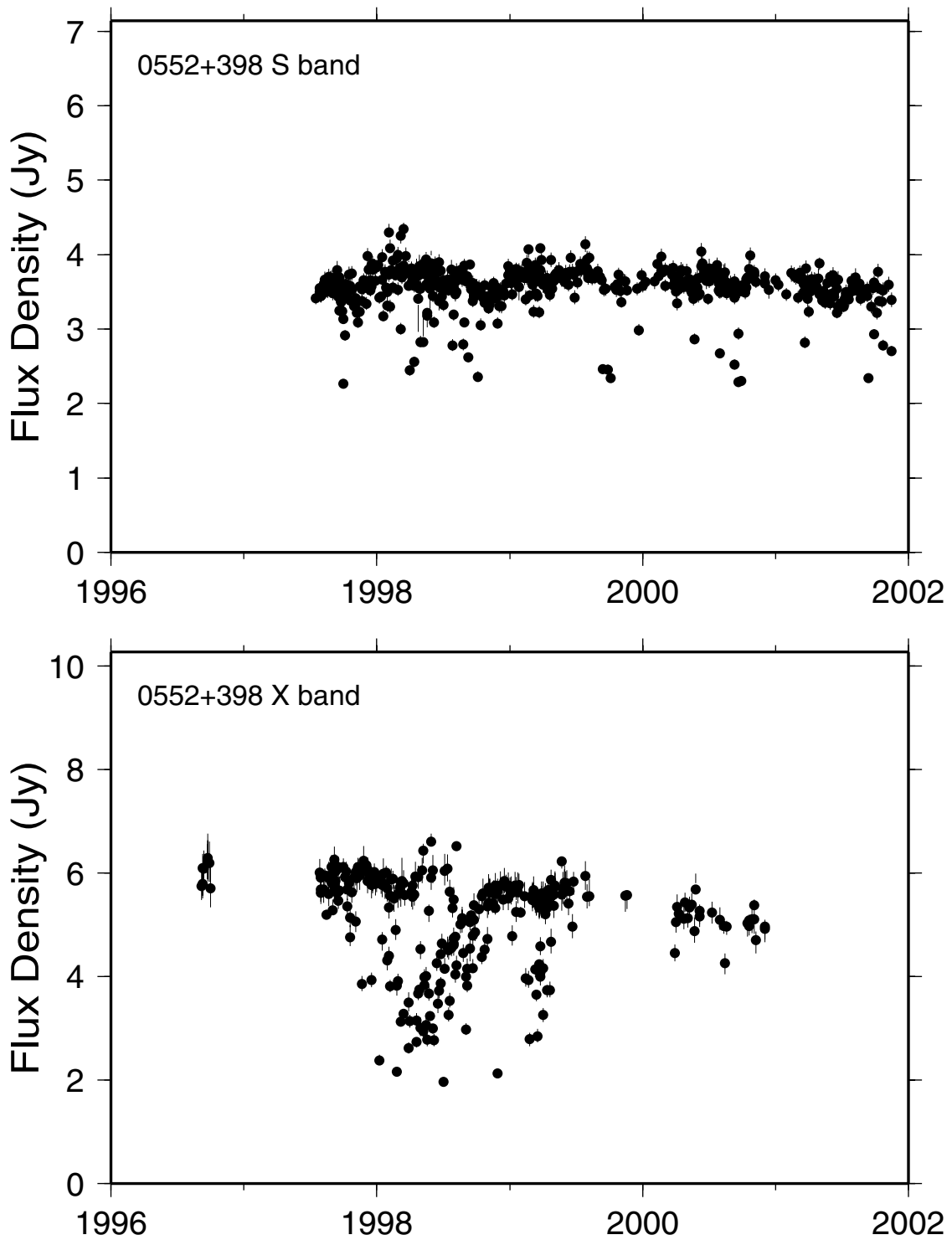


Figure 5.7 Flux densities of the 0552+398 at X band and S band.

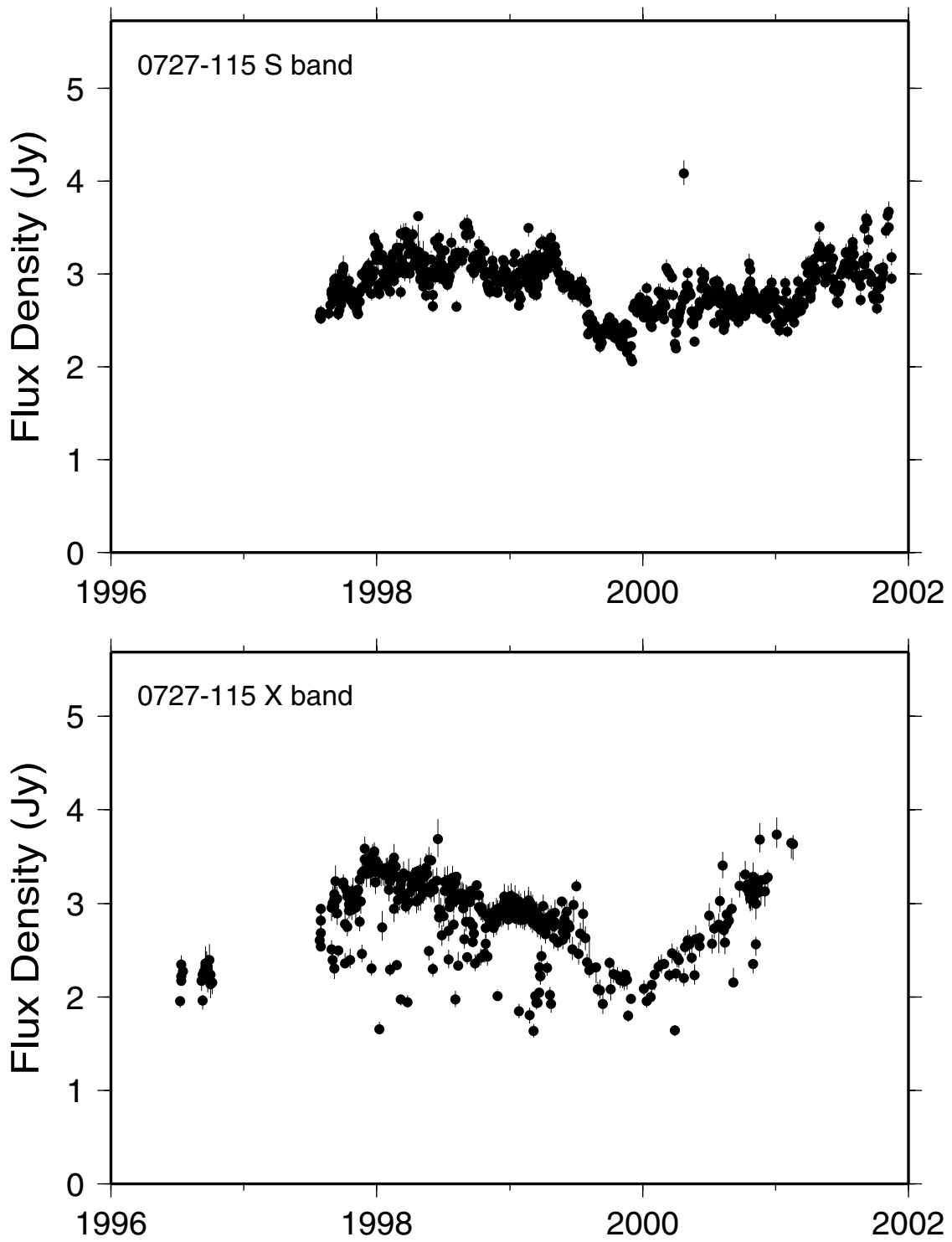


Figure 5.8 Flux densities of the 0727-115 at X band and S band.

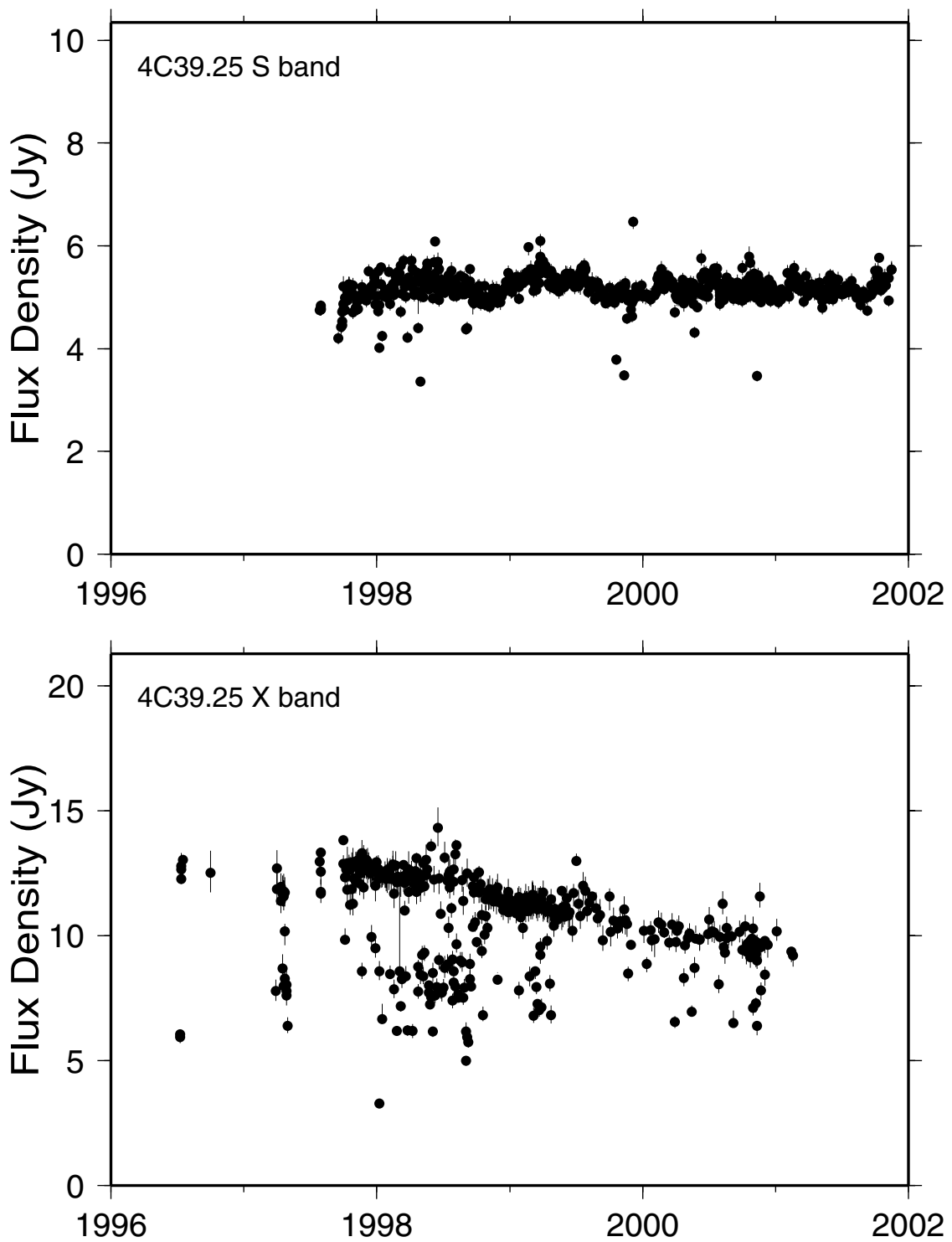


Figure 5.9 Flux densities of the 4C39.25 at X band and S band.

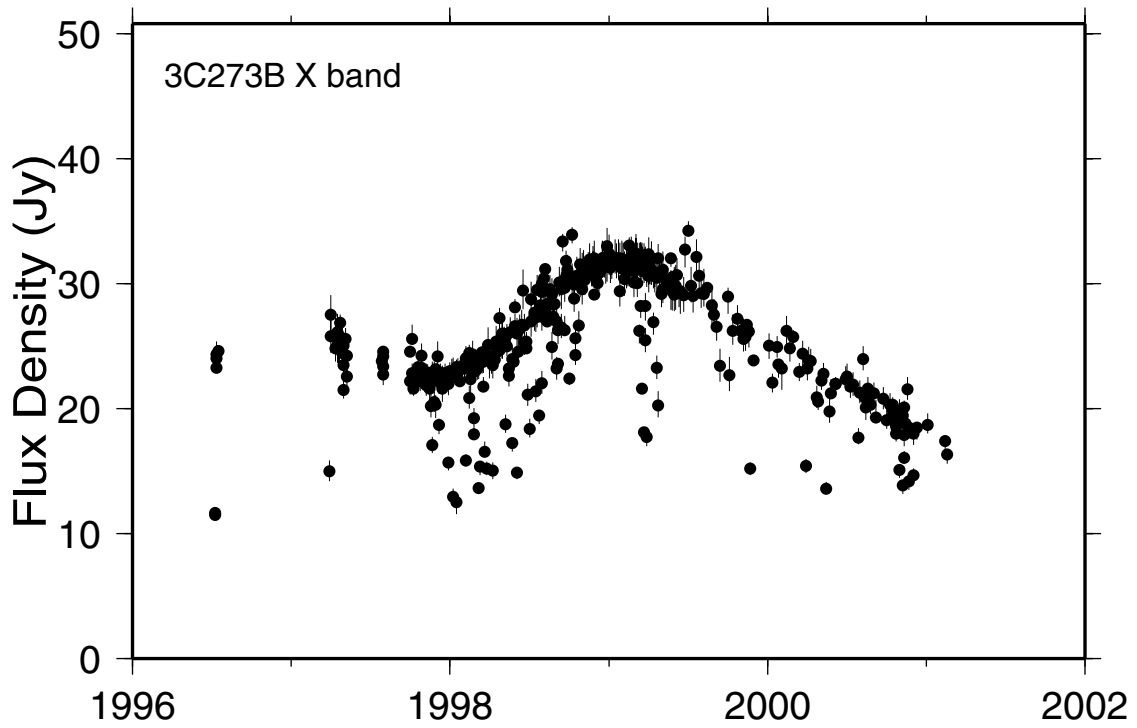
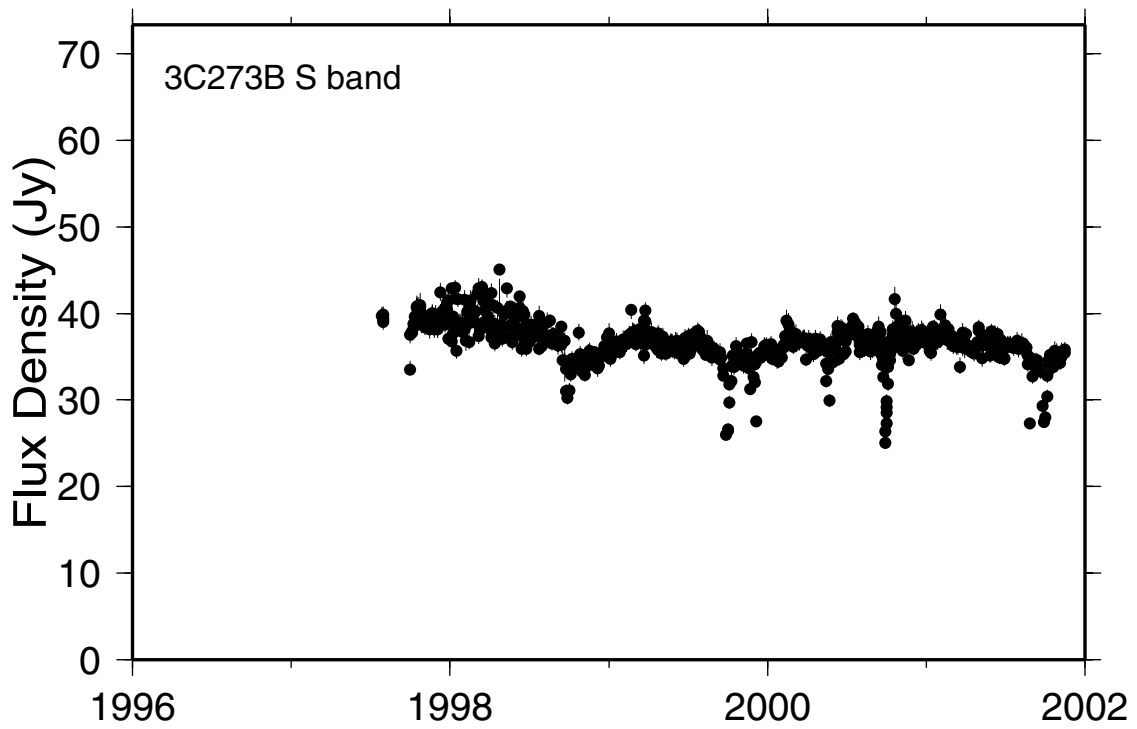


Figure 5.10 Flux densities of the 3C273B at X band and S band.

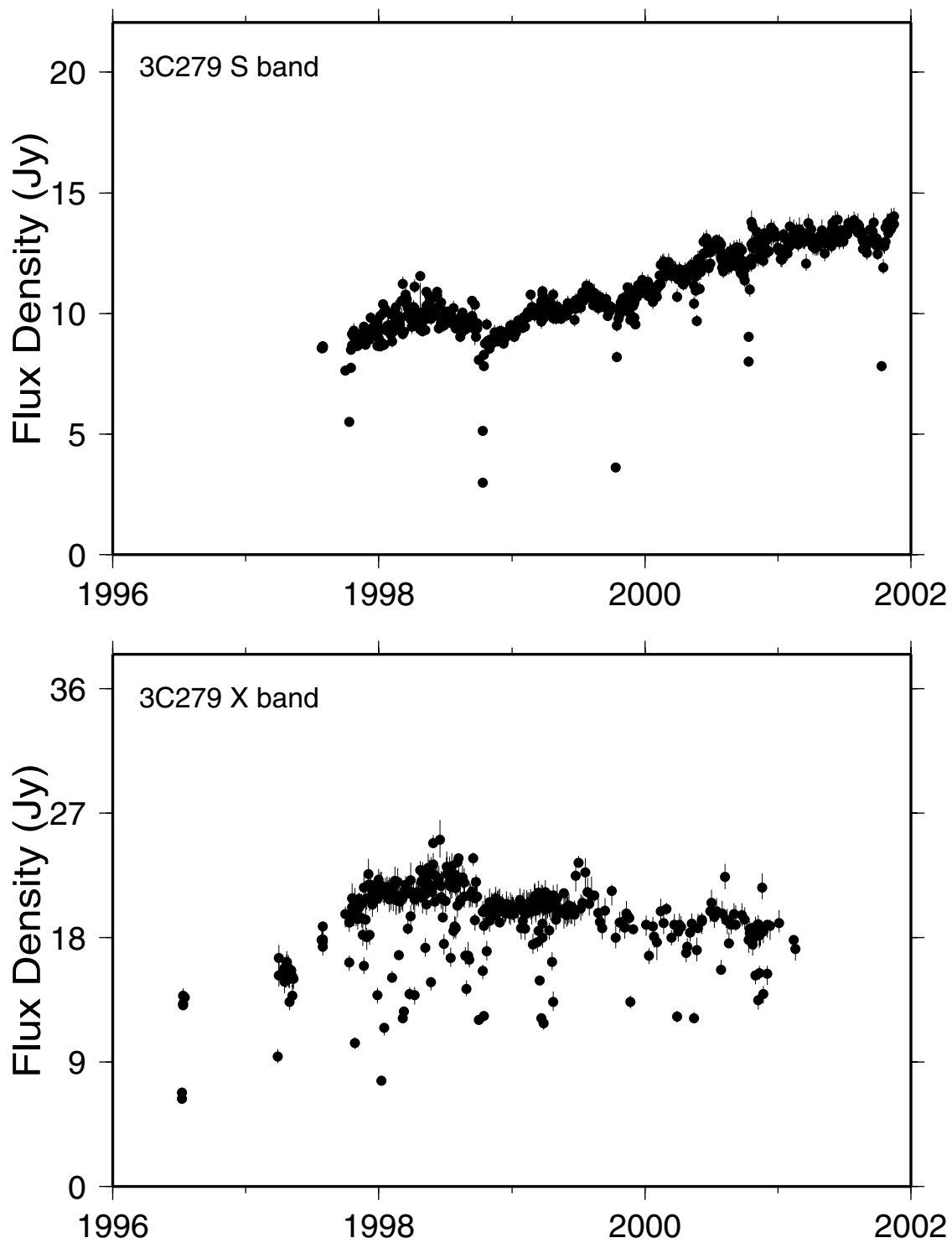


Figure 5.11 Flux densities of the 3C279 at X band and S band.

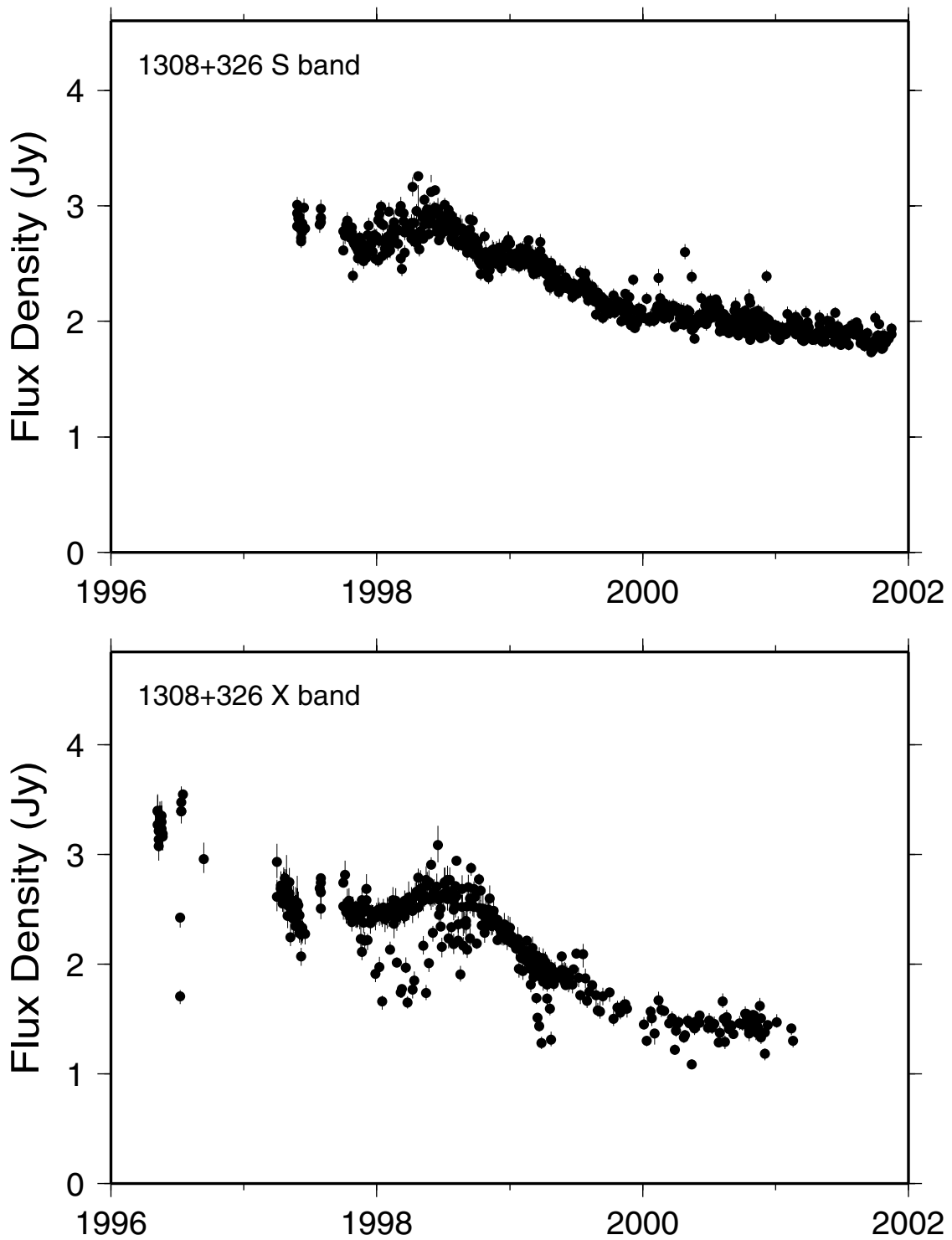


Figure 5.12 Flux densities of the 1308+326 at X band and S band.

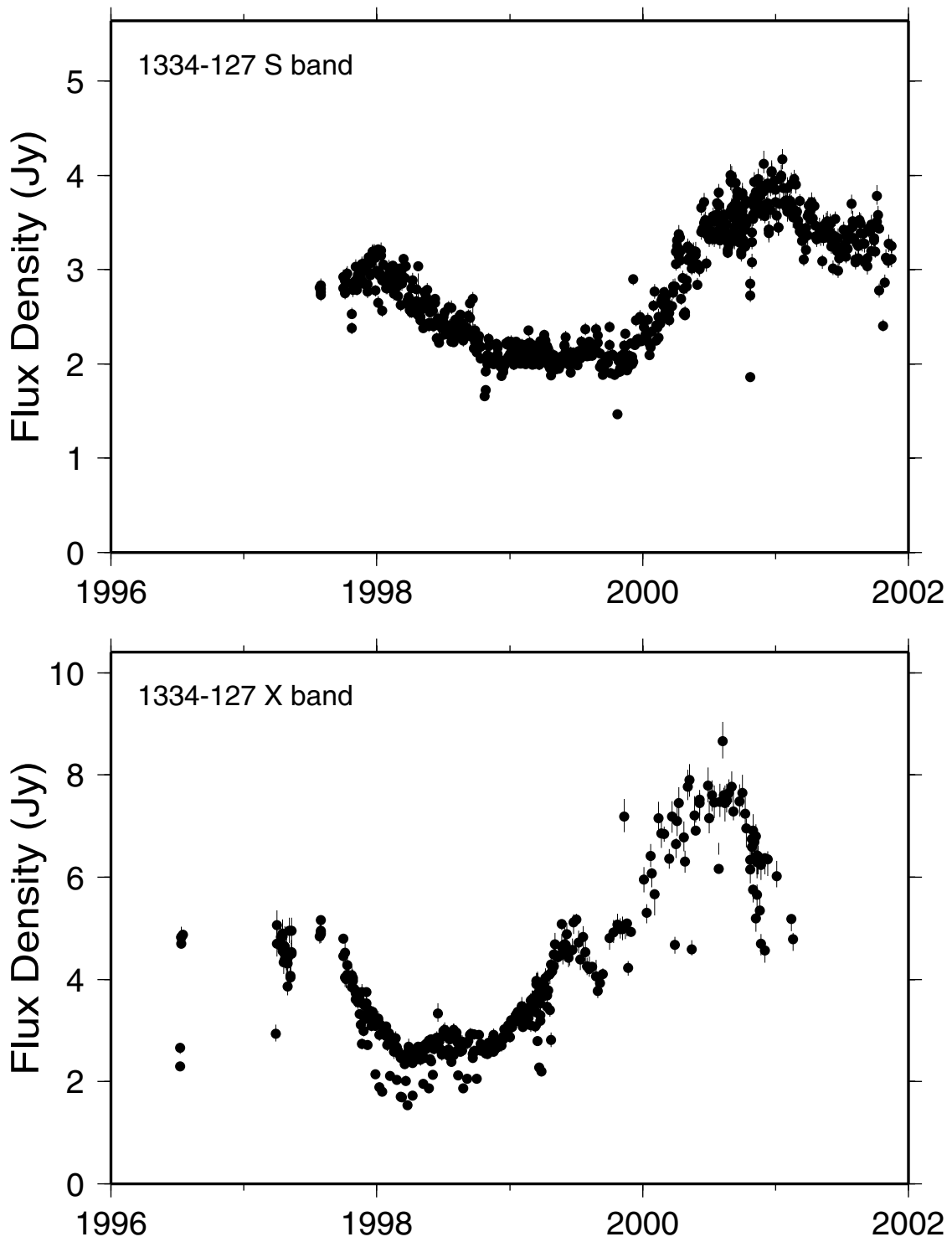


Figure 5.13 Flux densities of the 1334-127 at X band and S band.

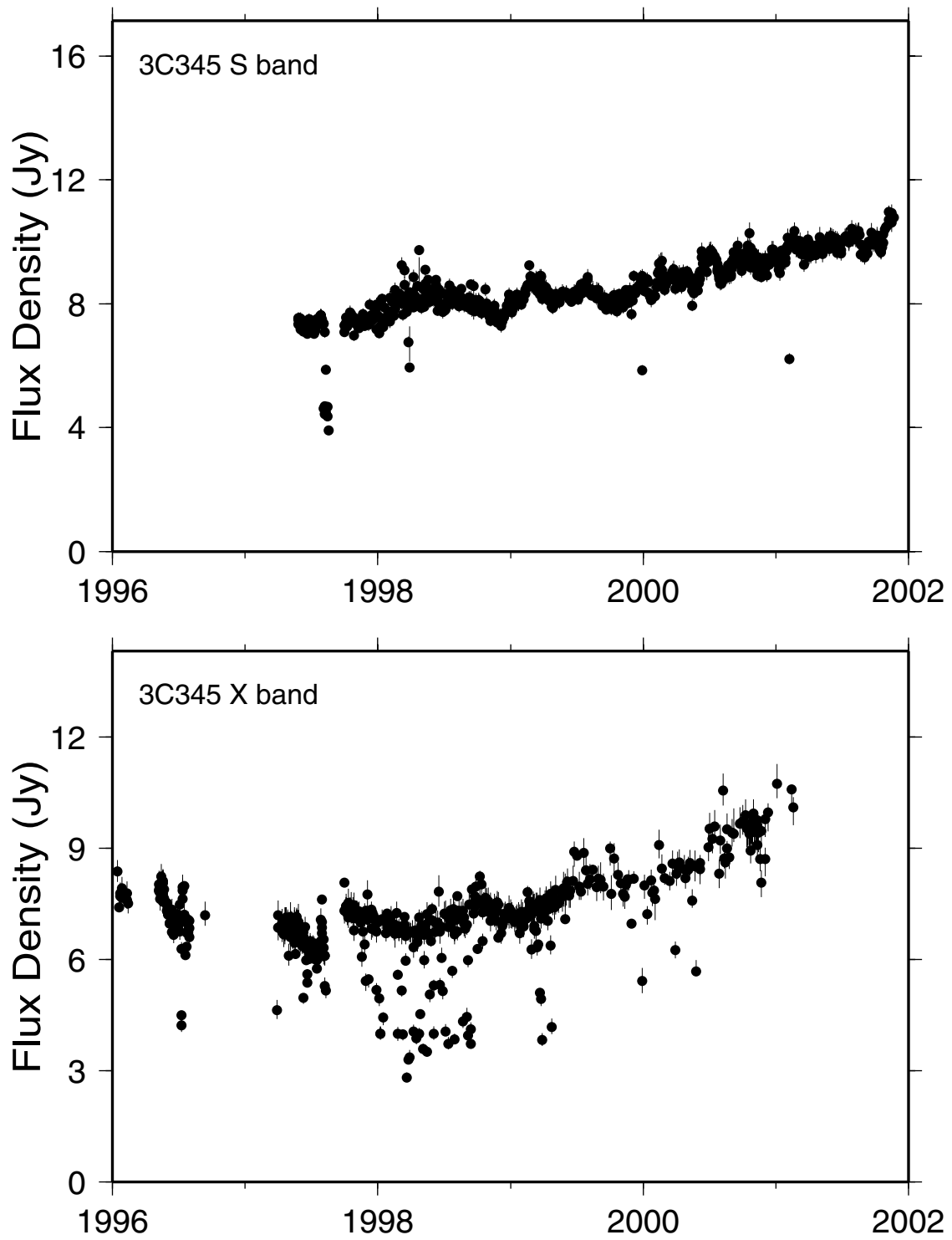


Figure 5.14 Flux densities of the 3C345 at X band and S band.

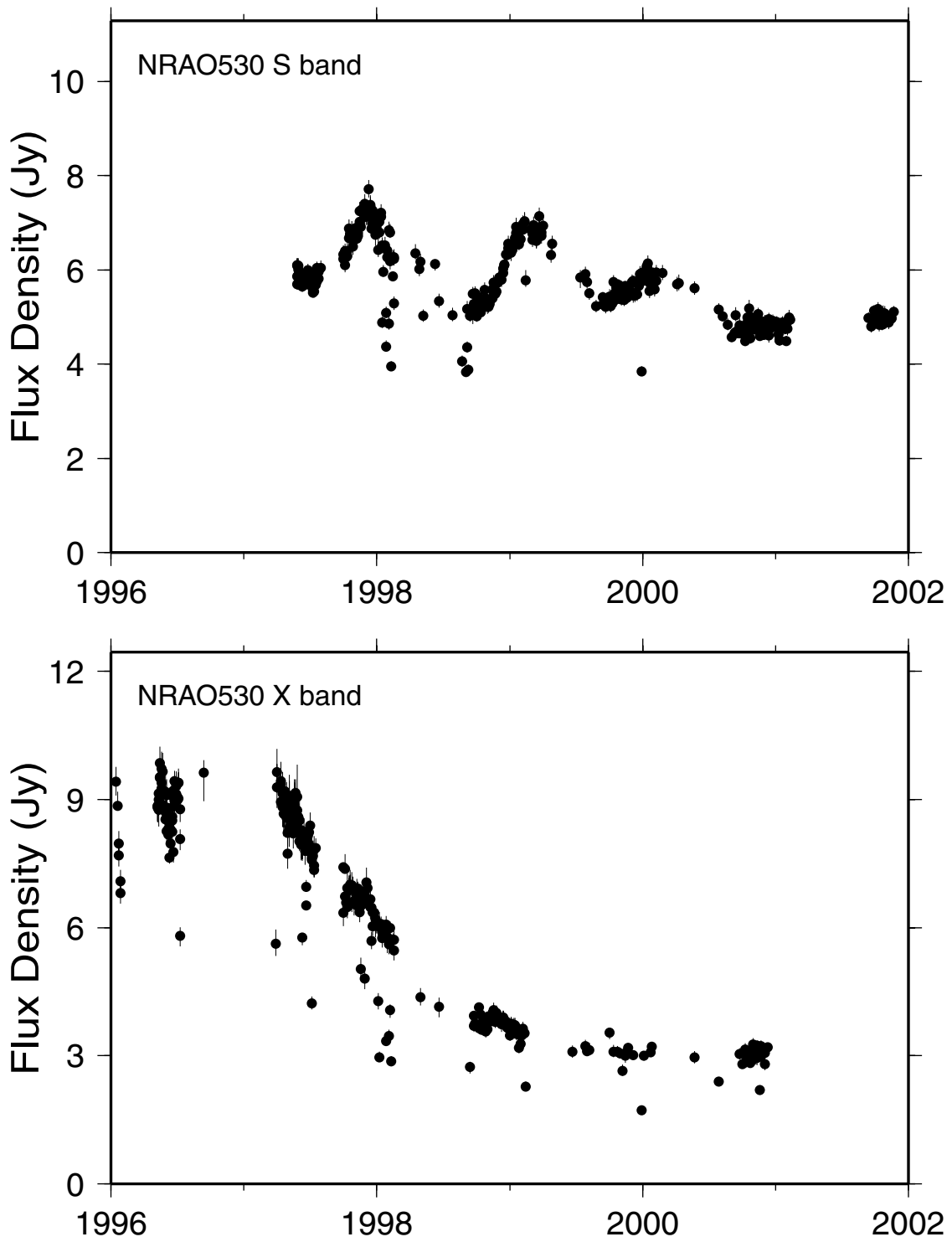


Figure 5.15 Flux densities of the NRAO530 at X band and S band.

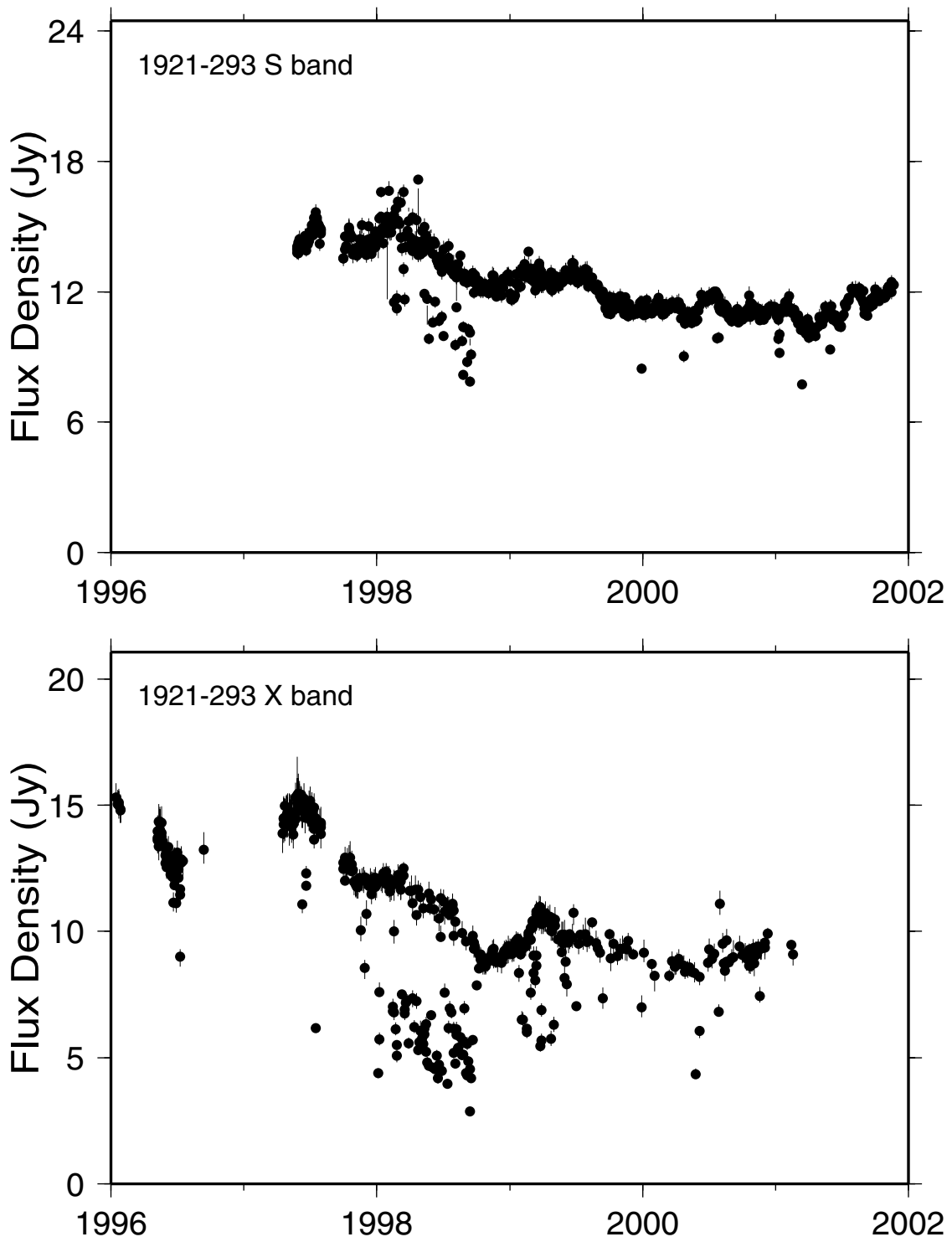


Figure 5.16 Flux densities of the 1921-293 at X band and S band.

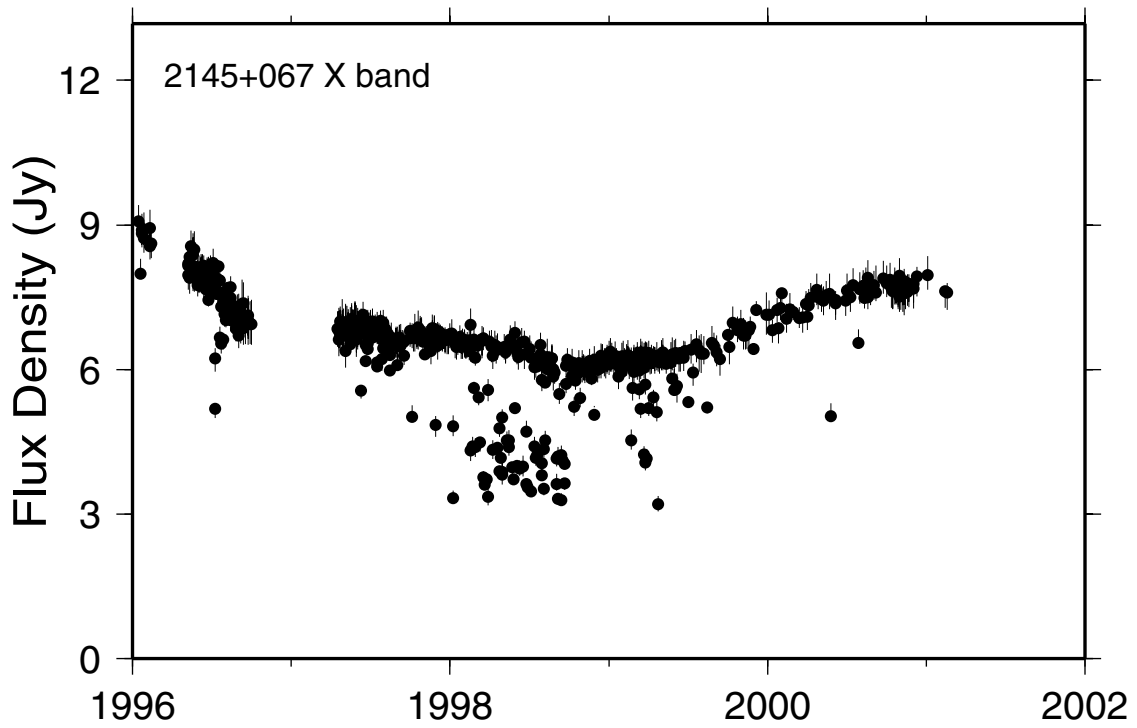
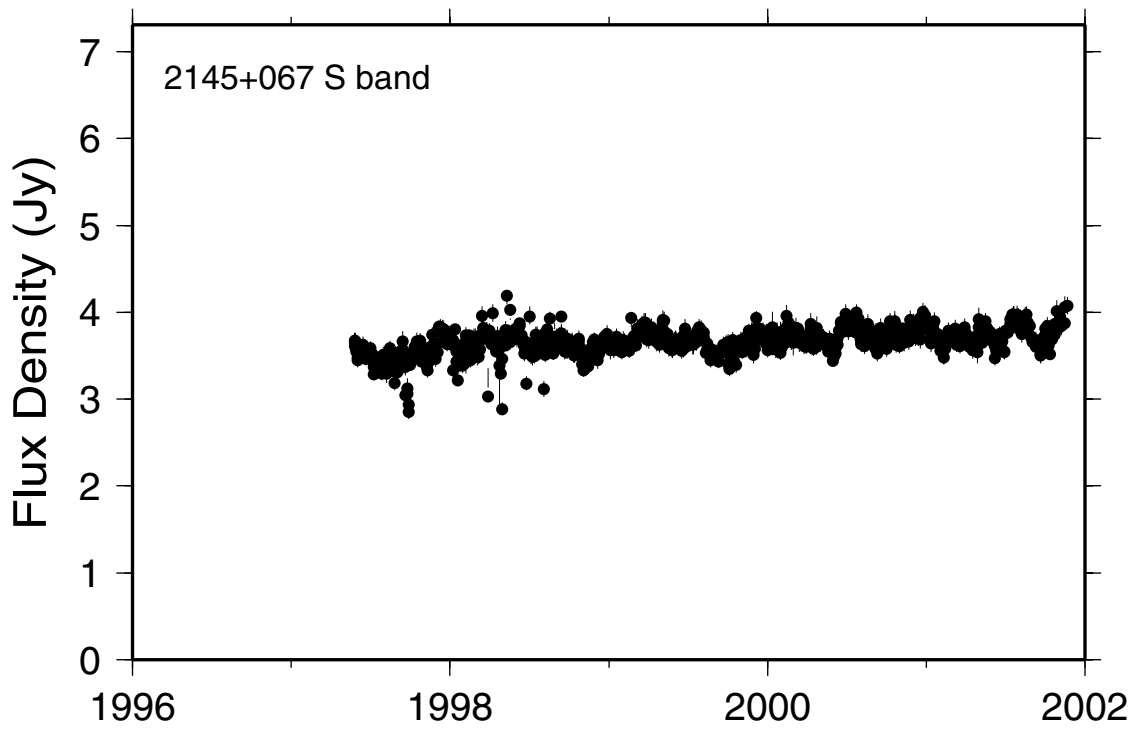


Figure 5.17 Flux densities of the 2145+067 at X band and S band.

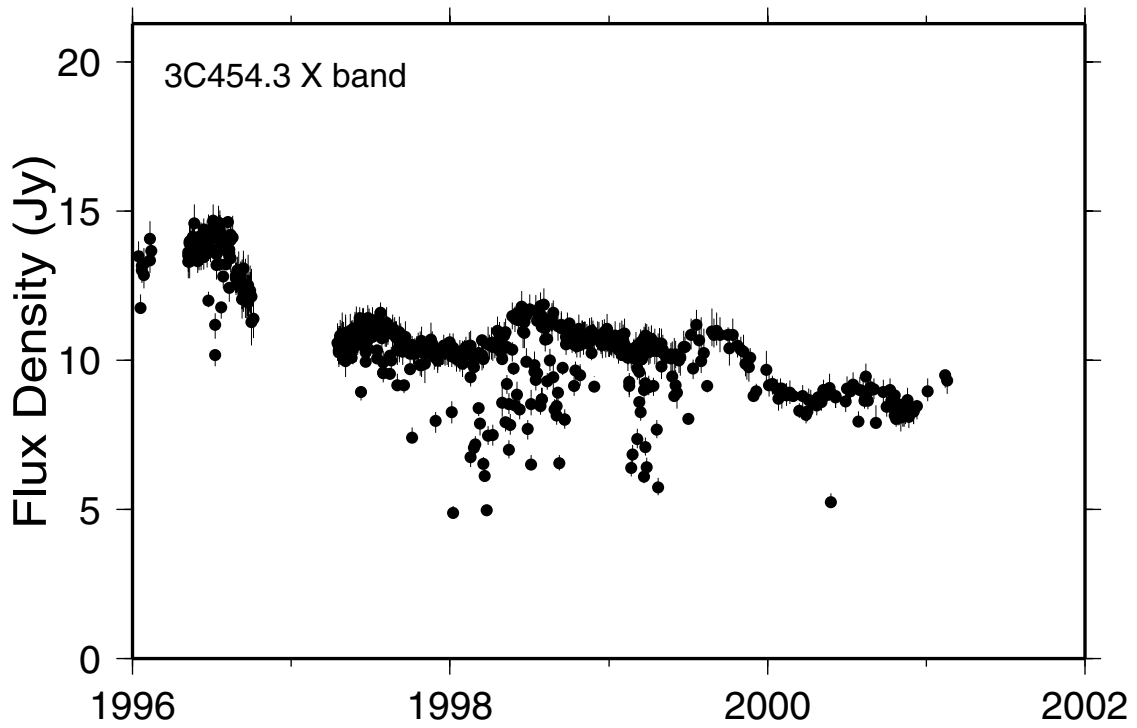
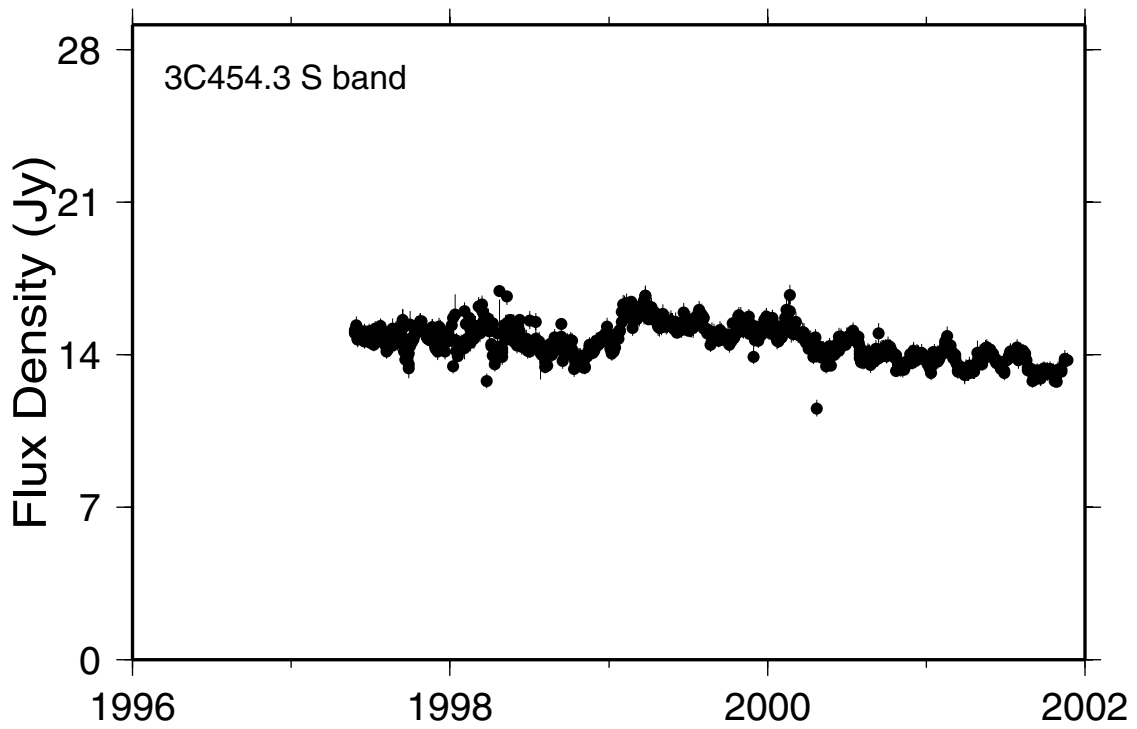


Figure 5.18 Flux densities of the 3C454.3 at X band and S band.

Chapter 6 Variation of EOP

6.1 Background

The real-time VLBI system and the automated data analysis system developed for the KSP made it possible to perform data analysis tasks right after all the observations in an experiment were finished. The feasibility of using KSP VLBI data to estimate the earth's rotation pole position (δx and δy) and the difference between UT1 and UTC was investigated using 6 months of the KSP VLBI data. In the data analysis, site coordinates of the four VLBI sites were fixed to the *a priori* ITRF96 site coordinates.

It was necessary because the KSP VLBI network is quite compact and sufficiently stable EOP values can not be estimated while the site coordinates are estimated at the same time. No *a priori* information was used for δx , δy , and UT1-UTC, so these values were assumed to be zero before the parameter adjustment. The other procedures and conditions were same as in the regular data analysis. In Figure 6.1, the estimated values are compared with the EOP97C04 data series maintained by the IERS. Since the KSP VLBI network is considerably compact compared to the size of the earth, there should be strong correlation between the estimated values of δx and δy . Nevertheless, the estimated values are consistent with the EOP97C04 which has been obtained by combining several datasets estimated by various space geodetic techniques. The results demonstrate that UT1-UTC and the earth's rotation pole positions can be estimated from the KSP VLBI data.

By using the 6 months of KSP VLBI data, earth's rotation pole position (δx and δy) and UT1-UTC were estimated. As in the regular data analysis, CALC (version 8.1) and VLBEST software were used. Site coordinates are provided as *a priori* information and fixed through the parameter adjustment process. No *a priori* information was used for δx , δy and UT1-UTC, so that these values were assumed to be zero before the parameter adjustment.

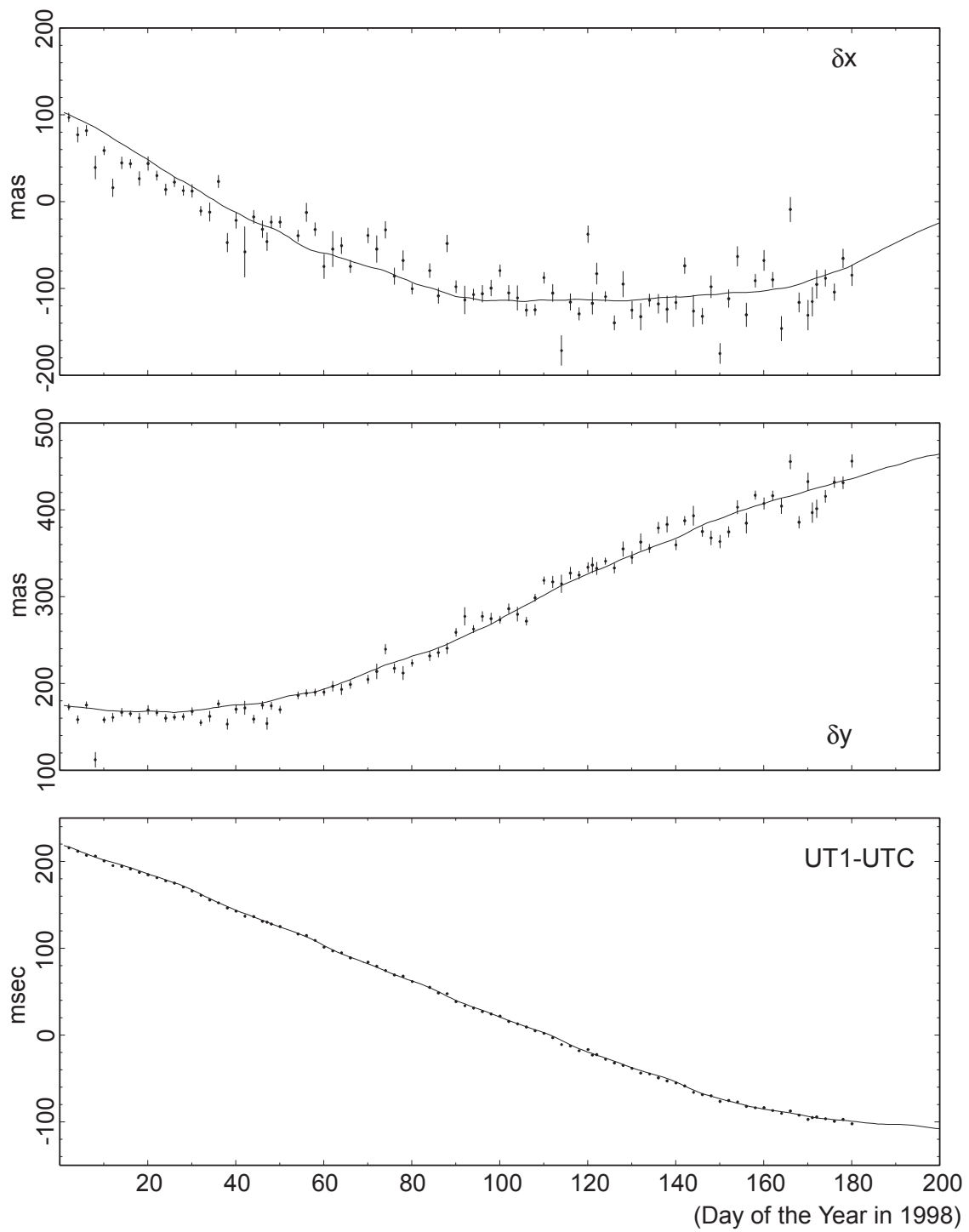


Figure 6.1 Estimated values of δx , δy , and UT1-UTC estimated from routine KSP VLBI sessions. Solid curve lines are the EOP97C04 data series maintained by the IERS.

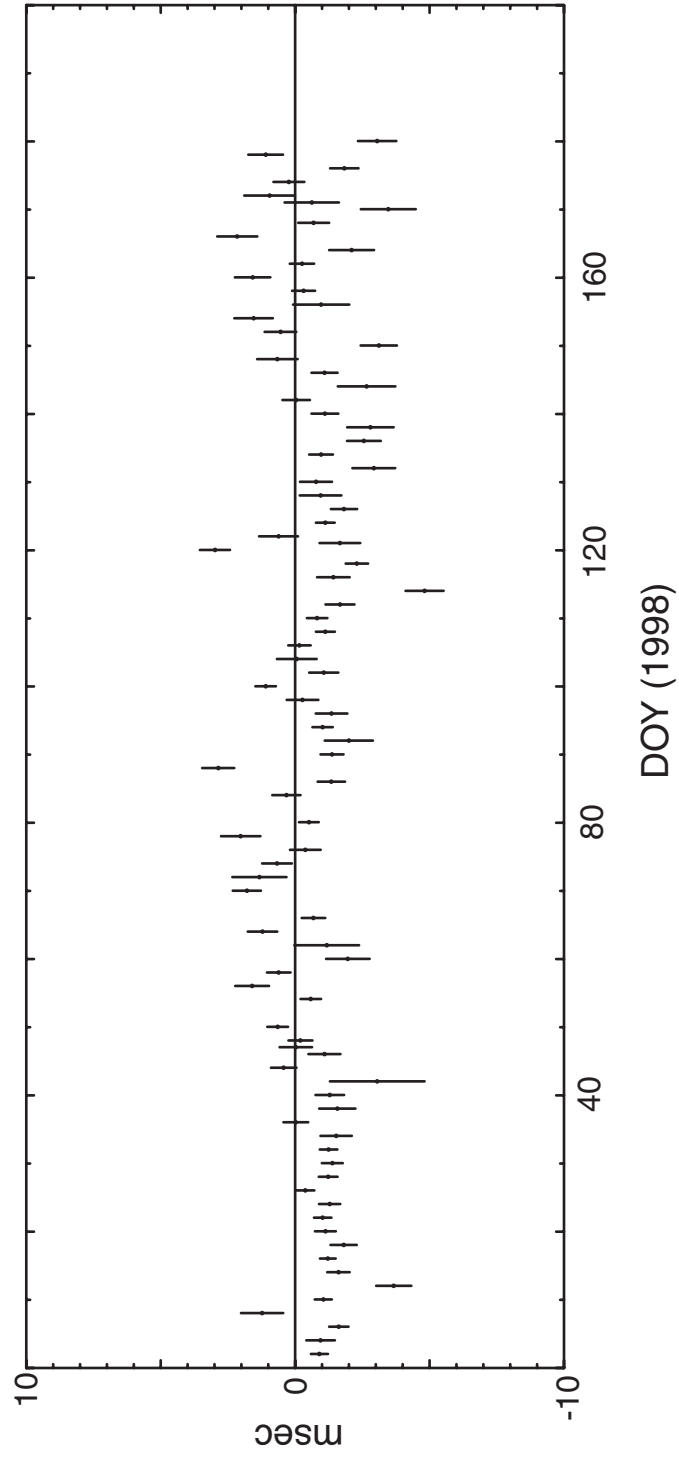


Figure 6.2 Deviation of the estimated UT1-UTC from the EOP97C04 values provided by IERS.

Table 6.1 Statistic characteristics of the formal errors of the estimated EOP.

	Average	Minimum
δx	10.0 mas	4.8 mas
δy	6.0 mas	3.1 mas
UT1-UTC	0.59 msec	0.29 msec

Estimated values are compared with the EOP97C04 data series maintained by IERS. Since the KSP VLBI network is compact compared to the size of the earth, there should be strong correlation between the estimated values of δx and δy . Nevertheless, the estimated values are consistent with the EOP97C04 which has been obtained by combining several datasets estimated by various space geodetic techniques. Figure 6.2 shows the difference between the estimated UT1-UTC and the UT1-UTC values from EOP97C04 data series. Table 6.1 shows the statistic characteristics of the estimated EOP values from the KSP VLBI data.

6.2 Kashima-Westford Experiments

Figure 6.3 and Figure 6.4 show the schematic route of the high speed network used in the e-VLBI test experiments. Two VLBI stations, one is 34-m and the other is 11-m, at Kashima and 11-m VLBI station at Koganei are connected to the Galaxy network under the collaboration between CRL and NTT laboratories. The maximum data rate of the Galaxy network is 2.4 Gbps and it supports ATM. At Kashima, an IP interface unit is connected to the ATM switch and it provides IP connection at the maximum data rate of 622 Mbps. The Galaxy network is then connected to the Super-SINET network at National Institute for Informatics at Hitotsubashi. In the United States, the 18-m Westford VLBI station is connected to the Abilene network operated by the Internet2 consortium. The speed of the backbone of the Abilene network is now at 10 Gbps. The Abilene network and the Super-SINET network are connected at New York with a trans-Pacific link. The connection between two networks is currently at 622 Mbps. There is another route which uses GEMnet between Galaxy and Abilene network. There is a plan to upgrade the speed of the GEMnet route to 155 Mbps in near

future, but the current speed is limited to 20 Mbps because of a bottleneck between Musashino and the Tokyo access point. During the test session on March 25, the route of Super-SINET was used.

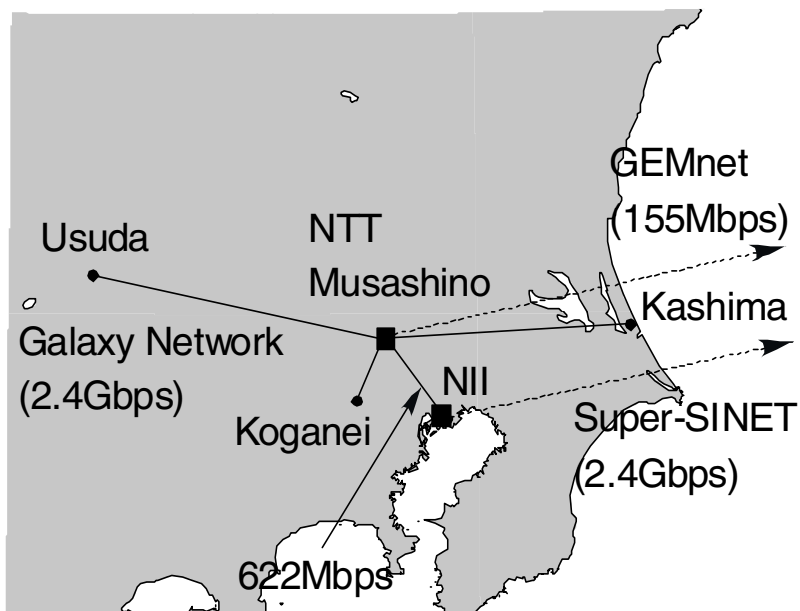


Figure 6.3 Configuration of the high speed network in Japan.

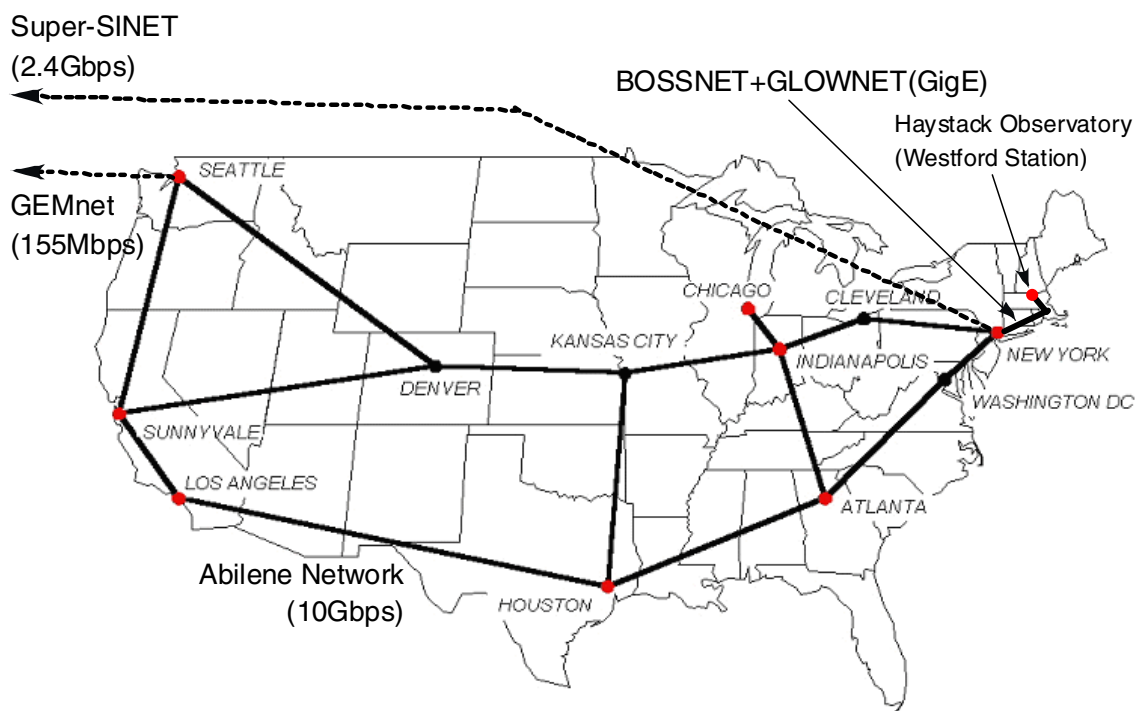


Figure 6.4 Configuration of the high speed network in the United States.

A test e-VLBI session was performed for two hours from 16:00 UT on March 25, 2003 with the Kashima-Westford baseline. The 34-m antenna VLBI station at Kashima and 18-m antenna station at Westford were used for the observations. This was the fourth test in the series of e-VLBI test observations. During the previous tests, successful detections of the fringes from the e-VLBI observations were demonstrated and the software developments have been continued with the obtained data sets.

At the Kashima station, K5 VLBI system was used to record observed data. At the Westford station, Mark5 VLBI system developed by Haystack Observatory was used to record observed data. The observed data were recorded to internal hard disks at each site and transferred to Kashima and Haystack Observatory after the observations by using FTP. For this purpose, a program was executed to extract the data from the Mark5 and to generate data files. At Haystack Observatory, K5 data files were converted their format and recorded to Mark5 system. After the conversion, both data recorded at Kashima and at Westford were processed for cross correlation processing using the Mark4 correlator at Haystack Observatory. At Kashima, Mark5 data files were converted to K5 file format and then both data recorded at Kashima and at Westford were processed for cross correlation processing by using the software correlator on the K5 VLBI system. After the cross correlation processing, bandwidth synthesis processing was done and two database files (one for X-band and another for S-band) were generated for data analysis. The total data volume was hence 56Mbps. The observations were performed with 14 channels (8 for X-band and 6 for S-band) and 2MHz for each channel. The file size of the Mark5 system was checked from the extracted files from the Mark5 disks. Since there are 16 input channels both in K5 and Mark5 systems, two channels were used as redundant channels.

After the data processing, CALC and SOLVE software were used to perform data analysis. In the estimation process, positions of both Kashima and Westford stations were fixed to the ITRF2000 values and the UT1-UTC was estimated along with the clock offset, clock rate, and the atmospheric zenith delay. The estimated UT1-UTC value is shown in the Table 6.2 as well as the values published in the Bulletin B of the IERS. As shown in the Table 6.2, the UT1-UTC was estimated with the uncertainty of 23.9 microseconds, which is comparable to the results from intensive sessions. The comparison of the estimated value with the results reported in IERS Bulletin B suggests there is a discrepancy between them. It is necessary to investigate the cause of the

discrepancy. Especially, the consistency of the station coordinates and a priori information used in the data analysis has to be set carefully.

Table 6.2 Estimated value of UT1-UTC from the Kashima-Westford e-VLBI session and reported values from IERS Bulletin B 183, May 2, 2003.

	Epoch (UT)	UT1-UTC (μ sec)
e-VLBI	20:00 on Mar. 25	-338727.0 \pm 23.9
IERS	00:00 on Mar. 25	-337951
IERS	00:00 on Mar. 26	-338610

Table 6.3 Time sequence from the observations to the data analysis. Time is in Japanese Standard Time and start from 22:00 on June 30.

Time	Event
22:00	Observations Start
00:00	Observations End
~04:20	File extraction and transmission From Kashima to Westford : 107Mbps (41.54GByte in 51m 35s) From Westford to Kashima : 44.6Mbps (41.54GByte in 2hr 04m 02s)
~08:10	File Conversion (Mark5 to K5)
~20:30	Software Correlation
~21:20	Bandwidth Synthesis Processing, Database Generation, Data Analysis

Next e-VLBI session was performed again for two hours from 13:00 UT on June 27, 2003. The observation mode, configuration of the observing systems, and the baseline were identical to the previous e-VLBI session performed in March, 2003. The purpose of the session was to demonstrate how fast the UT1-UTC can be actually estimated from the international e-VLBI session. Therefore, the file transfer servers as well as the network switches were carefully tuned to improve the file transfer speed

over the network. Because the transmission delay over the network is quite large, about 200 msec., the default buffer size of the servers had to be increased from 64 kBytes to more than 4 Mbytes. As the results of this tuning, the file transfer speed was improved from about 2.2 Mbps to more than 100 Mbps. Table 6.3 shows the actual time sequence of the observations, file transfers, and data processing during the e-VLBI session. As shown in the table, the file transfer speed reached to 107 Mbps in the direction from Kashima to Haystack Observatory. The opposite direction was not as fast, but the speed was about 45 Mbps. In total, the UT1-UTC was estimated within 21 hours and 20 minutes after the session finished. Thus the rapid estimation of the EOP less than one day was successfully demonstrated by the international e-VLBI observations and data analysis.

6.3 Discussions

Since file transfer speed became so fast, the longest time is required for data correlation processing. But since it is done by the software correlator, the time can be easily decreased by increasing the number of CPUs to be used to the correlation processing. File conversion is also time consuming processing, but this becomes unnecessary if K5 systems are used at both observing sites or file format between different systems become compatible. The discussions about the standard file format for e-VLBI have just begun, it is expected that the file conversion processing will become unnecessary in the near future. By combining these efforts, it will become feasible to estimate UT1-UTC within a few hours after the observations without major difficulties.

The successes of the series of e-VLBI experiments have many important meanings. Two different recording systems have been developed by two independent teams and these two systems were used but the compatibilities between the two different systems were easily achieved by preparing file conversion software programs. The establishment of the file format standard for e-VLBI will further improve the compatibilities among different systems. It was also demonstrated that the international network connection has been drastically improved recently and the e-VLBI observations with intercontinental baselines are becoming realistic. Finally, the success of the bandwidth synthesis and the data analysis in the from the data obtained with the K5 systems showed the improved performance of the prototype K5 VLBI data acquisition

terminal compared with the conventional systems.

In the future, we are planning to continue similar e-VLBI sessions until the e-VLBI observations become reliable and robust. Since the trans-Pacific network has more capacity than we have used, it is expected we can still increase the file transfer speed by investigating the bottleneck of the network route. In parallel, we are planning to develop a CPU array system for distributed correlation processing for fast and effective processing. The real-time data transfer and processing software programs will also be developed to further improve the promptness to obtain results from geodetic VLBI observations. After these system developments, it will become possible to perform routine e-VLBI sessions with international baselines for rapid turn around EOP measurements. To realize e-VLBI observations with isolated radio telescope sites, satellite communications have great possibilities. If the satellite communications are utilized in the real-time VLBI applications, variable communication delay will become the most different factor. It is highly desired to pursue the use of satellite communications in the e-VLBI experiments as soon as possible.

The KSP space geodetic network, with its longest baseline extending only 135 km, is relatively compact in the sense that space geodetic techniques are often applied to much longer distances. The compactness and remote operation capabilities of the KSP make it a unique and ideal test-bed for technical developments and system improvements. Regular and intensive VLBI, SLR, and GPS results will be compared in order to improve their consistency and accuracy. The precise ground survey measurements and repeated joint VLBI experiments with globally distributed VLBI observation sites play a very important role for the collocation studies to tie different space geodetic techniques.

The accuracy with which the EOP values are estimated can be improved by simply extending the baselines of the network. There is no technical reason this can not be done if a high-speed digital communication network is available. The development of the KSP VLBI system was thus an important first step towards a larger real-time VLBI network expected to enhance the capabilities of the VLBI technique. Although there is not a definite plan for international real-time VLBI experiments at present, opportunities to use international high-speed digital links are becoming feasible.

The International VLBI Service for Geodesy and Geodynamics was formed as a new international organization for VLBI research on 1 March 1999. CRL has been

designated to be one of the Technology Development Centers of the organization. It is important for CRL to continue its contributions and leadership in the developments of the VLBI technology. CRL is expected to play an important role in increasing the accuracy and the sensitivity of the VLBI technique and in standardizing VLBI systems.

Chapter 7 Conclusions

In this thesis, hardware and software developments to realize real-time and near-real-time VLBI observations, data processing and analysis were described. In the KSP VLBI system, real-time VLBI was realized by using the dedicated ATM network connecting the four observation sites around Tokyo. By using the system, it was successfully demonstrated that the real-time VLBI can almost eliminate the turn-around time to obtain results from observations. The system also made it possible to coordinate and run the VLBI sessions without any human operations by automating all the procedures, i.e. generating the observation schedule files, performing the observations according to the schedule files, correlating the transmitted data from four observing sites, performing post-correlation processing including bandwidth synthesis and database generation, and then analyzing data to obtain results. As the consequences, quite frequent VLBI sessions became possible and daily continuous VLBI sessions were actually demonstrated for 113 days from July 22, 2000. After the successful developments of the real-time VLBI system, further efforts were continued to realize near-real-time VLBI over the inter-continental baselines by using IP over the shared network environments. Prototype system of the VSSP has been developed as a realization of a part of the PC-based K5 system concept. Two domestic geodetic VLBI sessions were performed with the VSSP systems and the expected performance of the system was confirmed.

By using these real-time and near-real-time VLBI systems, various possibilities of real-time and near-real-time VLBI were presented through the actual observations. By using the KSP VLBI system, the extraordinary displacements of Tateyama and Miura VLBI sites caused by the volcanic activities near Izu islands were monitored. Such a dense monitoring with VLBI would not be possible without real-time VLBI capability of the KSP VLBI network. Flux densities of 16 radio sources were obtained as bi-products of the geodetic VLBI observations of KSP, and the results clearly suggested some of the strong radio sources are varying with time as a result of interstellar scintillations. Lastly, the ability of the rapid turn-around measurements of the Earth's Orientation Parameters was demonstrated by using the KSP VLBI network and an international baseline between Kashima and Westford stations. The Mark-5 system

was used at the Westford station and the correlation processing was performed at Haystack Observatory using the Mark-4 correlator and also at Kashima using the K5 software correlation programs. After the observations of the second session, UT1-UTC value was successfully estimated within one day and this turn-around time is expected to be further shortened by increasing the maximum bandwidth of the connecting network route and by using distributed correlation processing.

These results are clearly showing the part of the advantages of the real-time and near-real-time VLBI observations. These achievements were not possible with the conventional geodetic VLBI observations based on the tape-based observing and data processing systems. In the early developments of the VLBI technologies, emergences of the hydrogen maser systems and high speed data recorder systems played very important role. Similarly, the emergence and rapid growth of the high speed network technology are playing very important role in realizing real-time and near-real-time VLBI. The current growth of the maximum bandwidth of network is remarkable and it will provide us an opportunity to transfer observed data over inter-continental distances at the data rate which exceeds the maximum recording data rate to magnetic media in the near future. In such a situation, e-VLBI is expected to be able to expand the sensitivities of the VLBI observations. The current capacity limitations of the existing correlators can also be expanded by using distributed correlation processing. We expect the real-time and near-real-time VLBI will trigger the breakthroughs for various research fields in geodesy, geophysics, deep space navigation, astrometry, and astronomy in the foreseeable future.

References

Anderson, A. J. and A. Cazenave (Eds.) (1986), *Space Geodesy and Geodynamics*, Academic Press

Bare, C., B. G. Clark, K. I. Kellermann, M. H. Cohen, and D. L. Jauncey (1967), Interferometer Experiment with Independent Local Oscillator, *Science*, **157**, p. 189-191

Boucher, C., Z. Altamimi, and P. Sillard (eds.) (1999), *The 1997 International Terrestrial Reference Frame (ITRF97)*, IERS Technical Note 27, Central Bureau of IERS - Observatoire de Paris, Paris, France

Charlot, P. (1994), Evidence for source structure effects caused by the quasar 3C273 in geodetic VLBI data, in *VLBI Technology, Progress and Future Observational Possibilities*, ed. by T. Sasao, S. Manabe, O. Kameya, and M. Inoue, pp. 287-294, Terra Sci., Tokyo

Clark, T. A., B. E. Corey, J. L. Davis, G. Elgered, T. A. Herring, H. F. Hinteregger, C. A. Knight, J. I. Levine, G. Lundqvist, C. Ma, E. F. Nesman, R. B. Phillips, A. E. E. Rogers, B. O. Rönnäng, J. W. Ryan, B. R. Schupler, D. B. Shaffer, I. I. Shapiro, N. R. Vandenberg, J. C. Webber, and A. R. Whitney (1985), Precision Geodesy Using the Mark-III Very Long Baseline Interferometer System, *IEEE Trans. Geoscience and Remote Sensing*, **GE-23**, pp. 438-449

Eubanks, T. M., M. G. Roth, P. B. Esposito, J. A. Steppe, and P. S. Callahan (1982), An Analysis of JPL TEMPO Earth Orientation Results, *Proceedings of the Symposium No. 5: Geodetic Applications of Radio Interferometry*, International Association of Geodesy, Tokyo, Japan, May 1982, NOAA Tech. Rep. NOS 95 NGS 24, pp.81-90

Eubanks, T. M. (1993), Variations in the Orientation of the Earth, in *Contributions of Space Geodesy to Geodynamics: Earth Dynamics*, ed. by D. E. Smith and D. L. Turcotte, *Geodynamics Series*, **24**, American Geophysical Union, pp. 1-54

Fey, A. L., A. W. Clegg, and E. B. Fomalont (1996), VLBA observations of radio reference frame sources. I., *Astrophys. J. Suppl. Ser.*, **105**, pp. 299-330

Fey, A. L., and P. Charlot (1997), VLBA observations of radio reference frame sources. II. Astrometric suitability based on observed structure, *Astrophys. J. Suppl. Ser.*, **111**, pp. 95-142

Fiedler, R. L., E. B. Waltman, J. H. Spencer, K. J. Johnston, P. E. Angerhofer, D. R. Florkowski, F. J. Josties, W. J. Klepczynski, D. D. McCarthy, and D. N. Matsakis (1987), Daily observations of compact extragalactic radio sources at 2695 and 8085 MHz, 1979-1985, *Astrophys. J. Suppl. Ser.*, **65**, pp. 319-384

Heki, K., Y. Takahashi, T. Kondo, N. Kawaguchi, F. Takahashi, and N. Kawano (1987), The relative movement of the North American and Pacific Plates in 1984-1985 detected by the Pacific VLBI Network, *Tectonophysics*, **144**, pp. 151-158

Heki, K., Y. Takahashi, and T. Kondo (1990), Contraction of north-eastern Japan: evidence from horizontal displacement of a Japanese station in global very long baseline interferometry networks, *Tectonophysics*, **181**, pp. 113-122

Heki K., and Y. Koyama (1993), Eastward extrusion of the south China block: an evidence from Very Long Baseline Interferometry, *Proceedings of the General Meeting of the International Association of Geodesy*, Beijing, China

Herring, T. A., I. I. Shapiro, T. A. Clark, C. Ma, J. W. Ryan, B. R. Schupler, C. A. Knight, G. Lundqvist, D. B. Shaffer, N. R. Vandenberg, B. E. Corey, H. F. Hinteregger, A. E. E. Rogers, J. C. Webber, A. R. Whitney, G. Elgered, B. O. Ronnang, and J. L. Davis (1986), Geodesy by radio interferometry: evidence for contemporary plate motion, *J. Geophys. Res.*, **91**, B8, pp. 8341-8347

Herring, T. A. and M. R. Pearlman (1993), Future Developments and Synergism of Space Geodetic Measurement Techniques, in *Contributions of Space Geodesy to*

Geodynamics : Technology, ed. by D. E. Smith and D. L. Turcotte, pp. 21-25

Hirabayashi, H., P. G. Edwards, and D. W. Murphy (eds.) (2000), Astrophysical Phenomena Revealed by Space VLBI, Proceedings of the VSOP Symposium, Jan. 2000, ISAS, Japan

Kawano, N., T. Yoshino, F. Takahashi, K. Koike, and H. Kumagai (1982), Observations of Scintillation and Correlated Flux Using the Real-time VLBI System (K-2), Proc. Symp. No. 5: Geodetic Applications of Radio Interferometry, IAG, Tokyo, Japan, May 1982, NOAA Tech. Rep. NOS 95 NGS 24, pp.224-230

Kiuchi, H., S. Hama, M. Imae (1996a), K-4 and KSP VLBI Terminal, Proceedings of the Technical Workshop for APT and APSG 1996, pp. 166-170

Kiuchi, H., M. Imae, T. Kondo, M. Sekido (1996b), Real-time VLBI of the KSP, Proceedings of the Technical Workshop for APT and APSG 1996, pp. 125-129

Kondo, T., J. Amagai, H. Kiuchi, and M. Tokumaru (1991), Cross-correlation Processing in a Computer for VLBI Fringe Tests, J. Commun. Res. Lab., **38**, pp. 503-512

Kondo, T., H. Kiuchi, and M. Sekido (1996), KSP Correlator and Data Reduction System, Proceedings of the Technical Workshop for APT and APSG 1996, pp. 188-191

Kondo, T., N. Kurihara, Y. Koyama, M. Sekido, R. Ichikawa, T. Yoshino, J. Amagai, K. Sebata, M. Furuya, Y. Takahashi, H. Kiuchi, and A. Kaneko (1998), Evaluation of repeatability of baseline lengths in the VLBI network around Tokyo metropolitan area, Geophys. Res. Lett., **25**, pp. 1047-1050

Koyama, Y., K. Heki, M. Imae, T. Kondo, H. Kuroiwa, Y. Sugimoto, F. Takahashi, T. Yoshino, C. Miki, J. Amagai (1994), Horizontal Movements of Marcus VLBI Station due to the Pacific Plate Motion, Proc. CRCM'93, special issue of J. Geodetic Soc. Jpn., pp. 117-122

Koyama, Y. (1996), Excess Westward Velocities of Minamitorishima (Marcus) and Kwajalein VLBI Stations from the Expected Velocities Based on Rigid Motion of the Pacific Plate, *J. Geodetic Soc. Jpn.*, **42**, pp. 43-56

Koyama, Y., N. Kurihara, T. Kondo, M. Sekido, Y. Takahashi, H. Kiuchi, and K. Heki (1998), Automated geodetic very long baseline interferometry observation and data analysis system, *Earth Planets Space*, **50**, pp. 709-722

Koyama, Y., R. Ichikawa, T. Otsubo, J. Amagai, K. Sebata, T. Kondo, and N. Kurihara (1999), Recent Achievements in Very Long Baseline Interferometry, *J. Comm. Res. Lab.*, **46**, pp. 253-258.

Koyama, Y., T. Kondo, and N. Kurihara (2001), Microwave flux density variations of compact radio sources monitored by real-time very long baseline interferometry, **36**, No.2, pp.223-235

Koyama, Y., T. Kondo, J. Nakajima, M. Sekido, and M. Kimura (2003), VLBI Observation Systems Based on the VLBI Standard Interface Hardware (VSI-H) Specifications, *Proc. IVS Symposium in Korea, New Technologies in VLBI*, Nov. 2002, Gyeongju, Korea, ASP Conference Series, **306**, pp.135-144

Koyama, Y., T. Kondo, H. Osaki, A. R. Whitney and K. A. Dudevoir, Rapid Turn Around EOP Measurements by VLBI Over the Internet, *Proc. the XXIIIrd. General Assembly of the International Union of Geodesy and Geophysics*, Jul. 2003, Sapporo, Japan (in press)

Kunimori, H., F. Takahashi, M. Imae, Y. Sugimoto, T. Yoshino, T. Kondo, K. Heki, S. Hama, Y. Takahashi, H. Takaba, H. Kiuchi, J. Amagai, N. Kurihara, H. Kuroiwa, A. Kaneko, Y. Koyama, and K. Yoshimura (1993), Contributions and Activities of Communications Research Laboratory under the Cooperation with Crustal Dynamics Project, in *Contributions of Space Geodesy to Geodynamics: Technology*, eds. D. E. Smith and D. L. Turcotte, American Geophysical Union Geodynamics Series, **25**,

pp.65-79

Kurihara, N., K. Uchida, F. Takahashi, M. Imae, T. Yoshino, S. Hama, Y. Takahashi, and Key Stone Project Group (1996), The Crustal Deformation Monitoring System for the Tokyo Metropolitan Area (Key Stone Project), Proceedings of the Technical Workshop for APT and APSG 1996, pp. 65-69

Ma, C., and M. Feissel (Eds.) (1997), Definition and realization of the international celestial reference system by VLBI astrometry of extragalactic objects, IERS Tech. Note 23, Central Bureau of IERS, Obs. de Paris, Paris

Ma, C., E. F. Arias, T. M. Eubanks, A. L. Fey, A.-M. Gontier, C. S. Jacobs, O. J. Sovers, B. A. Archinal, and P. Charlot (1998), The international celestial reference frame as realized by very long baseline interferometry, *Astron. J.*, **116**, pp. 516-546

McCarthy, D. D. (1993), The Use of Crustal Dynamics Project Data to Predict the Orientation of the Earth, in Contributions of Space Geodesy to Geodynamics: Earth Dynamics, by D. E. Smith and D. L. Turcotte (eds.), Geodynamics Series **24**, American Geophysical Union, pp. 71-76.

Ryan, J. W., T. A. Clark, C. Ma, D. Gordon, D. S. Caprette, and W. E. Himwich (1993), Global Scale Tectonic Motions Measured with CDP VLBI Data, in Contributions of Space Geodesy to Geodynamics : Crustal Dynamics, ed. by D. E. Smith and D. L. Turcotte, Geodynamics Series, **23**, American Geophysical Union, pp. 37-49

Schuh, H., C. Patrick, H. Hase, E. Himwich, K. Kingham, C. Klatt, C. Ma, Z. Malkin, A. Niell, A. Nothnagel, W. Schlüter, K. Takashima, and N. Vandenberg (2002), Final Report, IVS Working Group 2 for Product Specification and Observing Program, in 2001 Annual Report, International VLBI Service for Geodesy and Astrometry, by N. R. Vandenberg and K. D. Baver (eds.), NASA/TP-2002-00817-0, pp. 13-45.

Sincell, M. W. (1997), Multiwavelength variability of the synchrotron self-compton model for blazar emission, *Astrophys. J.*, **477**, pp. 574-579

Steufmehl, H. (1983), AUTOSKED-Automatic creation of optimized VLBI observing schedules, Proceedings of the 8th Working Meeting on European VLBI for Geodesy and Astrometry, Report MDTNO-R-9243, Survey Dep. of Rijkswaterstat Delft, pp. IV22-IV29

Türler, M., T. J. Courvoisier, and S. Paltani (1999), Modelling the submillimeter-to-radio flaring behavior of 3C273, *Astron. and Astrophys.*, **349**, pp. 45-54

Wait, F. (1983), Precision measurement of antenna system noise using radio stars, *IEEE Trans. Instrum. Measure.*, **32**, pp. 110-116

Waltman, E. B., R. L. Fiedler, K. J. Johnston, J. H. Spencer, D. R. Florkowski, F. J. Josties, D. D. McCarthy, and D. N. Matsakis (1991), Daily observations of compact extragalactic radio sources at 2.7 and 8.1 GHz, 1979-1987, *Astrophys. J. Suppl. Ser.*, **77**, 379-404

Whitney, A. R. (2001), VLBI Standard Interface Specification, in 2000 Annual Report, International VLBI Service for Geodesy and Astrometry, by N. R. Vandenberg and K. D. Baver (eds.), NASA/TP-2001-209979, pp. 18-49

Whitney, A. R. (2003), The Mark 5 VLBI Data System and e-VLBI Development, in 2002 Annual Report, International VLBI Service for Geodesy and Astrometry, by N. R. Vandenberg and K. D. Baver (eds.), NASA/TP-2003-211619, pp. 22-33

Xia, S., H. Tamura, H. Hasegawa, J. Ooizumi, H. Kunimori, J. Amagai, and H. Kikukawa (1999), Local Tie at the Key Stone Sites, Proceedings of the Gemstone Meeting, Tokyo, Jan. 1999, pp. 85-89

Yen, J. L., K. I. Kellermann, B. Rayhrer, N. W. Broten, D. N. Fort, S. H. Knowles, W. B. Waltman, and G. W. Swenson, Jr. (1977), Real-Time, Very Long Baseline Interferometry Based on the Use of a Communications Satellite, *Science*, **198**, pp. 289-291

Yoshino, T. (1999), Overview of the Key Stone Project, *J. Comm. Res. Lab.*, **46**, pp. 3-6

Zensus, J. A. (1997), Parsec Scale Jets in Extra Galactic Radio Sources, *Annu. Rev. Astron. Astrophys.*, **35**, pp. 607-636

List of Publications

Yasuhiro Koyama, Jun Amagai, and Hitoshi Kiuchi, Precise Position Determination of New Kashima VLBI Station, *J. Comm. Res. Lab.*, **38** (1991) pp.335-340

Yasuhiro Koyama, Results of VLBI Experiments at the Communications Research Laboratory, IV. Experimental Results, IV.4 Minami-Torishima (Marcus) Experiments, *J. Comm. Res. Lab.*, **38** (1991) pp.543-551

Yasuhiro Koyama, Michito Imae, Noriyuki Kurihara, Chihiro Miki, Yuji Sugimoto, Taizoh Yoshino, Fujinobu Takahashi, Hitoshi Kiuchi, Shin'ichi Hama, Yukio Takahashi, Hiroshi Takaba, Takahiro Iwata, Yuko Hanado, Mamoru Sekido, Tetsuro Kondo, Jun Amagai, Akihiro Kaneko, and Kosuke Heki, Western Pacific VLBI Network, III. Geodetic Results of the Experiments, III.1 Movement of the Minamitorishima Station, *J. Comm. Res. Lab.*, **42** (1995) pp.43-55

Yasuhiro Koyama, Kosuke Hheki, Michito Imae, Tetsuro Kondo, Hiroshi Kuroiwa, Yuji Sugimoto, Fujinobu Takahashi, Taizoh Yoshino, Chihiro Miki, and Jun Amagai , Horizontal Movement of Marcus VLBI Station due to the Pacific Plate Motion, *Proceedings of the Eighth International Symposium on Recent Crustal Movements* (1993) pp.117-122

Yasuhiro Koyama, Excess Westward Velocities of Minamitorishima (Marcus) and Kwajalein VLBI Stations from the Expected Velocities Based on Rigid Motion of the Pacific Plate, *J. Geod. Soc. Jpn.*, **42** (1996) pp.43-57

Yasuhiro Koyama, Ryuichi Ichikawa, Tadahiro Gotoh, Mamoru Sekido, Tetsuro Kondo, Noriyuki Kurihara, Fujinobu Takahashi, Jun Amagai, Toshimichi Otsubo, Hideyuki Nojiri, Kouichi Sebata, Hiroo Kunimori, Hitoshi Kiuchi, Akihiro Kaneko, Yukio Takahashi, Shin'ichi Hama, Yuko Hanado, Michito Imae, Chihiro Miki, Mizuhiko Hosokawa, and Taizoh Yoshino, VLBI, SLR, and GPS observations in the Key Stone Project, *Proceedings of the IAG Scientific Assembly, Geodesy on the Move, Gravity,*

Geoid, Geodynamics, and Antarctica (September 3-9, 1997, Rio de Janeiro), IAG Symposia **119** (1997) pp.394-399

Yasuhiro Koyama, Noriyuki Kurihara, Tetsuro Kondo, Mamoru Sekido, Yukio Takahashi, Hitoshi Kiuchi, and Kosuke Heki, Automated Geodetic Very Long Baseline Interferometry Observation and Data Analysis System, Earth, Planets, and Space, **50** (1998) pp.709-722

Yasuhiro Koyama, Ryuichi Ichikawa, Tetsuro Kondo, Noriyuki Kurihara, Yukio Takahashi, Taizoh Yoshino, Kouichi Sebata, and Masato Furuya, Comparison of site velocities measured by VLBI and GPS in the Key Stone Project Network, Proceedings of the IAG Section 2 Symposium, Towards an Integrated Global Geodetic Observing System (October 5-9, 1998, Muenchen, Germany), IAG Symposia **120** (2000) pp.158-160

Yasuhiro Koyama, Takahiro Iwata, and Hiroshi Takaba, 3. KSP VLBI System, 3.1 Observation System, 3.1.4 Observation and System Management Software, J. Comm. Res. Lab., **46** (1999) pp.33-38

Yasuhiro Koyama, Kosuke Heki, Yukio Takahashi, and Masato Furuya, 3. KSP VLBI System, 3.3 Data Analysis System, 3.3.1 Data Analysis Software, J. Comm. Res. Lab., **46** (1999) pp.77-81

Yasuhiro Koyama, Eiji Kawai, Mamoru Sekido, Noriyuki Kurihara, Kouichi Sebata, and Masato Furuya, 7. Observation Results, 7.6 Tie of the KSP VLBI Network to the Terrestrial Reference System, J. Comm. Res. Lab., **46** (1999) pp.183-186

Yasuhiro Koyama, Ryuichi Ichikawa, Toshimichi Otsubo, Jun Amagai, Kouichi Sebata, Tetsuro Kondo, and Noriyuki Kurihara, Recent Achievements in Very Long Baseline Interferometry, J. Comm. Res. Lab., **46** (1999) pp.253-258

Yasuhiro Koyama, Tetsuro Kondo, and Noriyuki Kurihara, Microwave flux density variations of compact radio sources monitored by real-time Very Long Baseline

Interferometry, Radio Science, **36** (2001) pp.223-235

Yasuhiro Koyama, Geodetic Results from Domestic VLBI Observations, J. Comm. Res. Lab., **48** (2001) pp.13-16

Yasuhiro Koyama, Junichi Nakajima, Mamoru Sekido, Makoto Yoshikawa, Akiko M. Nakamura, Hisashi Hirabayashi, Tatsuaki Okada, Masanao Abe, Toshiyuki Nishibori, Tetsuharu Fuse, Steven J. Ostro, Dennis Choate, Reginald A. Cormier, Ron Winkler, Raymond F. Jurgens, Jon D. Giorgini, Keith D. Rosema, David L. Mitchell, Donald K. Yeomans, Martin A. Slade, and Alexander L. Zaitsev, Radar Observations of Near Earth Asteroids 6489 Golevka and 4197 (1982TA), J. Comm. Res. Lab., **48** (2001) pp.143-150

Yasuhiro Koyama, Tetsuro Kondo, Junichi Nakajima, Mamoru Sekido, and Moritaka Kimura, VLBI observation systems based on the VLBI Standard Interface Hardware (VSI-H) specifications, Proceedings of the IVS Symposium in Korea, New Technologies in VLBI, (November 5-8, 2002, Gyeongju, Korea), ASP Conference Series, **306**, pp.135-144

Yasuhiro Koyama, Tetsuro Kondo, and Hiro Osaki, Rapid Turn Around EOP Measurements by VLBI over the Internet, Proceedings of the XXIII General Assembly of the International Union of Geodesy and Geophysics (June 30-July 11, 2003, Sapporo, Japan) (*in press*)